CO_2 sequestration using brine impacted fly ash

By

Grace Nyambura Muriithi

Bsc Honours (Chemistry) - University of Nairobi

Submitted in fulfillment of the requirements for degree of Magister Scientiae in the Chemistry Department, University of the Western Cape

Supervisor: Dr Leslie F. Petrik

November 2009

ABSTRACT

Coal combustion accounts for over 40 % of the world's energy production and this figure is projected to increase with increasing human population and industrialization. The combustion of coal leads to the generation of waste products such as fly ash (FA), brine from water treatment, bottom ash, slag, flue gas desulphurization products (FGD) and gas emissions such as N_2O, and CO_2. The emissions contribute to air pollution and global warming, while FA, brines, and FGD are possible soil and water pollutants.

In order to minimize the environmental impact of coal combustion, mitigation of the effects of coal burning processes such as the waste products (FA, brine, bottom ash, slag and FGD) and gas emissions is required. This study investigated utilization of the Secunda FA (class F) and reverse osmosis (RO) Tutuka brine to sequester CO_2 in an attempt to make coal power production more environmentally sustainable.

It was hypothesized that South African FA and brine could sequester CO_2 through mineral carbonation. A statistical approach was undertaken to optimize the % $CaCO_3$ formed from FA/brine/CO_2 interaction with input parameters of temperature, pressure, particle size and solid/liquid ratio (S/L) being varied. The ranges adopted for the input parameters were: temperature of 30 ºC or 90 ºC; pressure of 1 Mpa or 4 Mpa; four particle sizes namely bulk ash, > 150 µm, < 20 µm and 20 µm- 150 µm particle size range; S/L ratios of 0.1, 0.5 or 1. The FA/ brine dispersions were carbonated in a high pressure reactor varying the above mentioned input parameters.

The fresh Secunda FA of various size fractions was characterized morphologically using scanning electron microscopy, chemically using X-ray fluorescence and mineralogically using qualitative X-ray diffraction. The carbonated solid residues on the other hand were characterized using quantitative X-ray diffraction, scanning electron microscopy, thermal gravimetic analysis and Chittick tests. The raw brine from Tutuka together with the carbonation leachates were characterized

using inductively coupled mass spectrometry and ion chromatography. Total acid digestion was carried out to evaluate the differences in the total elemental content in both the fresh ash and the carbonated solid residues.

The results suggested that South African FA from Secunda belongs to class F based on the CaO content as well as the total alumina, silica and ferric oxide content, while the RO brine from Tutuka were classified as $NaSO_4$ waters.

Mineral carbonation occurred and ranged between 2.75 % and 6.5 % of $CaCO_3$ depending on the input parameters.

Two polymorphs of $CaCO_3$ were identified in the carbonated residues i.e. calcite and aragonite.

The carbonated ash/brine leachates were cleaner with respect to major and trace element concentration compared to raw brine thus the carbonation process could be used to improve the quality of brines generated in the power industry. Removal of the major elements from brine was as follows Ca-74.8 %, Na- 28.7 %, Mg- 98 %, K- 82.9 %, SO_4- 20.8 %. Hundred percent removal was observed for traces of Fe, Al, Mn, Cu, Zn, Pb, Ni, As, Ti, Sr, Se, Si and NO_3. However Mo, V, B, and Cl concentrations increased by 72.5 %, 94 %, 48.2 % and 7.2 % respectively after carbonation at 90 °C, 4 Mpa, S/L ratio of 1 using the bulk ash.

The parameters found to be of most significance in the carbonation process were the main effects of temperature, particle size and S/L ratio while the interactions of temperature and particle size as well as the interaction of temperature with S/L ratio were also found to be significant. The statistical approach led to a clear understanding of the effect of each input parameter as well as the arising interactions. The conditions of 90 °C, 4 Mpa, using bulk ash at a S/L ratio of 1 resulted in the highest yield of % $CaCO_3$ with a value of 6.5 %.

Theoretically one ton of Secunda FA containing 9.2 % of CaO could sequester 0.083 tons of CO_2. With the optimized protocol developed in this study bearing in

mind that the carbonation efficiency is 75.54%, 1 ton of Secunda FA could sequester 0.062 tons of CO_2. This translates to 0.65 % of CO_2 produced annually at Secunda plant being sequestered in the FA/brine dispersions. In other words, 16 tons of FA are required to sequester a ton of CO_2 annually.

It was also observed that carbonation using brine resulted in higher carbonation efficiency than carbonation using water as the Ca^{2+} component in the brine contributed towards the Ca^{2+} concentration.

DECLARATION

I hereby declare that "CO_2 sequestration using brine impacted fly ash" is my own work, that it has not been submitted for any degree or examination in any other university, and that all the sources I have used or quoted have been indicated and acknowledged by complete references.

Grace Nyambura Muriithi   November 2009

Signed..........................

ACKNOWLEDGEMENTS

LIST OF ABBREVIATIONS

FA	Fly ash
CUB	Coal utilization by-products
FGD	Flue gas desulphurization products
EPA	Environmental Protection Agency
GHG	Greenhouse gases
CFC	Chlorofluorocarbons
UNFCC	United Nations Framework Convention on Climate Change
CDM	Clean development mechanism
EDR	Electro dialysis reversal
SRO	Spiral reverse osmosis
TDS	Total dissolved solids
ZLED	Zero liquid effluent discharge
S/L	Solid to liquid ratio
FBB	Fluidized boiler bed
ECOBA	European Coal Combustion Products Association
ASTM	American Society for Testing and Materials
RO	Reverse osmosis
AMD	Acid mine drainage
WHO	World Health Organization
MSF	Multi stage flash
MEB	Multiple effects boiling
MF	Microfiltration
UF	Ultrafiltration
NF	Nanofiltration
EDI	Electrodeionization
VC	Vapour compressor
TVC	Thermal vapour compressor
MVC	Mechanical vapour compressor
TOC	Total organic content
NTU	Nephelometric turbidity units
GCM	Global climate model

IPCC	International Panel on Climate Change
EIA	Energy Information Administration
DOE	Department of Energy
MEA	Mono-ethanolamine
DEA	Di-ethanolamine
PSA	Pressure swing adsorption
IGCC	Integrated gasification combined cycle
ECM	Enhanced coalbed methane
MSWI	Municipal solid waste incineration
pE	Electron activity
CHS	Calcium silicate hydrate
CASH	Calcium aluminosilicate hydrate
SEM	Scanning electron microscopy
SEM-EDS	Scanning electron microscopy-electron dispersive spectroscopy
XRD	X-ray diffraction
XRF	X-ray fluorescence
ICDD	International Center for Diffraction Data
AAS	Atomic absorption spectroscopy
ICPS	Inductively coupled plasma spectroscopy
NAA	Neutron activation analysis
LOI	Loss on ignition
ICPMS	Inductively coupled plasma mass spectroscopy
IC	Ion chromatography
ICPOES	Inductively coupled plasma optical emission spectroscopy
DOE	Design of experiments
TGA	Thermal gravimetric analysis
$PM_{2.5}$	Particulate matter (25 μm)
TRO	Tubular reverse osmosis
ANOVA	Analysis of variance
CE	Carbonation efficiency

TABLE OF CONTENTS

LIST OF TABLES

LIST OF FIGURES

ACADEMIC OUTPUT

The following conference presentations are based on this study.

Oral Presentations

Muriithi G.N; Petrik L.F; Gitari M.W; "CO_2 sequestration using brine impacted fly ash: The chemistry and potential for brine remediation", 6th Kenya Chemical Society & 8th East and Southern Africa Environmental/ Theoretical Chemistry International Conference, Mombasa, Kenya, 5th to 9th October 2009.

Muriithi, G.N; Gitari, M.W; Petrik, L.F;"CO_2 sequestration using brine impacted fly ash", INORG2009, South African Chemical Institute Inorganic Meeting, Bloemfontein, South Africa, 13th to 17th September 2009.

Poster presentations

Gitari M.W; Muriithi N.G; Petrik L.F; "Chemical and mineralogical changes in brine slurried coal fly ash: Implications for CO_2 sequestration and brine effluents remediation", International Conference on Coal Science and Technology (ICCS&T), Cape Town, South Africa, 26th to 29th October 2009.

Muriithi, G.N; Gitari M.W; Petrik, L.F; "Brine remediation using fly ash and accelerated carbonation", International mine Water Conference, Pretoria, South Africa, 19th to 23rd October 2009.

Muriithi, G.N; Gitari M.W; Petrik, L.F; "CO_2 capture in brine impacted fly ash "South African Chemical Institute 39th National Convention, Stellenbosch, South Africa, 30th November to 5th December 2008.

Poster Paper

Muriithi, G.N; Gitari M.W; Petrik, L.F; "Brine remediation using fly ash and accelerated carbonation", International mine Water Conference, Pretoria, South Africa. Peer reviewed by members of the International Scientific Committee (International Mine Water Conference).

DON'T QUIT

When things go wrong,
As they sometimes will,
When the road you're trudging seems all uphill,
When the funds are low and the debts are high,
And you want to smile, but you have to sigh,
When care is pressing you down a bit
Rest if you must, but don't you quit.

Life is queer with its twists and turns,
As every one of us sometimes learns,
And many a failure turns about
When he might have won had he stuck it out.
Don't give up though the pace seems slow
You may succeed with another blow.

Success is failure turned inside out
The silver tint of the clouds of doubt,
And you never can tell how close you are,
It may be near when it seems so far;
So stick to the fight when you're hardest hit
It's when things seem worst that you mustn't quit.

CHAPTER ONE

INTRODUCTION

1.1 BACKGROUND

Fossil fuel combustion provides more than 85 % of the world's energy needs, with 40 % of it being from coal combustion (Montes-Hernandez et al., 2009). Coal combustion is projected to increase owing to the increased demand for electricity (due to industrialization as well as population growth) and the availability of large coal reserves in different parts of the world (Figueroa et al., 2008; Wolf et al., 2004). However, the combustion causes the generation of coal utilization by-products (CUB) such as CO_2, SO_2 and NO_x as gaseous emissions, wastes such as fly ash (FA), flue gas desulphurization products (FGD) and brine generation as well degradation to the land through land filling of the generated wastes. These emissions contribute to air pollution, while waste FA, brines, and FGD are possible soil and water pollutants. To conform to the Environmental Protection Agency (EPA) emission regulations, some coal-fired power plants have employed effective methods to remove SO_2 from exhaust gases. Hydrated lime ($Ca(OH)_2$) is used as SO_2 sorbent in the form of a slurry. The lime slurry is sprayed into a spray dryer where SO_2 is removed from flue gas as gypsum. The slurry is evaporated and salts precipitated. The sorbent is then carried by the flue gas downstream to a particulate collection device e.g. electrostatic precipitators or bag filters. The by-product is a dry mixture of calcium sulfite/sulfate and various metal oxides, commonly known as flue gas desulphurization products (Xiaoxun et al., 2000). Similar mechanisms are however lacking for the CO_2 and NO_x streams and the current trend for FA particulate removal involves the use of bag filters that are not 100 % effective.

Global warming is attributed to a significant increase of the green house gases (GHG), namely CO_2, CH_4, N_2O, chlorofluorocarbons (CFC) and O_3 in the atmosphere. These gases absorb solar radiation that would otherwise be reflected back into space. A build-up of these gases inside the earth's atmosphere means more heat is trapped close to the planet's surface, causing a gradual warming that

is now considered to lead to changes in the planet's climatic conditions e.g. the excess heat causes more water to evaporate from the earth's surface, bringing drier conditions to some regions and more rainfall to others. Overall, the concentration of green house gases causes sporadic changes in standard weather patterns and could eventually make parts of the planet uninhabitable. The contribution of these GHG's towards global warming has been projected as:- CO_2 (50 %), CH_4 (20 %), CFC (15 %), N_2O (10 %) and O_3 (5 %). The 50 % contribution from CO_2 can further be projected as:- fossil fuel combustion (73 %), cement industry (2 %) and deforestation (25 %) (Lemos de Sousa et al., 2008). Of all GHG, the atmospheric concentration of CO_2 has risen from pre-industrial levels of 280 ppm to 380 ppm in 2005 (Bachu, 2008) while in 2007, approximately 29 Gt of CO_2 were added to the atmosphere from fossil fuels combustion and this is projected to increase to 43 Gt by 2030 (Kharaka et al., 2009). Inevitably, failure to reduce atmospheric CO_2 emissions significantly, will have far reaching consequences as pertains to global warming (Soong et al., 2006).

Due to this major threat, various steps have been taken internationally such as the formation of the United Nations Framework Convention on Climate Change (UNFCCC) and the ratification of the Kyoto protocol which brings constraints to emissions and requires a timetable for realization of the reduction by 5.2 % of the 1990 level during the 2008 - 2012 periods (Tunç et al., 2007). Although the protocol does not bring any limitations to developing countries, South Africa has acceded to it as an Annex 1 and thus its participation will be through the Clean Development Mechanism (CDM). The CDM allows industrialized countries with emission reduction commitments to meet part of their commitments by investing in projects that reduce emissions in developing countries. The projects need to support sustainable development in the host countries and must lead to emissions reductions that are real, measurable and long term in climate change mitigation such as energy efficiency, cleaner production, fuel switching and forestry (www.dme.gov.za/energy/coal.stm).

According to He et al., (2006), coal accounts for 65 % of the total primary energy consumption in China. On the other hand, USA and South Africa generate 51.7 % and 93 % respectively of their electricity from coal combustion (Klass, 2003; Eskom, 2006). In 1999 USA contributed 23 % to the total world's emissions of CO_2 while China contributed 13.17 % (Klass, 2003). However according to the Netherlands Environmental Assessment Agency, this scenario changed in 2006 when China's emissions surpassed those of the USA by 8 %. Currently China tops the list of CO_2 emitting countries for the first time since in 2005, CO_2 emissions of China were still 2 %below those of the USA. The European Union with a volume of emissions half that of China occupies the 3rd position followed by Russia, India and Japan respectively. Annually the electricity generating industry in South Africa produces over 218 million tons of CO_2 (Eskom, 2006) with Sasol Sasolburg and Sasol Secunda contributing 57 million tons of CO_2 per annum and a single stationary power station such as Tutuka contributing 8 million tons of CO_2 per annum (Englebrecht et al., 2004). It thus follows that a major advance in tackling global warming would be achieved in curtailing atmospheric emissions of CO_2 from the coal burning power plants.

Coal is an easily combustible rock that contains 50 % or more by weight and 70 % by volume of carbonaceous material. The mineralogy of the coal constituents is dependent on the geology of the surrounding environment of coal formation. The most common inorganic mineral constituents are clay minerals illite and kaolinite; sulphides such as pyrite and marcasite; carbonates like dolomite, ankerite, calcite and siderite and quartz. Clay minerals make up 60 - 90 % of the total mineral matter in coal and quartz is found in almost all coal and can comprise from 1 to 20 % of the inorganic compounds present in the coals. Many trace elements are present within coal deposits ranging from a few percent of the total composition to parts per million (ppm) (Gitari, 2006). FA is a by-product of coal combustion which consists mainly of spherical glassy particles of varying SiO_2, Al_2O_3 and Fe_2O_3 content. The chemical and physical characteristics of FA are controlled by the coal, the boiler temperature and its operating conditions and post combustion parameters; the minerals present in the coal dictate the elemental composition of

the FA while the boiler design and operation dictate the mineralogy and crystallinity of the ash. The crystallinity of FA would determine whether the metals are incorporated within the glassy phase or within the crystalline compounds. The metals in the glassy phase are expected to leach at a much faster rate than that from the crystalline phase (Eskom, 2001). FA contains trace concentrations of many toxic elements that are known to be detrimental to the environment and public health. These include Ni, V, As, Be, Cd, Ba, Cr, Cu, Mo, Zn, Pb, Se, U, Th and Rd (Eary et al., 1990). The extent to which these minor and trace elements are leached from FA upon contact with aqueous media such as acid mine drainage or brine will have an impact on the suitability of using FA as bulk fill upon disposal (Kim et al., 2003). Sukrut et al., (2002) observed that toxic metallic trace elements are present in coal thereby implying that these are passed onto the resulting FA. Consequently, to avoid contamination of soil and ground water, leaching of toxic metals should be considered before the ash is buried in landfills or used in manufacturing of cement.

Different characteristics of FA make it suitable for various applications, for instance as a source of silica it is used in the ceramic and glass industry (Ferreira et al., 2003). The silica and alumina have also been utilized in making zeolites (Somerset et al., 2008; Somerset et al., 2004; Querol et al., 2002; Querol et al., 1997). Its CaO content makes it suitable for use in cement and in concrete production as an extender, a replacement of concrete in building and construction. Amendment of acidic soils has been shown to be possible using FA which also provides nutrients such as potassium and phosphorous to the plants (Rosen et al., 1994). Several authors have also used FA in remediation of acid mine drainage and mine tailings, replacing conventional water cleaning chemicals (Gitari et al., 2008; Gitari, 2006; Robb and Robinson, 1995).

Sasol, a global petrochemical player uses large quantities of coal, steam and oxygen as feedstock for production of fuel and chemicals. 70 % of the coal is used for gasification (i.e.) coal to liquid fuel conversion and in the process CO_2 is emitted together with large amounts of coarse ash, about 7 million tons per year

(Ginster and Matjie., 2004). The remaining 30 % of the coal utilized, a finer coal fraction, is combusted to produce steam for generation of electricity leading to production of FA which is emitted with flue gas and is trapped by precipitators or bag filters. Sasol-Sasolburg and Sasol-Secunda produce a total of 4.75 Mt of FA per annum. Eskom on the other hand consumes approximately 109 million tons of coal annually producing 25 million tons of ash (Eskom, 2006). Tutuka, one of Eskom's coal fired power plants with a capacity of 3654 MW per annum produces 1.765Mt of FA per annum (Krüger, 2003).

Water requirements are high in both Secunda and Tutuka power stations; for instance Sasol Secunda uses 255 Ml/day of fresh water for steam generation, process cooling and as feed water for its coal to fuel and chemical processes. These waters are obtained from reservoir dams and thus need pre-treatment to clean and desalinate them through processes such as electro dialysis reversal (EDR) and spiral reverse osmosis (SRO). Brines are the by-product of the desalination process. They are highly saline solutions usually containing total dissolved solids (TDS) of over 35,000 mg/l. The brine streams contain residues of water softening chemicals (lime), flocculants (aluminium and iron sulphates, silicates), disinfectants (chlorine, sodium hypochlorite) antiscalants and antifoaming agents (Buhrmann et al., 1999). Previous analysis done on both Tutuka and Secunda brines showed them to be rich in Ca, Na, K, SO_4, Cl and Mg (Petrik et al., 2007). Also present are traces of Fe, Mn, Cr, V, Ti, P, Si and Al (Mooketsi et al., 2007)

Both Tutuka and Secunda are operated in accordance with the zero liquid effluent discharge (ZLED) policy. This implies that apart from seepage water losses no saline water is discharged to surface water resources. In Secunda, the brine streams are used for the hydraulic transport of FA usually in the form of a slurry which is then stockpiled in ash dumps. This implies that the ash dumps may act as a sink for the salts present in brine. Tutuka power station on the other hand utilizes a dry ash disposal system. FA is conditioned with the brine to a moisture

5

content of 12 % before being conveyed to the ash dumps. In the ash dumps it is further conditioned by irrigation with the high saline effluents for dust control.

CO_2 sequestration, which has currently gained increased attention, may allow for continued use of fossil fuels while ensuring reduced emissions. CO_2 abatement involves two major processes (Lemos de Sousa and Rodriguez, 2008); fixation in sinks (mainly biological fixation) or geological storage (capture and transportation). Geological storage is further divided into open systems (oceanic CO_2 lakes and diverse porous lithologies), mineral carbonation and closed systems (salt cavitation, deep saline aquifers, depleted oil and gas fields and coal seams). Biological fixation involves integration of photosynthetic functions of micro organisms such as microalgae by formation of new biomass that can be used e.g. as a food source for animals as it contains high crude protein content (Chae et al., 2006). Geological sequestration consists of capturing the gaseous CO_2 from emission sources and injecting it as a supercritical fluid into underground formations such as active and depleted oil and gas reservoirs, deep unminable coal seams, basalt formations and deep saline aquifers (United States Department of Energy, 1999). In these reservoirs the CO_2 can be stored by stratigraphic or structural trapping (physical isolation), solubility trapping (dissolved in the aqueous phase) and/or hydrodynamic trapping. However there is a potential for leakage regarding hydrodynamic trapping through imperfect confinement. The sequestration of CO_2 in saline aquifers proceeds by conversion into various carbonates such as calcite, magnesite, dolomite and siderite which can be stored in the aquifer formation for millions of years (Gunter et al., 2000). However, conversion of CO_2 into stable minerals in the geological formations is expected to be slow (hundreds to thousands of years) due to the slow kinetics of silicate mineral dissolution and carbonate mineral precipitation. Mineralogical carbon sequestration however could be significant in the proximity of the emission sources without the need of storing the gas into geological reservoirs.

This technology is called ex-situ mineral sequestration of CO_2 as originally proposed by Seifritz (1990) and first studied in detail by Lackner et al., (1995).

6

The basic concept behind mineral CO_2 sequestration (also known as mineral carbonation) is to mimic natural weathering processes in which calcium or magnesium silicates are transformed into carbonates.

Carbonation has been investigated as a possible state of the art technology for stabilization of municipal solid waste incineration ash for disposal by Ecke (2003); Ecke et al., (2002); Wu-Jang et al., (2007) and Rendek et al., (2006). These authors established that mobility of Pb and Zn is reduced by two orders of magnitude due to the predominance of $PbCO_3$ ($6<pH<9$) and $Zn(OH)_2$ ($9<pH<11$) respectively. Carbonation reactions of CaO are the most important processes that cause a decrease in ash pH and a formation of sorptive solid phases to adsorb heavy metals. pH was found to be a dominant parameter in metal leaching and metal leaching could be reduced by sorption in such newly formed minerals. Cd and Pb have a strong affinity for calcite and they could also form complexes with Fe and Al(hydr) oxides. However, carbonation increased the mobility of Cd due to the transition from $Cd(OH)_2$ to $CdCl_2$.

Mineral carbonation involves two major processes, direct and indirect carbonation. In direct carbonation, CO_2 reacts with solids like Ca/Mg silicate, forming dolomite. The mineral can also be slurried in water in an aqueous scheme before being carbonated. In indirect carbonation HCl is used to extract Ca and Mg from the silicate matrix (e.g. serpentine and wollastonite) giving rise to a hydroxide which is then carbonated. Other indirect carbonation routes have also been investigated for example use of acetic acid to generate Ca^{2+} cations from the Ca containing minerals such as wollastonite ($CaSiO_3$) that are then carbonated. Use of NaOH and acids are other viable means through which the reactive Ca and Mg can be extracted from the Ca/Mg silicate matrix (Huijgen and Coman, 2003).

Alkaline industrial wastes such as steel slag and concrete waste which are rich in Ca/Mg have also been studied, (Stolaroff et al., 2005) with respect to their utility as feedstock for mineral CO_2 sequestration. Their utilization is accompanied by three major advantages namely, their availability as waste products from

industries; the high reactivity due to their chemical instability and their low cost. Recently Montes-Hernandez et al., (2009) have studied the carbonation potential of coal combustion FA (class F). They suggested that carbonation occurs in two successive reactions, firstly the irreversible hydration of lime present in the ash and secondly the spontaneous carbonation of the calcium hydroxide suspension. Approximately 82 % of carbonation efficiency of FA is reported, moreover their experiments demonstrated that one ton of FA can sequester up to 0.026 tons of CO_2.

Soong et al., (2006) studied the CO_2 sequestration with brine solutions and class C FA. It was observed that exposure of brine to FA leads to an increase in Ca^{2+} concentration in the reaction mixture, this was attributed to the dissolution of CaO found in FA giving rise to $Ca(OH)_2$ which in turn increases the brine pH. The hydroxide further dissociates to give Ca^{2+} which reacts with CO_3^{2-} from the dissolution of carbon dioxide forming calcite. Thus the Ca, Mg and Fe in both FA and brine can react with CO_2 to produce the corresponding carbonates for safe and permanent storage of carbon dioxide. In addition, the Na^+ concentration in the brine is reduced. The concentration of CaO in the FA after exposure to brine decreased while that of NaCl increased. The observed increase in NaCl concentration in FA was linked to the decrease of Na^+ concentration in brine.

1.2 AREA OF STUDY

Sasol Synfuels in Secunda as well as Tutuka power stations situated in the Mpumalanga Province of South Africa were chosen as the study areas in this research. Both Tutuka and Secunda power stations utilize bituminous and anthracitic coal types with the generation of a class F FA whose lime content is below 10 %. Pre-treatment of water for boiler feed and cooling purposes in both sites leads to production of brines which are used in ash conditioning and transportation. A map of Mpumalanga province showing the location of the power plants is given in Figure 1.
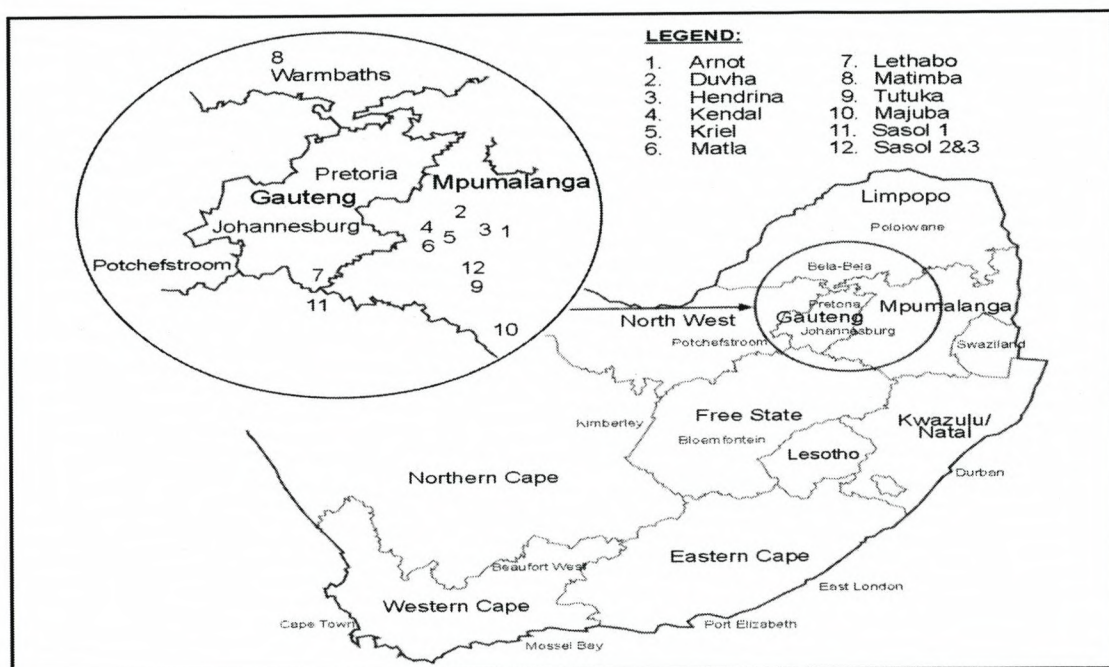
Figure 1.1: Location of the major coal fired power plants in South Africa (Krüger, 2003).

In their ash handling systems, Sasol (Secunda) slurries the FA before layering it in the ash dumps. Tutuka on the other hand moistens the dry FA (12 - 16 %) before heaping the ash in the dry dumps and eventually rehabilitating the dumps. The fact that these power stations utilize different disposal techniques for their FA coupled with different operating conditions in the two power plants made them suitable for comparative studies.

1.3 PROBLEM STATEMENT

Electricity generation from coal combustion is coupled with generation of huge amounts of FA particularly the South African coal whose calorific value is low with a high ash content of 30 - 40 %. Large volumes of waste waters (brines) are produced in coal power generation. Both brine and ash are made up of components which are available to leaching mechanisms thus making them detrimental to the environment (soil and underground water reservoirs). Coupled with this is the issue of CO_2 emissions that are a major cause of increasing the green house effect. Despite the numerous environmental issues associated with its combustion, coal will remain a major source of electric power in South Africa for

years to come owing to the relative lack of suitable alternatives to coal as an energy source coupled with the large coal deposits which can be exploited at extremely favourable costs (Randall, 2002). A viable utilization is thus sought of the waste products, to be used to capture the CO_2 gases emitted in the form of carbonates that are environmentally benign and stable.

Soong and co-authors used class C FA (from USA) whose lime content is very high (above 25 %) compared to the class F FA (less than 10 %) typically found in South Africa. However the South African FA is different in lime content and compaction and may not be suitable for carbonation. This study thus examines the feasibility of using South African (class F) FA together with brines for CO_2 sequestration. Of interest also will be the effect of carbonation on the FA and brine's elemental composition.

1.4 OBJECTIVES

The objective of this study is to investigate the feasibility of using South African FA and brine to capture CO_2 via mineral carbonation. This study thus seeks to establish answers to the following research questions:-

i) What is the chemical composition of FA and brine effluents produced at Sasol Secunda and Tutuka power stations?

ii) What mineral phases are likely to form during the ash/brine/CO_2 interaction?

iii) What is the mode of encapsulation of the CO_2 or brine components in the FA?

iv) To what degree can CO_2 be trapped in the ash?

v) What effect does carbonation have on both the FA and brine?

1.5 RESEARCH APPROACH

Firstly, characterization of the raw materials (FA and brine) was carried out. A statistical optimization approach for the carbonation experiment was then applied with a major emphasis on varying the following reaction parameters: - particle size, pressure, temperature and solid/liquid ratio (S/L). Characterization of the resulting solid residues and leachates was carried out to investigate the effect of

carbonation on the FA and brine solutions. Computation of the FA and brine capacity to sequester CO_2 was then carried out and the figures compared with literature values.

1.6 HYPOTHESIS

South African FA and brine are suitable for carbon capture via direct mineral carbonation.

1.7 SCOPE AND DELIMITATIONS OF STUDY

An extensive study had been carried out by the Environmental & Nano Sciences Research group (ENS) in the Chemistry Department, University of the Western Cape on the Secunda and Tutuka ash dumps with regards to characterization of the ash (Fatoba, 2007; Petrik et al., 2008). Also studied had been the brine streams from these two power plants. With this background knowledge, the potential of these two waste streams to sequester CO_2 was investigated. Characterization of the FA and brine was done and statistically designed experiments were used to evaluate the effect of temperature, pressure, S/L ratio and particle size on the degree of carbonation.

Thermal gravimetric analysis was only carried out on the samples from the experimental runs in which the highest degree of carbonation was achieved for both quantitative XRD and Chittick test due to cost constraints.

The statistical analysis only gives the most important concepts and the reader is thus referred to Design and Analysis of Experiments, 7th Edition by Montgomery (2009) for further assessment.

It proved impossible to carry out the carbonation experiments using the >150 µm fraction at a S/L ratio of 1. Immediately after mixing FA with brine a thick slurry was formed and this hampered stirring. Furthermore, no leachate could be

11

generated at the end of the experiment and this was required in order to investigate the effect of carbonation on the brine composition.

Due to the complexity of the D-optimal model design, optimization of the input parameters was not carried out. This model had the advantage of allowing the input variables to be varied at different levels unlike the case with restrictive models such as the 2^k model designs. Chapter 5 however clearly depicts the statistical significance of all the main effects and the significant interactions arising thereof.

1.8 OUTLINE OF SUBSEQUENT CHAPTERS

This study contains five more chapters as outlined below;

Chapter Two: This chapter will include the literature review regarding the genesis and problems of FA, brine and CO_2 and disposal from power plants as well as their subsequent impact on the surrounding environment. An overview of carbon capture and sequestration technologies will be reviewed with an in-depth look at mineral carbonation as the target of this study.

Chapter Three: The sampling techniques, experimental approach and analytical methods applied in the study will be set out in this chapter.

Chapter Four: Chapter Four will describe the characterization of the un-carbonated fly ash and brine samples and their characteristics.

Chapter Five: The carbonation results and the characterization of the subsequent residues and leachates, the main trends and patterns observed will be discussed in detail with regard to the research questions posed in this study.

Chapter Six: This chapter will summarize and discuss the findings from this study and tie it to the literature, drawing similarities, anomalies and giving possible reasons for them. From the observations, recommendations will be given for further research to generate answers to some of the questions that this study was not able to answer.

CHAPTER TWO

LITERATURE REVIEW

2.1 INTRODUCTION

The development level of a country is directly related to its economic and social development. One of the most important factors that plays an active role in achieving such development is energy. Energy can only be an impulsive force in industrialization and overall sustainable development of societies if it is supplied on time, in sufficient quantity, under reliable economic conditions with consideration and mitigation of the environmental impacts. The demand for energy increases rapidly in parallel with the population increase, industrialization and technological developments in developing countries in the world (Tunç et al., 2007).

Fossil fuel combustion provides more than 85 % of the world's energy needs with coal combustion accounting for 40 %. Coal combustion leads to emission of carbon dioxide which is a major contributor to environmental pollution. It is well known that CO_2 is the major green house gas (GHG) contributing 50 % of the total effect, followed by CH_4 and other contributors. Of all the GHG emissions, 50 % is derived from CO_2, with 73 % coming from fossil fuel utilization, 25 % from deforestation and 2 % from the cement industry (Lemos de Sousa et al., 2008).

South Africa's indigenous energy resource base is dominated by coal. Over 93 % of South Africa's primary energy needs are provided by coal (www.eskom.co.za). This is unlikely to change significantly in the next two decades owing to the relative lack of suitable alternatives to coal as an energy source. Many of the deposits can be exploited at extremely favourable costs and, as a result, a large coal-mining industry has developed. In addition to the extensive use of coal in the domestic economy, about 28 % of South Africa's coal production is exported, mainly through the Richards Bay Coal Terminal, making South Africa the fourth-largest coal exporting country in the world. South Africa's coal is obtained from

collieries that range from among the largest in the world to small-scale producers. As a result of new entrants, operating collieries increased to 64 during 2004. Of these, a relatively small number of large-scale producers supply coal primarily to electricity and synthetic fuel producers. (www.dme.gov.za/energy/coal.stm).

Sasol, the biggest local company listed on the Johannesburg Stock Exchange (JSE), produces synthetic fuels from low-grade coal and a small amount from natural gas. It operates the world's only coal-based synthetic fuels facility, and produces 36 % of liquid fuels consumed in South Africa. Sasol produces automotive fuels for consumers, premium fuels and lubricants for industry, as well as jet fuel, fuel alcohol and illuminating kerosene. It also converts natural gas to fuels and chemicals. (www.southafrica.info/doing_business/economy/infrastructure/energy.htm)

Eskom, the South African electricity supplying company operates a number of power plants within the Mpumalanga province where coal is utilized to generate electricity for both the local grid and for export. Both these companies therefore are faced with remediating the environmental impacts of coal combustion by-products as well as reducing CO_2 emissions to the environment.

2.2 FLY ASH

2.2.1 Generation and global recycling trends

Coal is composed of combustible organic matter with a variable amount of inorganic mineral matter. The coal combustion process produces solid coal utilization by-products (CUB's) from the non-combustible portion of the coal. These include FA, bottom ash, flue gas desulphurization (FGD) products and fluidized bed boiler (FBB) waste. In general, depending on the type of coal particle size and combustion conditions, 5 - 15 % of the coal remains as ash of which 3-10 % is unburnt organic material. However the ash content of South African coal, is much higher with a value of 40 %. The coal ash is subdivided into FA and bottom ash of which the former accounts for about 90 % by weight of the ash (Grossman and Nathan 1988). During combustion the mineral matter in coal is thermally altered into different minerals. The mineral constituents of the fired coal responsible for this chemical composition is comprised of the clay minerals,

illite ($[OH]K_2[Si_6Al_2]Al_4O_{20}$) and kaolinite ($[OH]_8Si_4Al_4O_{10}$); sulfides (such as pyrite cubic FeS_2 and marcasite orthorhombic FeS_2); carbonates like dolomite ($CaCO_3.MgCO_3$), ankerite ($2CaCO_3.MgCO_3.FeCO_3$), calcite ($CaCO_3$) and siderite ($FeCO_3$); quartz (SiO_2) and apatite ($Ca(PO_4)_3F$ (McCarthy et al., 1999, Lederman et al., 2003). At the furnace operating temperatures (typically in the range of 1400 – 16000 ºC) (Kutchko and Kim, 2006) the mineral matter within the coal may oxidize, decompose, fuse, disintegrate or agglomerate. Rapid cooling in the post-combustion zone results in the formation of spherical, amorphous (non-crystalline) particles. Expansion of trapped volatile matter can cause the particle to expand to form a hollow cenosphere. Minerals with high melting points may remain relatively unchanged. The heating and cooling have a significant effect on the composition and morphology of each particle (Kutchko and Kim, 2006). Larger particles of ash, called coarse ash, which make up the rest of the ash produced at the power station, drop down from the furnace and collect at the bottom in the ash hopper of the boiler. The lighter fraction termed FA is carried away from the boiler by the hot combustion gases and is separated from flue gas by electrostatic precipitators or bag filters. The resulting physical properties of the coal FA, such as moisture content, particle mass, glass composition and the proportion of unburned carbon are dependent on coal properties, the combustion temperature of the coal, the air flow, fuel ratio, coal pulverization size and rate of combustion (Nathan et al., 1999). FA particles range in size from 0.5 - 200 microns, have a hydrophilic surface and are extremely porous.

Coal combustion in power plants provides approximately 40 % of the world's electricity with the United States of America (USA) and China leading in the consumption of coal. According to He et al., (2006), coal accounts for 65 % of total primary energy consumption in China. USA on the other hand generates 51.7 % of its electricity from coal combustion according to Klass (2003). Worldwide currently, China is the largest producer of FA followed by Russia and the United States. The European Coal Combustion Products Association (ECOBA) member countries account for 90 % CUB's in Europe, producing 37.14 million tons of FA and utilizing about 48 % of it. In India Sushil and Batra (2006) reported that the major portion of FA produced is disposed in ash ponds and landfills while only 13

% is utilized. In South Africa, the quantity of FA generated per annum by Eskom power plants was estimated to be over 20 million tons (Eskom, 2001) and only about 5 % of it is utilized while the remaining is disposed of in ash dumps.

2.2.2 Physical, chemical and mineralogical characteristics of fly ash

FA is a fine residue composed primarily of spherical micron sized particles collected from dust collection systems after coal combustion. FA can be regarded as containing three different types of constituents; crystalline minerals (quartz, mullite, spinel etc), unburnt carbon particles and non-crystalline aluminosilicates glass. Fly ashes are classified by American Society for Testing and Materials (ASTM) into class F or C by their aggregate alumina, silica and ferric oxide contents. The distinction between class F and C is based on the sum of $SiO_2+Al_2O_3+Fe_2O_3$ in the FA. When the sum total is greater than 70 % the ash is classified as class F. When the sum is between 50 % and 70 % the ash is classified as class C (ASTM 618, 1993). Class C is also characterized by a higher lime content (between 20-30 %) compared to class F with a lime content of less than 10 %. South African FA is classified as class F.

Table 2.1: ASTM standards classification of fly ash (ASTM 618, 1993).

	Class F	Class C
$SiO_2 + Al_2O_3 + Fe_2O_3$, min %	70.0	50.0
SO_3, max %	5.0	5.0
CaO %	<10	>20
Moisture content, max %	3.0	3.0
LOI, max %	6.0	6.0
Available alkalis as Na2O, max %	1.5	1.5

All coal in a conventional utility boiler produces glasses and neoformed high temperature minerals comprising of aluminosilicates and oxides of iron that encompass other elements in minor and trace quantities that are possibly partitioned within them. In FA the glass occurs mainly as spherical dark globules in the matrix, whereas in the bottom ash, it has a massive smooth or frothy

appearance which has a dark colour. An appreciable amount of the coal FA is composed of hollow spheres known as "cenospheres" which are filled with CO_2 or N_2 and give FA its light weight characteristics. Cenospheres vary in size from 20-200 microns and can compose up to 20 % by volume of the ash (Nathan et al., 1999). The principal property of these spheres is that they are pozzolanic; this characteristic gives FA the cementitious behavior so that the pulverized coal FA represents a chemical reactivity that is directly correlated to the calcium content of the ash (Nathan et al., 1999).

The glass has two distinct types of colour shades (light and dark) and can either be spherical in shape or massive in appearance. The glass that has more iron is slightly lighter in shade as the shadow of iron oxide needles or dendrite patterns emerge from the lighter glass. Mullite is grainy, with low reflectance and occurs either within a sphere or within the matrix. Crystalline iron oxides occur mainly in the form of magnetite, hematite and ferrite spinel. The magnetite is whitish and occurs in at least three forms (euhedral crystals, dendritic and needle like or small grains). The dendritic form of ferrite spinel is observed to have originated from iron rich glass. Hematite has lower reflectance than magnetite which is slightly grayish white. Organic matter occurs mainly as char with a viscous flow pattern and abundant vesicles of various sizes. This phase is common in bottom ash. Quartz in both bottom ash and FA occurs either as discreet detrital grains (not affected in the combustion) or as fused silica that has a fuzzy appearance. The glassy spheres contain Si, Al, K, Ti and Fe and are of a darker shade compared to the iron rich spheres (mostly ferrite spinel or magnetite and some hematite) (Querol and Pires, 2004). The glass phase in ash is usually the main constituent involved in chemical reactions associated with ash utilization in the cement and concrete industry or in geopolymer and zeolite production. It also appears to be a major host within the ash for adsorbed trace elements, which may be loosely held to the glass surfaces and thus have significant potential for release into the surrounding environment. Glass in natural volcanic rocks is relatively unstable during chemical weathering and glass in coal ash may also be expected to break down with prolonged exposure, a process that may further release elements into surrounding environmental systems (Ward and French, 2006).

2.2.3 Particle size distribution of fly ash

The particle size distribution and surface area of FA are important parameters that give preliminary information about the interactions between the ash and aqueous solutions. The size of a particle is important because its surface may act as a site for deposition/condensation of volatile elements such as Cd, As, Hg, Mo and Se. The smaller the particle diameter, the greater the surface area relative to volume available for the adsorption of liquid and gaseous materials. According to Goodarzi, (2006), the particles of FA consist of three fractions, $PM_{>10}$, PM_{10} and $PM_{2.5}$. $PM_{>10}$ has particle size > 10μm while PM_{10} has particles of ≤ 10 μm. The $PM_{2.5}$ particles are ≤ 2.5 μm and have a bimodal size fraction with mean diameters of 0.05μm and 2.50 μm. Volatile elements are commonly enriched on the surfaces of these particles. Particle size distribution analyses of the South African and Colombian FA were carried out by Foner et al., (1999). They showed that 80 wt % of the South African and 75 wt % of the Colombian FA particles studied were found in fractions lower than 45 μm. Free lime in the South African ash was also found to be abundant in the small grain size-fractions. Several studies affirm that the most salient features of FA are the gradation effects of particle size on elemental concentration. Klein et al., (1995); Kaakinen et al., (1975); Davison et al., (1974), observed that As, Cd, Cu, Ga, Mo, Pb, S, Sb, Se, Tl and Zn tend to increase in concentration with decreasing FA particle size. Bosch (1990) investigated FA from some South African coal burning power stations and noted that there was a tendency for a higher concentration of trace elements in the FA to be associated with the smaller sized particles.

The most volatile elements which are the last to condense are partitioned to the smaller particles. Eary et al., (1990) observed that chalcophillic elements (As, Cd, Cu, Pb, Hg, Se, V and Zn) which tend to be present as sulphide minerals or associated with the organic fraction in coal, are generally more strongly volatilized during combustion and tend to become more enriched on particle surfaces than elements associated with silicate and oxide minerals in coal. The less volatile elements (Al, Ba, Ca, Ce, Co, Eu, Fe, Hf, La, Mg, Mn, Rb, Sc, Si, Sm, Sr, Ta, Th and Ti) on the other hand, show little tendancy to partition according to particle size. There are also elements such as Be, Cr, K, Na, Ni, and

U that exhibit an intermediate behavior. Other researchers such as Campbell et al., (1978); Lee et al., (1975) reported similar effects of particle size on elemental concentrations.

2.2.4 Ash Disposal

According to Sushil and Batra (2006), there are two different methods of FA disposal utilized by power stations in India. These are wet and dry disposal methods. In the wet disposal method, FA particles are collected by the precipitators before transportation to the ash ponds as a wet slurry. One of the power stations was reported to be using a 100 % dry ash extraction system and the ash is disposed and stored in the form of ash mounds after which it is sprayed with a polymer layer and vegetation is grown on top of it. Coal-fired power plants in the former Yugoslavia produce approximately 5 Mt of ash per year with 20 Kt being used in the cement industry and for production of paving slabs, building blocks and ready mixed concrete. The remaining ash is disposed in ash depositories (Ilic et al., 2003; Iyer, 2002). The large volume of unused FA is disposed in most cases to holding ponds, landfills and slag heaps (Iyer, 2002).

According to Foner et al., (1999), Israel used to dispose FA generated from power stations by dumping at sea and stockpiling in embankments around the power stations but this was stopped due to legislation prohibiting such disposal. Indiscriminate disposal of FA could have a negative effect on the environment through weathering and through leaching of the major and trace elements from the ash matrix, though this can be controlled to some extent by the practice of adequate water disposal techniques. If the FA is to be dry-land filled, it is often conditioned by adding only about 20 % water to avoid dust during transportation and dumping. Compaction of the ash and the formation of a pozzolanic crust also helps to limit leaching as a wetting front must first penetrate through a mass of dry ash before the underlying groundwater can be contaminated. Continuous rehabilitation of dry ash dumps is becoming common practice and involves covering the ash with a layer of soil and establishing suitable vegetation (Carlson and Adriano, 1993) further limiting leaching. For wet ash deposits, ash is slurried

19

with effluent water and piped to the ash dam where the ash particles settle to the bottom of the dam and the effluent is either discharged to receiving waters or pumped back to the power station for reuse (Carlson and Adriano, 1993).

South African power utilities also employ two different methods of disposal; dry disposal and dense slurry disposal. In Sasol's Secunda power station, the ash from hoppers is added to a stirred tank with continuous water addition to give a slurry with controlled density. This is then pumped continuously via pipes to the ash dam where the ash particles immediately settle out and the ash-water is either drained away via a penstock to the clear ash effluent dam, or percolates through the ash dump and is collected in a toe drain (Buhrmann et al., 1999). The ash water goes to the clear ash effluent dam, where it mixes with other wastewaters and after settling is pumped back for treatment using reverse osmosis (RO) and electro dialysis reversal (EDR) and the waste product (the salt laden concentrate) from these treatment processes is again used for hydraulic transport of more ash from the hoppers. In Eskom's Tutuka power station, the FA from the precipitators is moistened with brine (about 12 % - 16 % moisture content) before being transported to the ash dumps via a conveyor belt for disposal. The main disadvantage of this method is the possible dispersion of the fine particles by wind. Hence at the dumps, the ash is further irrigated with brine to keep it moist for dust control. One of the ways to ameliorate the negative impact of ash disposal would be rehabilitation of the ash-holding ponds by re-vegetation as is practiced in Tutuka. Other than Tutuka, Eskom has wet slurried power plants such as Kragbron, Komati and Grootvlei that are no longer operational.

2.2.5 Environmental impacts of fly ash

FA is considered hazardous to the environment due to possible release of the toxic elements contained in its matrix. The elements can cause air, surface water as well as ground water pollution. Air pollution results from emissions such as SO_2, NO_x and CO_2 in flue gas generated during coal combustion as well as dust from the ash dumps (Jones, 1995). Disposal in ash dumps takes up useful arable land and can cause discharge of particulate ash directly into the nearby surface water system.

Groundwater contamination is most likely to occur when wet ashing systems are employed due to the very high liquid to solid ratios of 10:1 to 20:1 typically used in slurries, which result in large volumes of water, containing soluble components dissolved from the ash (Jones, 1995). There is thus the potential for immediate groundwater pollution by downward percolation of contaminated pore water especially if the underlying soil is highly permeable. In addition, wet ashing systems reduce the possibility of cementation reactions (Jones, 1995). The long storage of ash in ponds under wet conditions and humid climate can cause leaching of toxic metals from ash that contaminate the underlying soil and ultimately the ground water systems (Hansen et al., 2002).

Groundwater pollution can occur in two ways: a gradual seepage of the ash pore water from the base of the deposit or, alternatively, in the event of a substantial rainfall event, liner failure and a subsequent flush out of any accumulated salts. Groundwater contamination from dry ash deposits however would be due to gradual seepage once the moisture front reaches the base of the deposit. Figure 2 shows the aqueous input and output streams around wet and dry ash deposits.
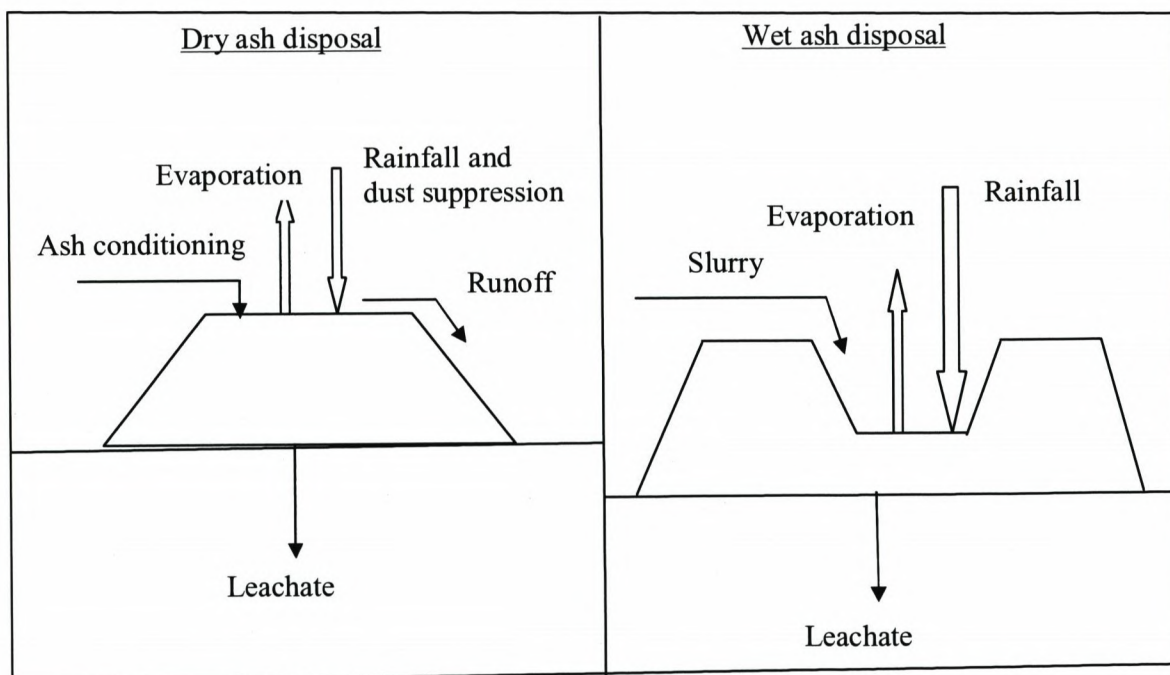
Figure 2.1: Aqueous input and output streams around wet and dry ash deposits (Adapted from Hansen et al., 2002)

The most notable feature of ash leachates is the extreme pH range, which can vary from 4.5 to 12. The pH of ash leachate determines the solubilities of the various trace metals concentrated on the surface of the ash particles. Most leachates also display relatively high soluble salt concentrations, usually with Ca^{2+} and SO_4^{2-} as the dominant cation and anion, respectively (Carlson and Adriano, 1993). The composition of leachate is also dependent on the quality of the water used for sluicing in wet disposal, and, to a lesser extent, on ash conditioning and dust suppression in dry disposal (Jones, 1995). The water used for these purposes is usually process water from the power station water circuit, which is typically high in dissolved salts (Notten, 2001).

The chosen ash disposal management method has a dominant effect on leachate composition and subsequent environmental performance. Environmental effects of FA are best exemplified in its application in soils and its effects on plants. Field and greenhouse studies have indicated that many chemical constituents of FA may benefit plant growth and improve agronomic properties of the soil (Chang et al., 1977). The effects on plants are primarily due to a shifted chemical equilibrium induced by the FA addition to soils. The concentrations of S, Mo, B in plant tissues have been shown to increase consistently with ash application to soil (Adriano et al., 1980). The increase in pH caused by ash application however leads to the deficiency of Mn, Zn, Cu, and Fe. Mo and Se form anionic species in fly ash amended soils and their uptake by plants is increased tremendously. B levels are elevated in South African ash and B is considered a major limiting factor for successful cropland utilization of ashes due to its phytotoxic effects. Se concentration in plant tissues consistently increased with FA treatment and the rate of increase was found to be proportional to either the rates of application or the Se content of the applied fly ash (Furr et al., 1978). Several authors have also noted that when inhaled, particles of FA less than 1μm in diameter may be deposited in the pulmonary tissue of the respiratory tract and gain entry into the blood stream (Adriano et al., 1980).

2.2.6 Utilization of fly ash

Globally less than 25 % of the total amount of FA produced is utilized. In 1993, about 88 million tons of FA, bottom ash, boiler slag and FGD residues were generated in the United States. Overall only 22 % of these solids were used for beneficial purposes (Gurdeep and Bradley, 2001). In China the FA emitted by the thermal power plants is $\approx$ 160 Mt. At present over 50 % of FA produced in China is used in different purposes such as bricks manufacture, construction of dams and in the cement industry (Nikolaos et al., 2009). In countries like Germany, Belgium and the Netherlands more than 95 % of the FA produced during 1996 was used in the construction industry. In the UK, FA utilization was approximately 50 % during 1998 while in Israel approximately 65 % of the FA generated so far was used for cement production. In South Africa, Eskom the national electric utility produces over 22 million metric tons of FA annually with only a small fraction (5 %) being utilized in the cement and brick making industry, while the major portion still requires disposal. This is costly since the resultant FA dumps require dust control and ultimately rehabilitation and utilization technologies that can reduce disposal volumes would be of direct financial benefits (Reynolds et al., 1999). The potential application of FA results in three main advantages (i) Use of a zero-cost raw material, (ii) The conservation of natural resources (such as alumina in cement manufacture) and (iii) Elimination of waste.

2.2.6.1 Utilization of ash as construction materials

This section takes an in-depth look at some of the application niches for FA.

i) Cement and concrete production

Cement is a fine powder that hardens on mixing with water. Portland cement, one of the most common types is made from limestone ($CaCO_3$) mixed with clays and other materials containing alumina and silica. Some FA types contain 24-27 % of lime (class C) and some silicates and aluminosilicates (Mangialardi et al., 1999). These types could potentially be used for production of cement powder. In South Africa 50 % of the cement clinker is made up of FA (Kruger and Krueger, 2005). Cement production is an activity that consumes large quantities of raw materials

and energy and emits large amounts of CO_2 (due to the conversion of $CaCO_3$ to CaO) which is a major contributor to the greenhouse effect and global warming. A large percentage of the energy is spent in decomposing $CaCO_3$ to CaO. In fact, for each ton of cement produced approximately the same quantity of CO_2 is emitted. Use of FA as a source of lime would ensure a reduction in CO_2 emissions as this decomposition step could be eliminated. FA is eminently suitable for cement extension due to the following of its characteristics, it is spherical, pozzolanic, low in alkalis, non expansive, of consistent quality and reactivity and has a low carbon content. The effect of the aforementioned properties is that less water is required to make concrete. This results in less shrinkage (cracking), improved density and easier placing. The low carbon content means that mineral admixtures used to modify concrete behavior (delay setting, aid flow etc) are not affected by FA (Kruger and Krueger, 2005). The pozolanicity of the FA means that the ultimate strength of the concrete with ash exceeds that of Portland cement only concrete (Kruger and Krueger, 2005). FA further increases resistance to corrosion and ingress of corrosive liquids by reacting with calcium hydroxide in the cement to form a stable, cementitious compound of calcium silicate hydrate.

The less soluble calcium silicate hydrate reduces the possibility of calcium hydroxide leaching from concrete. The reaction products also lead to the filling of capillary voids in the concrete mixture, thereby reducing the permeability of the concrete (Halstead, 1986). The FA acts as tiny ball bearings and improves the workability of the concrete. Addition of FA, when used in the correct proportions, ultimately results in a greater strength concrete than straight portland cement (Halstead, 1986). The beneficial blending of FA with portland cement arises from the fact that hydration reactions of the cement generates portlandite, $Ca(OH)_2$ and other hydrates (Taylor,1998). The FA reacts with the portlandite to produce more of the cementitious hydrates and thus contributes to higher strength concrete. Portland cement consists of four main compounds which react with water, to form products involved in cementation reactions. The four reactants are tricalcium silicate (alite, Ca_3SiO_5), dicalcium silicate (belite, Ca_2SiO_4), tricalcium aluminate ($Ca_3Al_2O_6$) and tetracalcium aluminoferrite ($Ca_4Al_2Fe_2O_{10}$). The hydration reactions of portland cement to generate portlandite proceeds according to the following reactions (Taylor, 1998):

$$2\,Ca_3SiO_5 + 6H_2O \rightarrow Ca_3Si_2O_7.3H_2O + 3Ca(OH)_2 \quad\text{...(2.1)}$$

$$2CaSiO_4 + 4H_2O \rightarrow Ca_3Si_2O_7.3H_2O + Ca(OH)_2 \quad\text{...(2.2)}$$
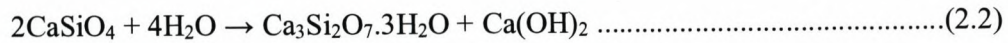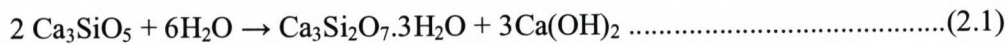
It is the portlandite from reactions (2.1) and (2.2) that reacts with fly ash to produce calcium silicate hydrate that adds more strength to the concrete.

ii) Utilization of ash for ceramics and glass production

The ceramic industry includes the manufacture of pottery and porcelain and building ceramics like bricks, tiles and stoneware. Ceramics are prepared from malleable earthy materials such as clay that are made rigid by high temperatures. Besides clays that confer cohesion and plasticity, ceramic pastes also include inert materials that provide structural support that helps to retain shape during drying and firing. Quartz is the most commonly inert used. Silica is also used in the glazing of ceramic bodies in combination with stiffeners and melting agents. When a glaze layer is applied to the ceramic body and then fired, the glaze ingredients melt and become glass-like. The ceramic industry is therefore a high consumer of silicate based materials and this makes it a potential candidate for FA application (Cioffi et al., 1994).

From a ceramic point of view, FA may be regarded as a pre-calcined non-plastic raw material similar to that used as chamotte (fragments of burnt fire-clay ground to powder and used with fresh fire-clay in making new vessels). Added to clay, it modifies the plasticity and consequently has a marked influence on the forming and drying of the ceramic mass. However the ceramic behaviour is very different from that of other non-plastics commonly used, such as sand or classical chamottes. The low silica content after firing reduces the possibility of cracking during rapid cooling; it also tends to act as a flux in clays and can result in a worthwhile reduction in firing temperatures (Queralt et al., 1997). A 20-30 wt % addition of FA increases the content of mullite and markedly improves the properties of stoneware products. The use of coal ash for glass-ceramic manufacture has also been investigated in recent years (Cioffi et al., 1994). Moreover, FA is presented as a fine dust so it can be directly incorporated into

ceramic pastes with almost no pre-treatment. One possible application for FA is to convert it to a glasslike substance by melting at high temperatures (above 1300 °C) a process called vitrification. Glass ceramics from FA are reported to have the following qualities; higher hardness, better workability, increased fracture toughness, strength and thermal shock resistance (Boccaccini et al., 1997). Potential applications for the resulting glass ceramics are floors of industrial buildings, outside and inside facing of walls and production of machine tool parts (Boccaccini et al., 1997).

2.2.6.2 Geotechnical applications of fly ash

i) Road pavement

Road pavement is a stratified multilayered structure consisting of a surface layer (made of bitumen or asphalt), a middle layer (base course and sub base) and the lowest layer (sub grade). The base course is the layer of material that lies immediately below the wearing surface of a pavement and has essentially a structural role. It consists of granular material (like stone fragments or slag) that can be stabilized with cementitious materials (cement, natural pozzolans etc). Between the base course and sub grade there is sometimes another layer called sub base which supports the base and is built with the same type of materials but is usually of inferior quality. FA application can be used as a substitute for sand and /or cement in cement stabilized bases and sub bases in road pavements (Mulder, 1996; Bolt et al., 1986).

ii) Embankments

Embankments are constructed from earth (soil) or stone materials and are used to keep back water (retaining walls, land reclamation etc). When soils do not present the desirable geotechnical properties it is common practice to stabilize them with lime or cement. This reduces soil compressibility and increases shear strength thus improving engineering properties. One potential application of FA is in soil stabilization as a substituent for lime or cement, taking advantage of FA pozzolanic characteristics (Tay et al., 1991; Show, 2003).

2.2.6.3 Agricultural applications of fly ash

The physical structure of FA often consists of cenospheres which show an increased surface area, capillary action and nutrient- holding capacity compared with sands (Fisher et al., 1976). FA is comprised primarily of fine sand- and silt-sized particles, therefore if applied at sufficient rates it can be used to change soil texture to increase soil water-holding capacity (Gangloff et al., 2000; Aitken et al., 1984; Adriano et al., 1980). Application of fertilizers to enrich soil and promote plant growth is a common practice. N, P and K are the three main elements commonly supplied in fertilizers while B, Cu and Mn are sometimes also added in small quantities. FA is rich in two out of three of these main nutrients; K and P, while N is lost during combustion. This means FA can potentially supply phosphorus and potassium replacing commercial fertilizers such as NPK. The fertilizer potential of municipal solid waste incineration (MSWI) FA was studied by Rosen et al., (1994) who found that plant growth in FA amended soils was 1.5 to 2 times greater than in non-amended soils and greater than in either phosphorus or potassium fertilizers amended soils.

Besides the fertilizing potential, FA could also be used in agriculture as a liming agent. Lime is often added to soil to reduce acidity. FA has high pH values and thus can substitute lime in reducing soil acidity. Rosen et al., (1994) confirmed the effectiveness of FA as a liming agent. Some elements like B, Cu, Mo and Zn are also essential plant nutrients and in certain quantities can even improve plant growth. However above a certain level they become phytotoxic. The addition of fly ash to the soil will increase its salt content due to the high levels of soluble salts present in the ash. These salts are of concern since they can induce salt stress in plants. Phytotoxicity due to high salinity is also reported (Glordano et al., 1983). Use of FA as a fertilizer and liming agent is however not large scale due to the small amounts that can effectively be applied to the soil because of nutrient balance and environmental concerns. The potential for using FA in agriculture depends on the specific crop and soil environment.

2.2.6.4 Other uses of fly ash

ii) Adsorbing materials

The use of adsorbing materials like activated carbon has been widespread for treatment of effluents. Another example is zeolites (mineral composed of hydrated aluminium silicates of alkali and alkaline earth metals) which are used in ion exchange processes such as water softening (Amrhein et al., 1996; Breck, 1984). Although natural zeolites occur in veins and cavities of basic igneous rocks, artificial zeolites from coal FA can be synthesized by hydrothermal treatment with NaOH (Mimura et al., 2001; Querol et al., 1997). These zeolites are environmentally safe but the effluents generated during synthesis contain high levels of metals such as Pb and Zn and the effluents thus must be treated before discharge. The zeolites can be used industrially as sorbents e.g. in removal of different ions and molecules from solution, waste water treatment to remove heavy metals form water, catalysis and as additives in detergents (Querol et al., 2002, Somerset et al., 2004).

ii) Sludge conditioning

Sludge originating from waste water treatment contains high amounts of water (up to 95 %) and needs to be dewatered to reduce the volume and disposal costs (Hwa and Jeyaseelan, 1997). Filtration is the most commonly used technique to dewater sludge. However waste water contains small amounts of oil that make dewatering difficult. To overcome this problem the sludge can be conditioned by the addition of filter aids. Use of FA as a chemical conditioner has been investigated by Hwa and Jeyaseelan (1997), their findings indicate that FA does facilitate the filtering process since it decreases both specific resistance and capillary suction time.

iii) Treatment of acid mine drainage (AMD)

Acid mine drainage (AMD) results from the reaction of pyrite with oxygen and water as follows:-

$$FeS_{2(s)} + 3.75O_2 + 3.5H_2O \rightarrow Fe(OH)_{3(s)} + 2SO_4^{2-} + 4H^+ \quad \text{.......................(2.3)}$$
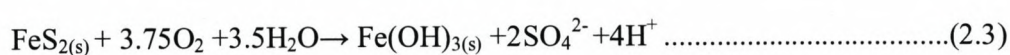
Due to the formation of SO_4^{2-} from elemental sulphur the pH of water decreases to acidic conditions (Gitari, 2006). As a result the pH of the water is lowered making it corrosive and unable to support many forms of aquatic life (Kimmel, 1993). Trace metals such as Zn, Cd and Cu present in AMD are toxic at extremely low concentrations and may act synergistically to suppress algal growth and affect fish and other marine life (Hoehn and Sizemore., 1995). Caustic materials such as hydrated lime ($Ca(OH)_2$, caustic soda (NaOH), ammonia (NH_3), pebble quick lime (CaO) and soda ash (Na_2CO_3) have been used to raise the AMD's pH (Robb and Robinson,1995). FA is a cheap and widely available source of lime and thus can be used in AMD remediation without additional use of liming agents or the standard water purification chemicals thus achieving water purification by co-disposal of two hazardous wastes (Petrik et al., 2003; Somerset et al, 2004). Moreover the sludges formed from the reaction of AMD and FA can be used to make high capacity zeolitic adsorbents.

2.3 BRINES

2.3.1 Introduction

Water is one of the most abundant resources on earth, covering three quarters of the planet's surface. However about 97 % of the earth's water is salt water in the oceans and only 3 % is fresh water (Peters et al., 2008). This small percentage of the earth's water, which supplies most of human and animal needs, exists in ground water, lakes and rivers. The only nearly inexhaustible sources of water are the oceans which however are of high salinity. It would be feasible to address the water shortage problem with sea water desalination, however the separation of saline constituents out of water requires large amounts of energy, which when produced from fossil fuels, can cause harm to the environment. On a global scale, manmade pollution of natural sources of water is becoming one of the largest causes for fresh water shortages. Added to this is the problem of uneven distribution e.g. Canada has a tenth of the world's surface fresh water but less than 1 % of its population (Le Dirach et al., 2005). Of the total water consumption worldwide, about 70 % is used by agriculture, 20 % is used by industry and only 10 % for household needs.

Brines are waters saturated or nearly saturated with salt and are commonly considered to be those waters more concentrated in dissolved materials than sea water (35 g of dissolved constituents per kg of sea water). Natural brines are waters with an extremely high concentration of dissolved constituents- elements, ions and molecules. They are commonly found at depth in the earth but they also are found at the earth's surface, most notably as a by-product of oil and gas test wells and production wells, hence they are known as oil-field brines. Owing to the high concentration of dissolved components such as Na and Mg, natural brines are of commercial interest especially in production of table salt. Subsurface caverns (especially those used for the mining of table salt), saline lakes (e.g. the Great Salt Lake (Utah, USA), the Dead Sea (Israel), and the Salton Sea (California, USA) and the saltwater ocean are three principal natural sources of brine. Brine can contain salt concentration more than five times greater than the salt content of average sea water. At 60 °F (15.5 °C) saturated brine is 26.4 % salt by weight, at 0 °C (32 °F) brine can only hold 23.3 % salt (Petrik et al., 2007).

Desalination involves the removal of salt constituents from sea water or from saline water to a usable level. All desalination processes involve three liquid streams: the saline feed water (brackish water or seawater), low-salinity product water, and very saline concentrate (brine or reject water). The saline feed water is drawn from oceanic or underground sources or can originate from human activities. It is separated by the desalination process into the two output streams: the low-salinity product water, and very saline concentrate streams. Although some substances that are dissolved in water, such as $CaCO_3$, can be removed by chemical treatment, other common constituents, like NaCl, require more technically sophisticated methods, collectively known as desalination (El-Manharawy and Hafezb, 2003). According to the World Health Organization (WHO), the permissible limit of salinity is 500 ppm and for special cases up to 1000 ppm. Most of the water available on earth has salinity of up to 10,000 ppm and sea water normally has salinity in the range of 35,000- 45,000 ppm in the form of total dissolved salts (Tiwari et al., 2003). Excess brackishness causes problems such as taste, stomach ailments and laxative effects. The purpose of

30

desalination therefore is to clean or purify brackish water or sea water and supply water with dissolved salts within the permissible limit of 500 ppm or less.

2.3.2 Desalination Technologies

In water recycling the treatment objectives include; minimizing volume of waste for disposal, achieving a zero liquid discharge, reducing total dissolved solids, achieving high quality water for reuse and minimizing capital and operating costs. Desalination can be achieved by using a number of techniques. Industrial desalination technologies use either phase change or involve semi-permeable membranes to separate the solvent or some solutes. All processes require a chemical pre-treatment of raw seawater to avoid scaling, foaming, corrosion, biological growth and fouling and also require a chemical post treatment (Parekh et al., 2003).

Phase change processes include multi-stage flash (MSF) and multiple effects boiling (MEB), while membrane processes include both pressure-driven processes and electrically-driven processes. Pressure driven processes include microfiltration (MF), ultrafiltration (UF), nanofiltration (NF) and reverse osmosis (RO) while electrically driven processes include electrodialysis reversal (EDR) and electrodeionization (EDI) vapour compression (VC), freezing, humidification/dehumidification and solar stills (Abufayed and Ghuel., 2001).

Multi-stage flash (MSF) and multiple effect boiling (MEB) processes consist of a set of stages successively decreasing temperature and pressure. MSF process is based on the generation of vapour from seawater or brine due to a sudden pressure reduction when seawater enters an evacuated chamber (Kalogirou, 2005). The process is repeated stage by stage at successively decreasing pressure. This process requires an external steam supply, normally at a temperature of about 100 °C. The maximum temperature is limited by the salt concentration to avoid scaling and this maximum limits the performance of the process. In MEB, vapours are generated due to the absorption of thermal energy by the seawater. The steam generated in one stage is able to heat the salt solution in the next stage because the next stage is at a lower temperature and pressure (Parekh et al., 2003). In thermal

vapour compressor (TVC) and mechanical vapour compressor (MVC), after initial vapour is generated from the saline solution, this vapour is thermally or mechanically compressed to generate additional vapour (Bouchekima, 2001).

The conversion of saline water to fresh water by freezing has always existed in nature and has been known to man for thousands of years. Desalination of water by freezing is a separation process related to the solid-liquid phase change phenomenon. When the temperature of saline water is reduced to its freezing point, which is a function of salinity, ice crystals of pure water are formed within the salt solution (Lewis et al., 2009) a phenomenon known as eutectic freeze crystallization. These ice crystals can be mechanically separated from the concentrated solution, washed and re-melted to obtain pure water (Safi et al., 1999).

Humidification/dehumidification processes are based on the fact that air can be mixed with large quantities of water vapour. Additionally, the vapour carrying capability of air increases with temperature (Bourouni et al., 2001). In this process, sea water is added into an air stream to increase its humidity. Then this humid air is directed to a cooling coil on the surface of which water vapour contained in the air is condensed and collected as fresh water.

Reverse osmosis (RO) and Electro-dialysis reversal (EDR) do not involve phase change but rather use of membranes. EDR process utilizes a direct current electric field to remove salt ions in the brackish water. According to Turek and Bandura, (2007), EDR is the desalination technique commonly known to be least sensitive to inorganic scaling compared to other techniques. EDR achieves relatively high water recovery levels and consequently high calcium suphate and calcium carbonate rich concentrates as wastes.

In EDR, an electric current migrates dissolved salt ions, including fluorides, nitrates and sulfates through an electro dialysis stack consisting of alternating layers of cationic and anionic exchange membranes. Periodically, the direction of ion flow is reversed by reversing the polarity of the applied electric current. Saline feed water containing dissolved salts is separated into positively charged sodium

and negatively charged chloride ions. These ions will move towards an oppositely charged electrode immersed in the solution i.e. cations move to the cathode while anions move to the anode (Shaffer et al., 1980). A large number of alternating cation and anion membranes are stacked together, separated by plastic flow spacers that allow the passage of water. The streams of alternating flow spacers are a sequence of diluted and concentrated water which flows in parallel to each other. To prevent scaling, inverters are used which reverse the polarity of the electric field every 20 minutes (Safi et al., 1999). Since energy requirements are proportional to the water's salinity, EDR is more feasible when the salinity of the feed water is not more than 6000 ppm of total dissolved salts. Similarly due to the low conductivity which increases the energy requirements of very pure water, the process is not suitable for water of less than about 400 ppm dissolved salts (Bouchekima et al., 2001).

In the RO process, water from a pressurized saline solution is separated from the dissolved salts by flowing through a water-permeable membrane. The permeate (the liquid flowing through the membrane) is encouraged to flow through the membrane by the pressure differential created between the pressurized feed water and the product water, which is at near-atmospheric pressure. The remaining feed water continues through the pressurized side of the reactor as brine. No heating or phase change takes place. The major energy requirement is for achieving the initial pressurization of the feed water. For brackish water desalination the operating pressures range from 250 to 400 psi, and for seawater desalination from 800 to 1 000 psi. In practice, the feed water is pumped into a closed container, against the membrane, to pressurize it. As the product water passes through the membrane, the remaining feed water and brine solution becomes more and more concentrated. To reduce the concentration of dissolved salts remaining, a portion of this concentrated feed water-brine solution is withdrawn from the container. Without this discharge, the concentration of dissolved salts in the feed water would continue to increase, requiring ever-increasing energy inputs to overcome the naturally increased osmotic pressure (Bouchekima et al., 2001).

A reverse osmosis system consists of four major processes: (1) pretreatment, (2) pressurization, (3) membrane separation, and (4) post-treatment stabilization.

Pretreatment involves removal of suspended solids, adjusting the pH, and adding a threshold inhibitor to control scaling caused by constituents such as calcium sulphates. In pressurization the pressure of the pretreated feed water is raised to an operating pressure appropriate for the membrane and the salinity of the feed water. The permeable membranes inhibit the passage of dissolved salts while permitting the desalinated product water to pass through. Applying feed water to the membrane assembly results in a freshwater product stream and a concentrated brine reject stream (Safi et al., 1999). Because no membrane is perfect in its rejection of dissolved salts, a small percentage of salt passes through the membrane and remains in the product water.

Reverse osmosis membranes come in a variety of configurations. Two of the most popular are spiral wound and hollow fiber membranes. They are generally made of cellulose acetate, aromatic polyamides, or, nowadays, thin film polymer composites. Both types are used for brackish water and seawater desalination, although the specific membrane and the construction of the pressure vessel vary according to the different operating pressures used for the two types of feed water (Shaffer et al., 1980). The product water from the membrane assembly is then stabilized through pH adjustment and degasification before being transferred to the distribution system for use as drinking water. The product passes through an aeration column in which the pH is elevated from a value of approximately 5 to a value close to 7. In many cases, this water is discharged to a storage cistern for later use.

The feed water to Tutuka power plant in the Mpumalanga Province of South Africa uses a combination of 50 % mine water and 50 % cooling water as its feed. The combined water is saline with maximum conductivity of 5500 S/cm. The main contaminants present in these waters are listed in Table 2.2 below.

Table 2.2: Main contaminants in Tutuka feed waters (Adopted from Buhrmann et al., 1999)

Ion	Concentration
Calcium, (ppm)	300
Magnesium, (ppm)	200
Sodium, (ppm)	1100
Chloride, (ppm)	700
Aluminium, (ppm)	400
Sulphate, (ppm)	1500
Copper, (ppm)	500
Iron, (ppm)	500
Barium, (ppb)	90

Since the mine water is first stored in an open dam and the cooling cycle provides ideal conditions for organic growth, the organic content of the water is naturally high, with total organic content (TOC) up to 65 ppm. At Tutuka the combined mine/cooling water is supplied to a clarifier for softening by the addition of lime as well as the removal of turbidity with the aid of flocculants and coagulants. A 50 % reduction in alkalinity and 93 % reduction in turbidity is achieved. The clarifier overflow is subjected to pH control by the addition of HCl, followed by gas chlorination to control biological activity in the downstream sand filters. Suspended solids are removed in a battery of pressure sand filters where turbidity is reduced to below 2 Nephelometric Turbidity Units (NTU). A final set of 5 m cartridge filters situated directly before the RO unit serves as a safety barrier in order to prevent solids contamination of the membranes. The RO plant is composed of three identical modular units in order to ensure a minimum of 66 % capacity at all times. Each unit is equipped with a high pressure feed pump and operates independently. Permeate (product) from the three units is combined in a single product tank from where it is returned to the power station cooling circuit. Brine (waste) from the units is concentrated further by means of two vacuum condensers before disposal on the ash heaps (Buhrmann et al., 1999).

Sasol Synfuels (Secunda) utilizes large quantities of water to produce steam for gasification, process heating, electricity generation and for general process cooling. Both EDR and RO are utilized since RO can produce the high water quality while EDR can achieve the high water recovery required at Sasol. The membrane desalination facility consists of a clariflocculator (clarifier, reaction

zone and flocculation chamber built in one unit), sand filters, a 6,800 m^3/day RO system and a 7,600 m^3/day EDR system (Persechino and Gottberg, 2001). After the water is pretreated, it is fed to the EDR facility. The EDR acts as a roughing demineralizer to remove most of the minerals. The EDR product is then fed to the RO system. The RO plant produces water that is sent directly to the boiler water treatment plant for final polishing. The RO concentrate is returned to the EDR as a concentrate makeup which the EDR process concentrates further. This integrated membrane system allows Sasol to achieve 70 % water recovery while producing water with 20 ppm TDS, ten times better than their raw water intake (Persechino and Gottberg, 2001).

2.3.3 Disposal

Desalination technologies such as RO processes have increasingly been adopted to produce fresh water from alternative sources such as sea water and brackish water due to water scarcity. However, desalination applications have always been limited by the disposal costs of the produced concentrated waste brine. In coastal regions, brine can possibly be discharged into the ocean, but this is not feasible for inland areas. For inland desalination plants, various treatment options are currently being used to concentrate the brines as much as possible in order to reduce the volume prior to disposal (Buckley et al., 1987). The major strategies for brine disposal at inland sites are limited to three general categories namely; deep well injection, evaporation ponds and solar ponds (Ahmed et al., 2001). Several other systems for utilization of brine have been proposed which include among others irrigation of salt tolerant plants (halophytes) and brine shrimp farming (Rhee et al., 1993).

Zero discharge effluent which involves concentration of the effluents to form crystallized salts has also been used in certain situations where brine streams are relatively large and available land is limited. This technology has generally been applied to waste water disposal from power plants, oil refineries and some mining operations (Saripalli et al., 2000). Deep well injection is considered the most cost effective when compared with other systems in practice for inland based

desalination plants. Drawbacks to this technology are selection of a suitable well site, costs involved in conditioning the waste water, possibility of corrosion and subsequent leakage in the well casing, seismic activity which could cause damage to the well and subsequently result in ground water contamination as well as the uncertainty in the estimation of the well's half life (Ahmed et al., 2001).

Evaporation ponds are applied primarily in regions with low rainfall and where climatic conditions are favourable for steady and relatively rapid evaporation rates. This is widely practiced in the Middle East and to a lesser extent in arid regions of Australia (El Saie et al., 2002). The principal environmental concern associated with evaporation pond disposal is pond leakage which may result in subsequent aquifer contamination. On the other hand it could lead to resource recovery measures such as aquaculture, brine shrimp farming and salt production (Ahmed et al., 2001). Though the application is a relatively simple and straight forward method, this technology is however limited to relatively small desalination plants and generally restricted to arid climatic conditions (Ahmed et al., 2001). Mickley et al., (1993) identified the factors that influence the selection of a disposal method. These include volume or quantity of concentrate, quality of constituents of concentrate, physical or geographical location of the discharge point of the concentrate, availability of receiving site, permissibility of the option, public acceptance, capital and operating costs, and ability for the facility to be expanded.

2.4 FLY ASH/BRINE INTERACTIONS

FA and brine co-disposal is widely used to moisten the ash and to encapsulate the brine components within the ash matrix. According to Ecke et al., (2003), the alkalinity in FA, primarily present as CaO, is used to neutralize brine. Direct mixing of various ratios of brine and FA to a predetermined pH in the co-disposal scenario enhances the formation of gypsum and soil components in ash residues (Mooketsi et al., 2007). Precipitation of aluminosilicates and metal hydroxides as well as iron compounds occurs at a pH of 10. Desalination or evaporation brines could be contacted with coal ash, possibly resulting in the irreversible retention of

the brine species into the coal ash mineral matter, resulting in an environmentally safe brine disposal option (Ecke et al., 2003).

Mooketsi et al., (2007) suggested that brine treated residues have elevated leachate electrical conductivity and Na, K, Ca, Cl and SO_4 concentration as compared to untreated ash residues due to the applied brine. They further postulated that the lime in FA improves the leachate quality in terms of the overall TDS as well as the electrical conductivity, and Cl and SO_4 content. The decrease in the SO_4 concentration observed is a result of reaction between the sulphates species present in brine and lime to form insoluble $CaSO_4$. This reaction consumes the SO_4 thus reducing the labile form of S species such as Na_2SO_4 in the brine. They concluded that most of the brine species like Na, Cl and SO_4 could be stabilized within the ash matrix.

2.5 CARBON DIOXIDE

The term "global warming" refers to the measured increase in the earth's average temperature. This is caused by the buildup of key green house gases in the atmosphere accumulated from continual combustion of fossil fuels and land use changes over the 20th century (Weubles and Jain, 2001). The difference between the incoming radiation energy and the outgoing radiation (also known as radiative forcing) is investigated by using global climate models (GCMs) that represent the interaction of the atmosphere, land masses, oceans and ice-sheets. By predicting how the global climate will respond to various perturbations, projections can be made to determine how global climate will change under different conditions. Under the six illustrative emission scenarios used by the International Panel on Climate Control (IPCC), CO_2 levels are predicted to increase over the next century from 369 ppm to between 540-970 ppm (Nakicenovic and Swart, 2000).

This translates to an increase in global average temperatures of between 1.4 and 5.8 °C (Watson, 2001) in turn leading to an increase in extreme weather events and a rise in sea levels. The USA current emissions of 6000 million tons per year are projected to increase to 8000 million tons per year by 2030 due to increased

consumption of fossil fuels (coal, petroleum and natural gas). The Energy Information Administration (EIA) within the Department of Energy (DOE) estimates that the combined CO_2 emissions from China and India in 2030 from coal use will be three times that of the USA (China 8286 Mt of CO_2, India 1371 Mt of CO_2, USA 3226 Mt of CO_2) (Figueroa et al., 2008). According to the Netherlands Environmental Assessment Agency, China's 2006 CO_2 emissions surpassed those of the USA by 8 %. China tops the list of CO_2 emitting countries for the first time since in 2005, CO_2 emissions of China were still 2 % below those of the USA. The European Union with a volume of emissions about half that of China, occupies the 3rd position followed by Russia, India and Japan respectively. According to Engelbrecht and co-authors, (2004), South Africa produces over 427 Mt/a of CO_2 as demonstrated in Table 2.3. Sequestrable emissions are from point sources and it is potentially possible to capture the CO_2. Non-sequestrable emissions are spread over a large area and it is not possible to capture the CO_2.

Table 2.3 : 2000 CO_2 emissions by industry sector in South Africa (Engelbrecht et al., 2004)

Sequestrable CO_2		Amount (Mt/a)	%
Electricity production		161	65
Industrial processes		28	11
Other energy		30	12
Manufacturing		30	12
	Total	249	100
Non sequestrable			
Waste		10	6
Agriculture		48	27
Fugitive		42	24
Transport		40	22
Heat production		37	21
	Total	178	100
TOTAL		427	

Table 2.3: CO_2 emissions from Eskom power stations (Engelbrecht et al., 2004).

Power station	Location	Power output (MW)	CO_2 emitted (Mt/a)	CO_2 conc. (%)
Hendrina	Hendrina	1338	11	12-15
Arnot	Middleburg	1104	9	12-15
Kriel	Leandra/Secunda	1992	15	12-15
Matla	Leandra/Secunda	2877	22	12-15
Duvha	Witbank	2601	19	12-15
Lethabo	Vanderbijl	2463	18	12-15
Kendal	Kendal	2819	22	12-15
Tutuka	Standerton	1023	8	12-15
Majuba	Majuba/Volksrust	590	4	12-15
Matimba	Ellisras	2715	21	12-15
Other		1350	12	12-15
		TOTAL	**161**	

Table 2.4: CO_2 emissions from Sasol synthetic fuel plants (Engelbrecht et al., 2004).

Plant	Location	CO_2 source	CO_2 emitted (Mt/a)	CO_2 conc. (%)
Sasol 1	Sasolburg	Boilers and heaters	7	10-15
		Downstream of gasifiers	4	90-98
Sasol 2	Secunda	Boilers and heaters	9	10-15
		Downstream of gasifiers	14	90-98
Sasol 3	Secunda	Boilers and heaters	9	10-15
		Downstream of gasifiers	14	90-98
		TOTAL	**57**	

Tables 2.4 and 2.5 show that the combined CO_2 emissions from Eskom and Sasol amount to 218 Mt/a. This represents 87.5 % of the total sequestrable South Africa's CO_2 emissions of 249 Mt/a (Eskom, 2000).

These emissions are mainly present in the form of flue gas with a CO_2 concentration of 10 - 15 % (186 Mt/a). The remainder of the CO_2 (32 Mt/a) is emitted in a concentrated form (90 - 98 %) and in a pressurized form (20 bars) (Engelbrecht et al., 2004; Scholes and Van der Merwe, 1998).

The increase in CO_2 emissions is unsustainable and will soon exceed the levels required for stabilization, currently estimated at 400-450 ppm (Bristow et al., 2004). Furthermore the radiative forces experienced from CO_2 today is a result of emissions during the last 100 years (Penner et al., 1999). This implies that some impacts of anthropogenic climate change may yet remain undetected and will ensure that global warming will continue for decades after stabilization.

The transport sector accounts for 26 % of global CO_2 emissions (Chapman, 2007), of which roughly two thirds originates from the wealthiest 10 % of countries (Lenzen et al., 2003). In order to reduce CO_2 emissions from road transport, a significant modal shift onto public transport is required (Waterson et al., 2003). Trains and buses provide the obvious solution but additional 'zero carbon' walking and cycling are real alternatives. Aviation is more environmentally damaging due to emission of other GHG which are directly released into the upper atmosphere, where localized effects can be more damaging than the effects of CO_2 alone (Cairns and Newson, 2006).

2.5.1 Environmental impacts of carbon dioxide

The combustion of fossil fuels injects amounts of CO_2 into the atmosphere that are large compared to the uptake capacity of natural sinks. CO_2 is not just a potent GHG; it is chemically reactive and physiologically active. A well established consequence of excess CO_2 in the air is the acidification of the surface ocean, which causes a reduction in the carbonate ion concentration. Doubling CO_2 in the air would not only lower the pH of surface ocean water by 0.3 but it would also reduce the carbonate ion concentration by a factor of 2. Recent experimental data suggests that the reduction of the carbonate ion concentration greatly affects the growth rate of coral reefs by inhibiting calcification. China's CO_2 emission from fossil fuels combustion increased from 394 to 966 million tons of carbon from 1980 to 2003 (an annual growth rate of 3.98 %). In 2003, China contributed $\approx$ 14.1 % of the world total CO_2 emissions, outdone only by the USA (Xuedu et al., 2006). In 1999, USA contributed 23 % of the world's emissions of CO_2 while Japan and Germany each contributed 12 % (He et al., 2006).

Warming of the climate system is unequivocal as is now evident from observations of increases in global average air and ocean temperature, widespread melting of snow and ice and rising global average sea level. Thermal expansion of the oceans have contributed about 57 % of the sum of the estimated individual contributions to the sea level rise with decrease in glaciers and ice caps contributing about 28 % and losses from the polar ice sheets contributing the remainder. Decrease in precipitation will lead to droughts while glacial meltdown and rise in sea level will lead to flooding. Increased flood risk poses challenges to society, physical infrastructure and water quality. Increased frequency of cardio-respiratory diseases is also projected due to higher concentration of ground level ozone in urban areas related to climate change and altered spatial distribution of some infectious diseases (IPCC, 2007).

Widespread mass losses from glaciers and reduction in snow cover over recent decades are expected to accelerate throughout the 21st century reducing water availability, hydro power potential and changing seasonality of flows in regions supplied by melt water from major mountains ranges (e.g. Hindu-Kush, Himalaya, Andes) where more than one-sixth of the world's population currently lives. In Africa, by 2020 between 75 to 250 million people will be exposed to increased water stress due to climate change. Yields from rain fed agriculture could be reduced by up to 50 %. Agricultural production including food access in many African countries will be severely compromised which will further adversely affect food security and exacerbate malnutrition (IPCC, 2007). Towards the end of the 21st century sea level rise will affect low lying coastal areas with large populations while 5 to 8 % increase in arid and semi-arid land in Africa is envisaged under a range of climate scenarios by the year 2050 (IPCC, 2007).

2.5.2 Carbon capture technologies

In consideration of how best to improve CO_2 capture, there are three technological pathways that can be pursued for CO_2 capture from coal-derived power generation. These are post-combustion capture, capture during combustion (oxyfuel combustion) and pre-combustion capture (Figueroa et al., 2008).

Post combustion capture

Post combustion capture occurs when CO_2 is removed from the flue gas of power station boilers and heating furnaces. The best proven technique to separate CO_2 from flue gas is to scrub it with mono-ethanol amine (MEA) solution. The MEA from the scrubber is heated with steam to release high purity CO_2. The CO_2 free amine is re-circulated to the scrubber. More than a dozen plants worldwide separate CO_2 from flue gas using MEA scrubbing. In these cases the CO_2 is used in industrial applications such as soft drinks industry. The disadvantages of post combustion capture are that the equipment sizes are large due to the large flue gas volumes and the low CO_2 concentration in the flue gas (10-15 %). Special measures need to be taken to minimize contamination of MEA by impurities in the flue gas such as SO_x and NO_x (Engelbrecht et al., 2004).

Capture during combustion (oxyfuel combustion)

Capture during combustion occurs when the fuel is burned with oxygen. Flue gas is re-circulated to the combustor to reduce the combustion temperature. The advantages of this method are that the flue gas stream has a high CO_2 concentration (85 %) and the flow rate is much lower (5 times) than the flue gas from conventional combustion using air. This stream can be sequestrated after dehydration and compression before transport and injection into deep geological formations. The disadvantage of capture during combustion is that an air separation plant is required to produce oxygen for combustion and large volumes of flue gas need to be re-circulated (Figueroa et al., 2008).

Pre-combustion capture

During pre-combustion capture of CO_2, the fuel is pre-gasified with oxygen and steam under pressure. The gas that is produced is cleaned to remove impurities such as H_2S, NH_3 and particulates. The cleaned gas is reformed and shifted to produce CH_4, CO_2, CO and H_2. The CO_2 can be removed using the Benfield process. The Benfield process absorbs the CO_2 in hot potassium carbonate solution that is diethanolamine (DEA) promoted. At Sasol (Sasolburg and Secunda) 30 Mt/a CO_2 is produced from the Benfield process at a concentration of 90-98 % (Figueroa et al., 2008). At this high concentration the CO_2 only requires

dehydration and compression before transport and injection into deep geological formations. More recently, pressure swing adsorption (PSA) has become the technology of choice for the removal of CO_2 from pressurized fuel gas streams in developed countries (Figueroa et al., 2008). The process uses solid adsorbents that selectively absorb CO_2 from mixtures with CO, CH_4 and other hydrocarbon gases under pressure. When the vessel is depressurized, the CO_2 is released and the adsorbent is ready for the next absorption cycle. The cleaned gas can be used to produce liquid fuels or it can be combusted in a gas turbine to produce electricity using the integrated gasification combined cycle process (IGCC). The advantages of pre- combustion capture are that the CO_2 pressure is higher giving a higher driving force for CO_2 separation and more compact equipment. The disadvantage is that oxygen and steam are required for gasification. A reformer and shift converter is also required to convert the CO and methane in the gas to H_2 and CO_2 (Engelbrecht et al., 2004).

2.6 DEVELOPMENT OF MINERAL CARBONATION TECHNOLOGIES

In 2000, the burning of coal generated 37.8 % of all CO_2 arising from fossil fuels. A major advance in tackling global warming could therefore be achieved by curtailing atmospheric emissions of CO_2 from coal power plants. One approach to achieving this objective would be to sequester CO_2 (Arenillas et al., 2005).

CO_2 sequestration which has currently gained increased attention, allows for continued use of fossil fuels while ensuring reduced emissions to the atmosphere. CO_2 abatement involves two major processes (Lemos de Sousa and C. Rodriguez, 2008) i) fixation in sinks (mainly biological fixation) and ii) geological storage (capture and transportation). Geological storage involves storage in open systems - diverse porous lithologies, mineral carbonation and use of closed systems such as salt cavities, deep saline aquifers, depleted oil and gas fields and coal seams (enhanced coal bed methane (ECM) or pure sequestration).

There is only one significant biological process by which CO_2 is removed from the atmosphere and stored in the terrestrial biosphere (Chae et al., 2006). It is

known as photosynthesis, and occurs within the chloroplasts of green plants, including algae, in the presence of light in the wavebands 400 to 700 nm. Research being carried out at Jacob's University in collaboration with Nelson Mandela Metropolitan University since August 2008, seeks to use microalgea generated in photo bioreactors for CO_2 sequestration. Once harvested, the microalgea are turned into dry biomass through photosynthesis using the CO_2 from flue gas streams of various industries and eventually converted into biofuels, glycerine and protein. It is envisaged that this "green technology" could ultimately be rolled out across other parts of Africa (Willemse, 2009).

Geological sequestration consists of capturing the gaseous CO_2 from emission sources and injecting it as a supercritical fluid into underground formations such as active and depleted oil and gas reservoirs, deep unminable coal seams, basalt formations and deep saline aquifers (United States, Department of Energy, 1999). In these reservoirs the CO_2 can be stored by stratigraphic or structural trapping (physical isolation), solubility trapping (dissolved in the aqueous phase) and/or hydrodynamic trapping. However there is a potential for leakage regarding hydrodynamic trapping through imperfect confinement. The CO_2 in saline aquifers is converted into various carbonates such as calcite, magnesite, dolomite and siderite which can be stored in the aquifer formation for millions of years (Gunter et al., 2000). However, conversion of CO_2 into stable minerals in the geological formations is expected to be slow (hundreds of years) due to the slow kinetics of silicate mineral dissolution and carbonate mineral precipitation and thus sequestration within saline aquifers will only be effective in the long run.

Mineral carbon sequestration could be significant in the proximity of the emission sources without the need of storing the gas into geological reservoirs. This technology is called ex-situ mineral sequestration of CO_2 as originally proposed by Seifritz (1990) and first studied in detail by Lackner et al (1995).
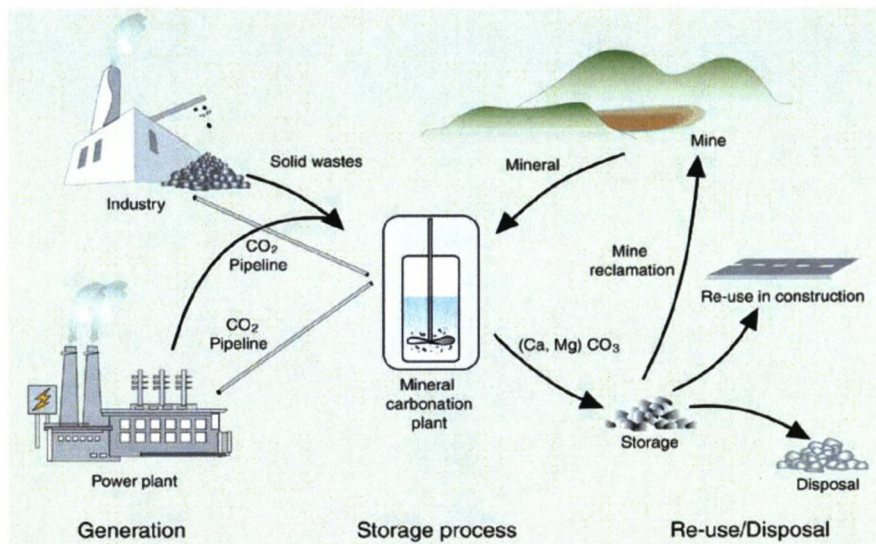
Figure 2.2: Material fluxes and process steps associated with the ex-situ mineral carbonation of silicate rocks or industrial residues (Adapted from IPCC report, 2005)

Mineral carbonation is a mimicry of natural weathering processes in which calcium or magnesium silicates are transformed into carbonates for long term sequestration since carbonates are more thermodynamically stable than CO_2. The sources of Ca and/or Mg are either primary mineral deposits (e.g. olivine, serpentine, basalt, and wollastonite) or alkaline solid wastes (e.g. FA, steel slag and mine tailings)

Two main routes have been proposed for mineral carbonation, namely direct carbonation and indirect carbonation.

Direct route

This section expounds further on the direct and indirect forms of mineral carbonation.

Direct gas- solid carbonation

The direct route involves direct gas-solid carbonation where CO_2 reacts with solids such as Ca/Mg silicates:

$$Ca/Mg\ silicate(s) + CO_2\ (g) \rightarrow (Ca/Mg)\ CO_3 + SiO_2(s) \quad\dots\dots\dots\dots\dots\dots\dots\dots(2.4)$$
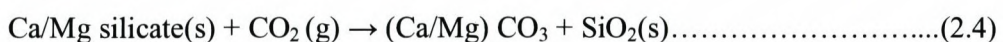
This route provides a simple process design and a better ability to apply the reaction heat generated unlike the three-phase carbonation route (Huijgen and Coman, 2003).

Aqueous carbonation

Since the presence of water enhances the reaction rate of carbonation (through formation of the hydroxide which further reacts to form the carbonate), (O'Connor et al., 2001) the Ca/Mg mineral in this case is slurried with water and carbonated directly at elevated CO_2 pressures and temperature. It is important to note that elevated temperatures and pressures are applicable for primary mineral deposits and mine tailings and not for industrial wastes. The process involves three simultaneous steps, first, carbon dioxide dissolves in the water phase resulting in a mildly acidic environment with HCO_3^- as the dominant carbonate species.

$$CO_2(g) + H_2O \rightarrow H_2CO_3(aq) \rightarrow H^+ + HCO_3^-(aq) \dots\dots\dots\dots\dots\dots(2.5)$$

Secondly, Ca/Mg leaches from the mineral matrix facilitated by the protons present

$$Ca/Mg \; silicate(s) + 2H^+ \rightarrow (Ca/Mg)^{2+}(aq) + SiO_2(s) + H_2O(l) \dots\dots\dots(2.6)$$
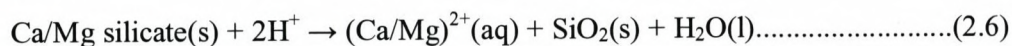
Finally, magnesium or calcium carbonate precipitates.

$$(Ca/Mg)^{2+}(aq) + HCO_3^- \rightarrow (Ca/Mg)CO_3(s) + H^+(aq) \dots\dots\dots\dots(2.7)$$
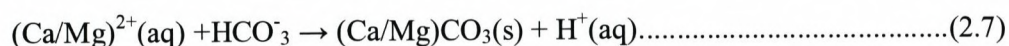
Salt additives may be used in aqueous carbonation, first, to increase the ionic strength of the solution and secondly, to possibly form complexes with dissolved Ca/Mg thus lowering the Ca/Mg activity in solution and enhancing the release of Ca^{2+}/Mg^{2+} ions from the silicate mineral (O'Connor et al., 2001).

Direct molten salt process

The direct molten salt process involves carbonation of serpentine in $MgCl_2.3.5H_2O$ as proposed by Wendt et al., (1998)

$$Mg_3Si_2O_5(OH)_4(s) + 3CO_2(g) \rightarrow 3MgCO_3(s) + 2SiO_2(s) + 2H_2O(l)\dots\dots\dots(2.8)$$
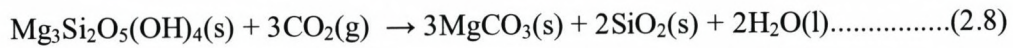
However the high costs associated with the use of corrosive chemicals, the make-up HCl or $MgCl_2$ required and the energy consumption make this process route economically unattractive.

Indirect route

Since the carbonation of Ca/Mg(hydr)oxides is much faster than that for the silicates, some processes have been proposed based on the extraction of the reactive compounds i.e. Ca and Mg, conversion to hydr(oxides) and subsequent carbonation.

HCl extraction route

HCl is used to extract Ca or Mg from the silicate matrix as was proposed by Lackner et al., (1995). Using serpentine as an example, Mg is extracted from the mineral using HCl.

$$Mg_3Si_2O_5(OH)_4(s) + 6HCl(l) + H_2O(l) \rightarrow 3MgCl_2.6H_2O(aq) + 2SiO_2(s)\dots\dots(2.9)$$
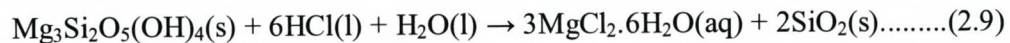
The solution is heated to recover the HCl. Overall, the process step can be given as:-

$$MgCl_2.6H_2O(aq/l) \rightarrow MgCl(OH)(l) + HCl(l) + 5H_2O(l)\dots\dots\dots\dots\dots(2.10)$$

The MgCl(OH) reforms to magnesium hydroxide when water is reintroduced.

$$2\,MgCl(OH)(l) \rightarrow Mg(OH)_2(s) + MgCl_2(l/s)\dots\dots\dots\dots\dots\dots\dots\dots(2.11)$$
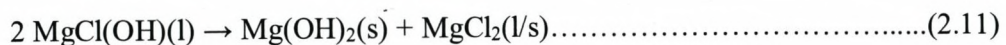
Finally the hydroxide is carbonated.

$$Mg(OH)_2(s) + CO_2(g) \rightarrow MgCO_3(s) + H_2O(l/g)..............................(2.12)$$
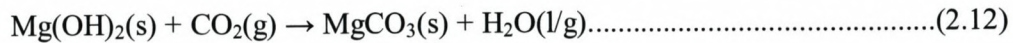
The major drawbacks of this approach are the costs associated with the use of HCl (i.e. make-up and the need for corrosion resistant materials) and the energy consumption caused by the water evaporation step.

Indirect molten salt process

In order to reduce the energy consumption caused by the H_2O evaporation in the HCl extraction route, other extraction agents such as $MgCl_2$ are applied. Using serpentine as an example, the serpentine is first dissolved in the molten salt (Wendt et al., 1998).

$$Mg_3Si_2O_5(OH)_4(s) + 3MgCl_2.3.5H_2O(l) \rightarrow 6Mg(OH)Cl(l) + SiO_2(aq) +$$
$$2.5H_2O(l)..(2.13)$$
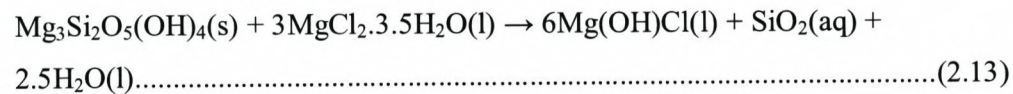
Then the silica is precipitated at temperatures of about 150 °C, water added and $Mg(OH)_2$ precipitates.

$$2Mg(OH)Cl(l) + nH_2O(l) \rightarrow MgCl_2.nH_2O(l) + Mg(OH)_2(s)..........................(2.14)$$

The $MgCl_2$ is dehydrated partially in order to recover the solvent at temperatures of between 110-250 °C.

$$MgCl_2.nH_2O(l) \rightarrow Mg_2.3.5H_2O(l) + (n3.5)H_2O(l)..(2.15)$$
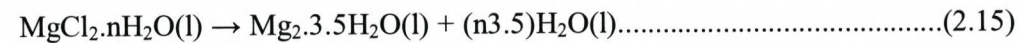
The $Mg(OH)_2$ is then separated and carbonated. However, the presence of the energy consuming partial dehydration and evaporation stages make this route unattractive (Huijgen and Coman, 2003).

Acetic acid route

Acetic acid is used to separate Ca from a silicate rich mineral (Kakizawa et al., 2001). Carbonation of wollastonite, for example using acetic acid follows two steps; first wollastonite is treated with acetic acid,

$$CaSiO_3(s) + 2CHCOOH(l) \rightarrow Ca^{2+}(aq) + 2CH_3COO^-(aq) + H_2O(l) +$$

$$SiO_2(s)..(2.16)$$
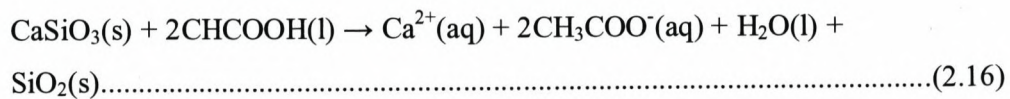
Then the calcium is carbonated and the acetic acid is recovered in a combined step,

$$Ca^{2+}(aq) + 2CH_3COO^-(aq) + CO_2(g) + H_2O(l) \rightarrow CaCO_3(s) +$$

$$2CH_3COOH(l)..(2.17)$$
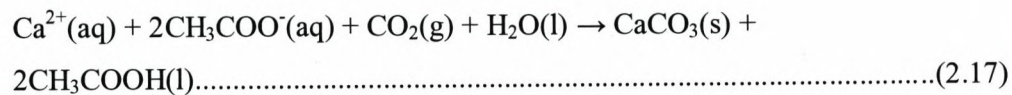
The irreclyclability of acetic acid makes this route costly. Eloneva et al., (2008) also applied acetic acid in their fixation of CO_2 by carbonation of calcium derived from blast furnace slag but found this process to be energy intensive and thus economically unviable.

Application of NaOH

NaOH is used to enhance the extraction of calcium from its three-dimensional structure in which it is kept by Si and Al atoms. Goff et al., (1998) developed this approach for mineral CO_2 sequestration in an attempt to overcome disadvantages associated with the aqueous carbonation route (i.e.) elevated temperatures, use of additives and possible heat treatment. The process was also tested and further developed by Zevenhoven et al., (2008) for blast furnace slag but it was also found not to be economically viable.

$$3CaAl_2Si_2O_8(s) + 4CO_2(g) + 8NaOH(aq) \rightarrow 3CaCO_3(s) +$$

$$Na_8(AlSiO_4)_6CO_3.2H_2O(s) + 2H_2O(l)..................................(2.18)$$
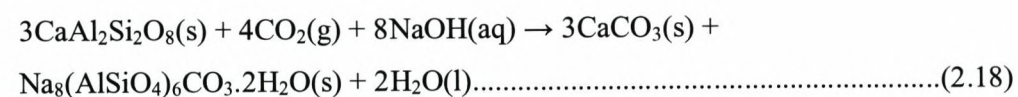
Three major drawbacks are however reported for this route; firstly, the reaction times are too long for industrial application; secondly, the feed stock has to be milled to less than 10 μm thus causing high energy consumption because of the grinding; and thirdly, large quantities of NaOH are required. Other processes that can be used include formation of iron carbonates for possible CO_2 storage but the major drawback is the consumption of the potentially valuable iron ore. Application of the enzyme carbonic anhydrase has also been studied (Simsek et

al., 2002; Simsek et al., 2001; Medina et al., 2000). The enzyme catalyses the hydration of CO_2 and could therefore enhance the carbonation rate of mineral CO_2 sequestration.

2.7 CARBONATION OF MUNICIPAL WASTES

Carbonation, which involves exposure of the solid waste residues to a CO_2 rich environment leading to formation of carbonates, has been studied on municipal solid waste incineration (MSWI) ash as a stabilization mechanism of the ash to reduce leaching of the mobile trace elements such as Ba, Mo, Sb, Zn, Pb, Cr, Cu, Se and Hg. In some European countries such as Belgium, the total concentration values for some elements have been regulated for example As, Cd, Cu, Cr, Hg, Ni, Pb and Zn. Hence several stabilization techniques have been proposed ranging from physical methods such as sieving and dia-magnetic separation to chemical means such as washing and carbonation (Sabbas et al., 2003). Carbonation however is widely accepted in most European countries owing to the fact that carbonation also reduces CO_2 emissions in the process. The ash is left to mature for 6 - 12 weeks after quenching and after this natural maturation, leaching for several metals appears to be lowered compared to the fresh ash.

Several authors (Kaibouchi and Germain, 2003; Freyssinet et al., 2002; Meima et al., 2002) have postulated that carbonation is the process responsible for the reduced metal mobility after maturation. Van Gerven et al., (2005), reported that while carbonation has a positive effect on the leaching of Cu and Ba (reduction in their leaching), leaching of the oxyanions Cr, Mo and Sb remains constant or even increases. They explained that at high pH, solubility of Cr is controlled by $BaCrO_4$ and that of Mo by $CaMoO_4$ together with oxyanions substitution of sulphates in ettringite, $(Ca_6Al_2(SO_4)_3(OH)_{12}.26H_2O)$. Sulphate substitution is also the controlling factor for Sb solubility. When pH decreases, ettringite dissolves and sulphates, Cr, Mo and Sb ions come back into solution. Sulphate then precipitates with Ba, dissolving even more Cr as a result. In acidic conditions, oxyanions undergo sorption to amorphous iron and Al oxides (Meima et al., 2002) thereby decreasing their concentration in the leachate. A possible explanation for

the oxyanion's behavior is that at high pH, the carbonate ion competes with the oxyanions in precipitation or sorption reactions resulting in a higher Cr, Mo and Sb leaching at pH 11.5 from carbonated ash than from un-carbonated ash. In addition, at this high pH, carbonate formation dissolves ettringite (Nishikawa et al., 1992) leading again to Cr, Mo and Sb coming into solution. Ecke, (2003), identified Pb, Zn Cr, and Cd as the potential major pollutants in FA from MSWI. Based on chemical equilibrium calculations, it was postulated that carbonation leads to a reduced mobility of Pb and Zn due to the predominance of $PbCO_3$ at pH 6-9 and $Zn(OH)_2$ at pH 9 -11 respectively, while the availability of Cr is a function of both carbonation and electron activity. A change in Cd mobility could not be deduced though. Their investigations found that due to the effect of carbonation, the leachability of Pb and Zn decreased by two orders of magnitude. Carbonation increased the mobility of Cd possibly due to the transition from $Cd(OH)_2$ to $CdCl_2$ (Ecke et al., 2002). According to Ecke et al., 2003, the mobility pattern of Cr can be attributed to electron activity (pE) rather than other factors such as CO_2 or pH. At pE 4, highly mobile hexavalent Cr-VI dominates the FA leachate system. As a function of time, the FA samples can be exposed toward more oxidizing conditions due to the impact of atmospheric O_2, i.e., the mobilization of Cr is favoured. On the other hand, mixing FA with water might facilitate the chemical reaction with other elements and, thus, the reduction of Cr-VI to Cr-III, which is characterized by a much lower mobility, as in $Cr(OH)_3$. Significant impacts might arise from the formation of calcium silicate hydrates (C-S-H) or calcium alumino-silicates hydrates (C-A-S-H) (Ecke et al., 2002). Through bonding and adsorption, the crystalline matrix may retain the metals. An effect that enhances the sequestering of a variety of cations such as Pb, Cd, Cu, Zn, etc. is probably the adsorption onto $CaCO_3$ leading to co-precipitation (Schwartz and Ploethner, 2000; Morse and Bender, 1990). This is a possible explanation for the reduced availability of Cu. However, the mobility pattern of Cd must be attributed to other processes because carbonation was observed to increase Cd mobilization when leached at pH 10.

Rendek et al, (2006) concurs that carbonation is an important step in weathering process and that it involves the CO_2 dissolution in water at initially alkaline

conditions. This causes pH to decrease as calcite precipitates until the material is in equilibrium with CO_2. However at acidic pH, HCO_3^- ions dominate the system hence carbonates will dissolve. Thus aqueous phase equilibrium with CO_2 promotes carbonate precipitation under basic conditions, while acidic conditions favour carbonate dissolution (Soong et al., 2004). Moreover, heavy metals (Cd, Cr, Pb, and Zn) can be trapped in the newly formed minerals. Calcite is the predominant newly formed mineral during bottom ash maturation, combined with aluminium hydroxides and various sulfates (Freyssinet et al., 2002). On weathering the CO_2 source is the atmospheric CO_2. However, it has been proved that the natural carbonation process can be accelerated; using different sources of CO_2 and a few methods have already been developed at laboratory scale on different MSWI ash and other calcium rich residues (Van Gerven et al., 2005). Moreover, accelerated carbonation may represent a proper pre-treatment stage prior to either recycling or land filling the ash (Sabbas et al., 2003). The carbon dioxide source can be either pure CO_2 or any other CO_2-rich gas such as certain industrial emissions. Consequently, using bottom or FA, CO_2 sequestration capacity to treat industrial emissions could be another interesting possibility of ash utilization. This process could both help reduce the greenhouse effect and reduce FA storage duration by accelerating weathering reactions (Anthony et al., 2000).

2.8 CARBONATION OF FLY ASH LEACHATES

Soong and co-authors (2006) studied the CO_2 sequestration process using brine solutions and class C FA. It was observed that exposure of brine to FA leads to an increase in Ca^{2+} concentration in the reaction mixture, which is attributed to the dissolution of CaO found in FA giving rise to $Ca(OH)_2$ which in turn increases the brine pH. The hydroxide further dissociates to give Ca^{2+} which reacts with CO_3^{2-} from the dissolution of carbon dioxide forming calcite. In addition, the Na^+ concentration in the brine is reduced (Mooketsi et al., 2007). The concentration of CaO in the FA after exposure to brine decreases while that of NaCl is increased. The observed increase in NaCl concentration in FA is linked to the decrease of Na^+ concentration in brine. Analysis of the solid precipitate formed after fly

ash/brine/CO_2 interaction indicated the presence of two major phases $CaCO_3$ (90 %) and NaCl (9 %) (Soong et al., 2006).

The following reactions explain the process of carbonate formation in ash/brine/CO_2 mixture:

$$CO_2 + H_2O \leftrightarrow H_2CO_3 \dots\dots\dots\dots\dots\dots\dots\dots\dots\dots\dots\dots\dots\dots\dots(2.19)$$

$$H_2CO_3 \leftrightarrow H^+ + HCO_3^- \dots\dots\dots\dots\dots\dots\dots\dots\dots\dots\dots\dots\dots\dots(2.20)$$

$$HCO_3^- \leftrightarrow H^+ + HCO_3^{2-} \dots\dots\dots\dots\dots\dots\dots\dots\dots\dots\dots\dots\dots\dots(2.21)$$

$$CaO + H_2O \leftrightarrow Ca(OH)_2 \dots\dots\dots\dots\dots\dots\dots\dots\dots\dots\dots\dots\dots\dots(2.22)$$

$$Ca(OH)_2 \leftrightarrow Ca^{2+} + 2OH^- \dots\dots\dots\dots\dots\dots\dots\dots\dots\dots\dots\dots\dots(2.23)$$

$$Ca^{2+} + CO_3^{2-} \leftrightarrow CaCO_3 \dots\dots\dots\dots\dots\dots\dots\dots\dots\dots\dots\dots\dots\dots(2.24)$$
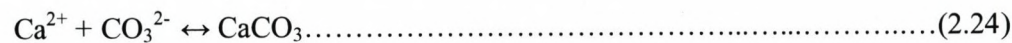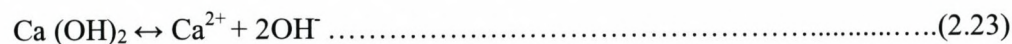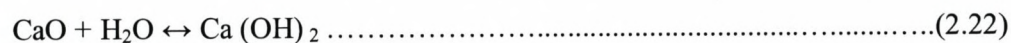
Other ions present in both FA and brine such as Mg and Fe can also be carbonated to form dolomite, siderite or magnesite for safe and permanent storage of carbon dioxide as illustrated by the following reaction mechanisms (Soong et al., 2006).

$$Ca^{2+} + Mg^{2+} + CO_3^{2-} \leftrightarrow CaMg(CO_3)_2 \dots\dots\dots\dots\dots\dots\dots\dots\dots(2.25)$$

$$Fe^{2+} + CO_3^{2-} \leftrightarrow FeCO_3 \dots\dots\dots\dots\dots\dots\dots\dots\dots\dots\dots\dots\dots\dots(2.26)$$

$$Mg^{2+} + CO_3^{2-} \leftrightarrow MgCO_3 \dots\dots\dots\dots\dots\dots\dots\dots\dots\dots\dots\dots\dots(2.27)$$

Montes-Hernandez et al., (2009) have also investigated the mineral sequestration of CO_2 by aqueous carbonation of coal FA (class F with 4.1 % of CaO) and they found that one ton of FA could sequester up to 0.026 tons of CO_2. It is important to note that class F bottom ash is expected to have a higher sequestration capacity due to the higher CaO content compared to that of the same class FA.

2.9 CHARACTERIZATION OF FLY ASH MINERAL PHASES AND BRINE SPECIES

In the study of CO_2 sequestration using brine impacted FA, various characterization techniques were used to identify species in the fresh ash, weathered ash, brines and the products of carbonation. Some of the techniques applied for characterization are discussed below.

2.9.1 Morphological analysis by Scanning Electron Microscopy (SEM)

SEM is a type of electron microscope capable of producing high-resolution images of a sample surface creating a three dimensional appearance useful for judging the surface structure and morphology of the sample. Scanning electron microscopy examines structure by bombarding the specimen with a scanning beam of electrons and then collecting slow moving secondary electrons that the specimen generates. These are collected, amplified and displayed on a cathode ray tube. The electron beam and the cathode ray tube scan synchronously so that an image of the surface of the specimen is formed. Specimen preparation includes drying the sample in the oven at 100 ºC and making it conductive to electricity if it is not already. SEM is typically used to examine the external structure of objects that are as varied as biological specimens, rocks, metals, ceramics and almost anything that can be observed in a dissecting light microscope. Sputter coating is necessary where the sample for analysis is not conductive. This is a physical vapour deposition process that uses a plasma generated by ionizing a low pressure inert gas such as argon with a target of a noble metal. The metals most commonly used are gold, silver, platinum, palladium and chromium. Except for chromium, all have good sputtering yields and can be sputtered in a low partial pressure atmosphere after evacuation with a mechanical vacuum pump. The heavier metals such as gold also have high secondary electron yields, making imaging much easier (Goldstein et al., 2003).

55

2.9.1.1 Scanning electron microscopy- Electron dispersive spectroscopy (SEM-EDS)

SEM-EDS is useful in obtaining rapid qualitative elemental analysis of an unknown sample. This method detects all elements from boron to uranium and is usually non-destructive. Two methods are used to determine the x-rays that are produced: (1) energy-dispersive analysis, which separates and detects x-rays of specific energy and displays them as histograms, whereas (2) wavelength-dispersive analysis uses the reflection of x-rays of a crystal at a characteristic angle to detect x-rays of specific wavelengths (Goldstein et al., 2003).

2.9.2 Mineralogical analysis by X-ray Diffraction (XRD)

XRD is an analytical technique which uses the diffraction pattern produced by bombarding a single crystal with x-rays to solve the crystal structure. The diffraction pattern is recorded and then analyzed to reveal the nature of the crystal. This technique is widely used in chemistry and biochemistry to determine the structures of an immense variety of molecules including inorganic compounds, DNA and proteins. When single crystals are not available, related techniques such as powder diffraction or thin film x-ray diffraction coupled with lattice refinement algorithms such as Rietveld refinement may be used to extract similar, though less complete information about the nature of the crystal (Szostak, 1989).

XRD utilizes the fact that x-rays of similar wavelength (λ) to the distance between lattice planes in a crystal (d) are diffracted by the nuclei of atoms. At certain angles of incidence of the x-rays to the lattice planes (θ), the diffracted x-rays positively interfere, creating a peak in the detected signal. The angles at which this occurs are defined by the Bragg's law: ($n\lambda=2d\sin\theta$). If the angle of incidence (θ) and the wavelength (λ) are known, the spacing (d) of the reflecting atomic planes can be determined from the above equation. The lattice spacing is characteristic of the mineral, thus the x-ray diffraction method can be used for the identification of minerals and for analysis of mixtures of minerals. XRD instruments plots peaks of 2θ (abscissa) vs. intensity (ordinate), i.e. peaks are

shown against double the incident angle (i.e., incident + diffracted) (Murad et al., 1994).

2.9.3 Chemical analysis by X-ray Fluoresence (XRF)

XRF utilizes the characterization of X-ray spectral information to determine the bulk elemental composition of solid samples. X-ray spectra are created by the interaction of an x-ray source with the electrons of the sample atoms. The excitation source causes ejection of an inner shell electron from a sample atom, creating a vacancy in the electron shell and leaving the atom in an excited state (Bekkum et al., 1991). During de-excitation, an electron transition occurs from an outer shell to fill this vacancy. The change in energy associated with the transition takes the form of x-ray radiation which is detected and analyzed. XRF is widely used for the analysis of solid environmental, geological, biological, industrial and other samples. Compared to other competitive techniques such as Atomic Absorption Spectroscopy (AAS), Inductively Coupled Plasma Spectroscopy (ICPS) and Neutron Activation Analysis (NAA), XRF has the advantage of being non-destructive, multi-elemental, fast and cost-effective. Furthermore, it provides a fairly uniform detection limit across a large portion of the periodic table and is applicable to a wide range of concentrations, from a 100 % to few parts per million (ppm). Its main disadvantage is that analyses are restricted to elements heavier than fluorine and that a large sample is required (Kalnicky and Singhvi, 2001).

2.9.4 Ion Chromatography (IC)

Ions in solution are detected by measuring the conductivity of the solution. In IC, the mobile phase contains ions that create a background conductivity making it difficult to measure the conductivity due only to the analyte ions as they exit the column. This problem is reduced by selectively removing the mobile phase ions after the analytical column and before the detector (Jarvis et al., 1992). This is done by converting the mobile phase ions to a neutral form or removing them with an eluent suppressor which consists of an ion-exchange column or membrane. A

high concentration of any one ion may interfere with the resolution and sometimes the retention, of others (Eaton et al., 1995). Most samples require dilution for determination of major ions by ion chromatography, which can introduce additional errors. Generally the minimum detectable concentrations for anions by this method are near 0.1mg/l for Br^-, Cl^-, NO_3^-, NO_2^-, PO_4^{3-} and SO_4^{2-} (Eaton et al., 1995).

2.9.5 Inductively Coupled Plasma Mass Spectroscopy (ICP-MS)

ICP-MS gives very high sensitivity for the determination of elements and even isotopes in solution. This technique has the ability to detect to the very low parts per billion (ppb) levels of most elements in an aqueous sample. In ICP-MS, a plasma or gas consisting of ions, electrons and neutral particles is formed from argon gas. The plasma is a very aggressive ion source and virtually all molecules in a sample are broken up into their component atoms because of the high temperatures (6727 °C) at which the ion source operates (Eaton et al., 1995). A radio frequency signal is fed into a tightly wound, water-cooled coil where it generates an intense magnetic field. In the centre of this coil is a specially made glass or quartz plasma torch where the plasma is formed. The plasma is generated in the argon gas by "seeding" the argon with a spark from a Tesla unit (similar to that used on a car spark plug). When the spark passes through the argon gas, some of the argon atoms are ionized and the resultant cations and electrons are accelerated toward the magnetic field of the radio frequency coil. Through a series of inelastic collisions between the charged particles (Ar^+ and electrons) and neutral argon atoms, a stable high temperature plasma is generated. The plasma is used to atomize and ionize the elements in a sample. When the sample aerosol passes through the plasma, it collides with the free electrons, argon cations and neutral argon atoms. The result is that any molecules initially present in the aerosol are quickly and completely broken down to charged atoms. The resulting ions are then passed through a series of apertures (cones) into the high vacuum mass analyzer. The isotopes of the elements are identified by their mass-to-charge ratio (m/e) and the intensity of a specific peak in the mass spectrum is

proportional to the amount of that isotope (element) in the original sample (Jarvis et al., 1992).

2.9.6 Thermal Gravimetric Analysis (TGA)

Thermal stability of the carbonated residues can be determined to give information about the adsorbed water as well as to quantify the amount of carbonates formed during the carbonation process. The most common sources of TGA disturbances and errors in the sequence of their frequency of occurrence are:- unstable buoyancy forces, convection forces, electrostatic forces, condensation of volatile products on sample surface, thermal expansion of the balance beam and turbulent drag forces from gas flow. The static buoyancy is related to the gas density and it is the most problematic factor hence gas handling is critical in TGA analysis (Czarnecki and Sestak, 2000).

2.9.7 Total acid digestion

Acid attack is the most widely used method of dissolving silicate rocks and has evolved into two forms. In one form the entire sample is taken up into solution so that the major elements and in particular silicon and aluminum may be determined. In the other method, if silicon is not determined, it is removed as volatile silicon tetra fluoride (SiF_4) during sample attack by fuming in the presence of hydrofluoric acid. The resultant solution is more stable since fluorosilic acid tends to hydrolyze and precipitate on standing or dilution. Hydrofluoric acid (HF) is the only acid that will readily dissolve silicate material partly due to the solubility of the hexafluorosilicate ion (SF_6^{2-}) in acid aqueous solution. However HF is not used alone and is applied together with other acids such as nitric acid and hydrochloric acid (Potts, 1992).

2.9.8 Carbonation experiments

Different strategies can be used for the optimization of carbonation. The classical method of experimental optimization involves changing one variable at a time keeping the others constant (Shi et al., 2009). This method however requires a

large number of experiments to illustrate the effect of individual factors. In addition, this does not consider the effect of interactions of various parameters (Montgomery, 2009). Use of statistical methods, helps to select important parameters from a large number of factors and the interactions between important variables can be understood easily.

2.9.8.1 Statistical Design of Experiments

The need to develop statistical theory for designing experiments stems from the inherent variability of experimental results (Mead, 1991). As the complexity of the experiments increases, and the differences of interest become relatively smaller, then the precision of the experiment becomes more important for instance in the control of industrial processes. The design of experiments software allows one to come up with a design that considers all the factors optimizing on the outcome of the response variable. The D-optimal criterion, one of the several optimalities, was developed to select design points in a way that minimizes the variance associated with the estimates of specified model coefficients.

The D-optimal factorial design is designed for use with categorical factors as an alternative to the general factorial design option. The general factorial design builder may produce designs with more runs than one is willing to run. The D-optimal design on the other hand chooses an ideal subset of all possible combinations, based on the specified model (Design Expert 7.1 User's manual, 2001).

2.10 SECTION SUMMARY

The disposal of both FA and brine is of major concern to the coal fired power plants due to their impact on the natural environment such as ground water systems. Coupled with this disposal problem is the issue of CO_2 emissions to the environment that are responsible for the global warming effect. It is thus imperative that proper means of disposal of these wastes is devised in order to continue with more sustainable use of natural resources such as coal without further harming the environment in the process.

Understanding the chemistry of the interaction of South African FA /brine / CO_2 is therefore important so as to predict their behavior and interactions in the ash dumps. As has been previously shown coal FA has the capacity to sequester CO_2 in the form of carbonates. This interaction has also been found to be of great influence during the weathering process as has been studied on municipal solid waste incineration where it has been found that carbonation stabilizes the ash by locking up some of the mobile trace elements such as Pb, Cu, Zn, and Hg through co-precipitation (Van Gerven et al., 2005; Ecke et al., 2003; Meima et al., 2002).

One of the main objectives of this study as clearly stated in section 1.4 was to study the CO_2/brine/FA interaction as a possible means of CO_2 capture as well as brine effluents remediation through encapsulation of the salts in the ash matrix. Since no study has been carried out so far on the effect of carbonation on the composition of FA and brine upon the interaction of class F fly ash, brine and CO_2, this study aims to investigate this phenomenon. Soong and co-authors (2006) in their study of FA/brine/CO_2 interaction utilized class C FA whose CaO content is very high (above 25 %) as opposed to the South African FA (class F) whose lime content is less than 10 %. Consequently, this study also intends to look into the CO_2 sequestration potential of the South Africa's class F FA and local industrial generated brines.

The literature search thus sets the pace for the experimental section of this study. Chapter three outlines the analytical techniques used in the study giving the chemicals used, their purity, instrumentation and the set up for each analytical equipment used.

CHAPTER THREE

EXPERIMENTAL AND ANALYTICAL METHODS

Chapter three describes the experimental and analytical methods used to achieve the objectives of this study.

3.1 MATERIALS AND METHODS

A list of chemicals used in the study is given in Table 3.1 below while the analysis of CO_2 gas used is given in section 3.1.1.

Table 3.1: A summary of chemicals used

Chemical	Supplier	Purity
Hydrochloric acid	Merck	Min 37 %
Sodium chloride	Merck	99.0-100.5 %
Sodium bicarbonate	SP Scientific	99.8 %
Methyl orange indicator	Merck	
Calcium carbonate	Kimix	Min 55 %
Nitric acid	Kimix	Min 55 %
Hydrofluoric acid	Merck	Min 48 %

3.1.1 Carbon Dioxide Analysis

The CO_2 used for the carbonation study was of a technical grade (CO_2, TEC) obtained from Afrox with the following analysis which was carried out by the supplier (Afrox):

Molecular weight = 44.011

Specific volume at 20 °C, 325 kPa = 5471 kg

Critical temperature = 31 °C

Relative density at 1 atmosphere = 1.53

Density at 0 °C, 325 kPa = 1.977kg/m^3

Flammability = not applicable

3.2 SAMPLE COLLECTION AND PREPARATION

The fresh FA samples used in this study were collected from the precipitators at Sasol Synfuels in Secunda and Tutuka power station in the Mpumalanga province of South Africa. Brine samples were collected from the water circulation of both Tutuka and Secunda power plants though for the carbonation experiments, it is Tutuka brines that were utilized. The FA samples were stored in tightly sealed containers to exclude air and placed in dark cool cupboards away from heat, out of direct sunlight and away from fluctuating temperatures. Brine samples were kept in the fridge for a maximum period of 24 hours at 4 °C to prevent their degradation before analysis.

Size fractionation of FA samples was carried out to evaluate whether the composition of FA as well as its reactivity varies across the different size fractions. Furthermore the obtained fractions were used for subsequent experiments. Different sizes of sieve apertures were chosen, these were 150, 106, 90, 75, 63, 53, 45, 32, 25 and 20 micron sieves. The sieves were arranged from highest to the lowest size with the highest size on top and the lowest at the bottom. 250g of dried bulk FA were placed in the highest size sieve and the stack of sieves was placed on the Endecott mechanical shaker. The shaker was switched on and timed to shake for one hour. Each size fraction was weighed, placed in a plastic container and labeled awaiting analysis by XRD and XRF. The <20 μm fractions, >150 μm fractions, 20 μm-150 μm fraction and the bulk ash were used for the carbonation experiments and the justification for use of these fractions is set out in section 3.4.1.

3.3 ANALYTICAL METHODS

3.3.1 Scanning Electron microscopy (SEM)

Scanning electron microscopy was carried out in order to understand the morphology of fresh ash, weathered ash as well as the carbonated solid residues.

3.3.1.1 Sample preparation

The fly ash samples were oven-dried at 110 °C for eight hours in preparation for the SEM-EDS analysis. A carbon adhesive tape was mounted onto an aluminium stub, and a small amount of sample applied onto the adhesive tape which is a special carbon conductive glue. The samples were then gold-coated to make them conductive with an Edward sputter coater.

3.3.1.2 Instrumental set up

Analysis was done with a Hitachi X-650 Scanning Electron Microanalyser equipped with a CDU- lead detector at 25 kV and a tungsten filament.

3.3.2 X-ray Diffraction (XRD)

XRD was carried out to identify and also quantify the different phases in the fresh ash and the carbonated solid residues.

3.3.2.1 Sample preparation for qualitative XRD

The samples were analyzed as is without any additional sample preparation. 5g of the sample was placed on polycarbonate samples holders and clipped into the instrument's sample holder.

3.3.2.2 Instrumental set up for qualitative XRD

Diffraction patterns for each fraction were collected using a Bruker AXS D8 Advance diffractometer coupled with a Cu-Kα radiation at 40kV and anode current of 40mA with a PSD Lynx-Eye, Si- strip detector. The measured range of 2θ angles were from 10° to 70° while the diffraction patterns were collected with a step of $\Delta 2\theta = 0.03°$ and counting time of three seconds in every step. Mineral identification in this study was done by comparison with published d-spacing data and relative intensities for the major peaks from the International Centre for Diffraction Data (ICDD PDF database, 1998) and EVA software from Bruker.

3.3.2.3 Sample preparation for quantitative XRD

Different size fractions of the FA earlier obtained (section 3.2.2) by sieving using an Endecott mechanical shaker were analyzed using quantitative XRD. This analytical method was also used to quantify $CaCO_3$ formed during the carbonation experiments. After addition of 20 % Si (99 % pure) for determination of amorphous content and milling in a McCrone micronizing mill, the samples were prepared for XRD analysis using a back loading preparation method. Due to the amorphous nature of FA, one cannot clearly establish a minimum sensitivity however the standard errors do give an indication of the accuracy.

3.3.2.4 Instrumental set up for quantitative XRD

The samples were analysed with a PANanalytical X'Pert Pro powder diffractometer with X'Celerator detector and variable divergence and receiving slits with Fe filtered Co-Kα radiation. The phases were identified using X'Pert Highscore plus software. The relative phase amounts (wt %) were estimated using the Rietveld method (Autoquan programme).

3.3.3 X-Ray Fluorescence (XRF)

X-ray fluorescence analysis was carried out to quantify the chemical composition of the fresh ash. XRF was however not carried out on the weathered ash as explained in the delimitations earlier. There is no literature on the use of XRF for quantitative analysis of carbonated solid residues; hence this technique was not applied to determine carbonates.

3.3.3.1 Sample preparation

All the size fractions obtained by fractionation as well as the bulk ash were analysed using X-ray fluorescence. 9 g of each sample was mixed with 2 g of the binder which is made up of 10 % C-wax binder and 90 % EMU powder. The mixture was thoroughly shaken, poured into the mould and pelletized at a pressure of 15 tons for about 1 minute using a Dickie and Stockler manual pelletizer. Loss

on ignition (LOI) was measured by placing the samples in the furnace at 1000 °C for at least 45 minutes.

3.3.3.2 Instrumental set up

XRF analyses of the FA samples were done on a Philips PW 1480 X-ray spectrometer. The spectrometer is fitted with a Chromium tube, five analyzing crystals namely LIF 200, LIF 220, GE, PE and PX and the detectors are a combination of gas-flow proportional counter and a scintillation detector. The gas flow proportional counter uses P10 gas, which is a mixture of 90 % argon and 10 % methane. Major elements were analyzed on the pellet at 40 kV and 50 mA tube operating conditions and trace elements were analyzed on a powder briquette at 50 kV and 40 mA tube operating conditions. Matrix effects in the samples were corrected for by applying theoretical alpha factors and measured line overlap factors to the raw intensities measured with the SuperQ Philips software.

3.3.4 Ion Chromatography (IC)

Ion chromatography was used to identify and quantify the anionic species in the brines and the carbonation leachates.

3.3.4.1 Sample Preparation

All the aqueous samples used in the study were filtered through a 0.2 μm pore membrane filter to remove suspended solids and then diluted with ultra pure water to obtain EC values of between 50 and 100 μS/cm.

3.3.4.2 Instrumental set up

Sulphates, chlorides, nitrates and phosphates were analyzed using a Dionex DX-120 ion chromatograph with an Ion Pac AS14A column and AG14-4 mm guard column.

3.3.5 Inductively Coupled Plasma Mass Spectroscopy (ICP-MS)

ICP-MS was used to identify the major, minor and trace elements in the brines and the carbonation leachates.

3.3.5.1 Sample preparation

All the aqueous samples used in the study were filtered through a 0.2 μm pore membrane filter to remove suspended solids and then diluted with ultra pure water to obtain EC values of between 50 and 100 μS/cm. The samples were acidified to pH less than 2 in order to stabilize the cations.

3.3.5.2 Instrumental set up

The majors were analyzed using a Varian Radial ICP-AES, while traces were done on an Agilent 7500ce ICP-MS, using a High Matrix Introduction (HMI) accessory and He as collision gas.

3.3.6 Chittick Tests for determination of % $CaCO_3$

The determination of $CaCO_3$ was made using the Chittick apparatus as described by Dreimanis (1962) and is based on the volumetric evolution of carbon dioxide when carbonates react with dilute hydrochloric acid.

3.3.6.1 Methodology

Two solutions are required for the test: diluted hydrochloric acid and coloured reservoir fluid which were prepared as follows:

Dilute Hydrochloric acid

A 6 N solution of HCl was made by adding 109.4 g of concentrated HCl to a litre of ultra pure water.

Reservoir fluid

In a 1 L Erlenmeyer flask, 100 g of NaCl was dissolved in distilled water. 1 g of $NaHCO_3$ was added and 2 ml of methyl orange solution. A 1:5 dilute sulfuric

acid was added until the solution turned a deep pink colour, the solution was stirred and topped up to the 1 L mark. 1.70 g of FA was weighed and placed in the reaction container which was then tightly capped. The level of the coloured liquid in the burette and the reservoir was leveled by opening the stop cork. A slight negative pressure was created by lowering the reservoir level by about 3 ml of the level in the burette. 20 ml of 6 N HCl was introduced and the mixture agitated. Simultaneously a stop watch was started as the acid was introduced and the displacement of the coloured liquid in the burette by evolving CO_2 was read after 1 minute and after 20 minutes. The reading at 1 minute was recorded as R_1 while that at 20 minutes was recorded as R_{20}. A schematic of the Chittick test set-up is as shown in Figure 3.1.
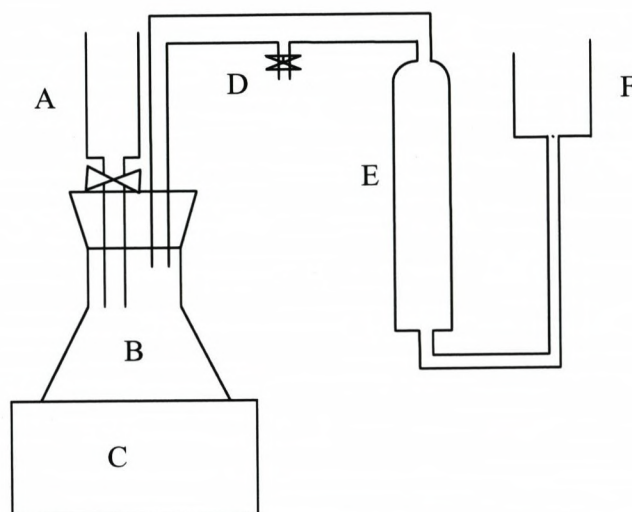
Figure 3.1: Schematic of Chittick test apparatus

Where: A = Pipette (with acid)   D = Leveling stopcock

B = Reaction vessel   E = Measuring burette

C = Magnetic stirrer   F = Reservoir fluid

Correction factors were calculated for each reading and used to determine the % $CaCO_3$. This was done by reacting 0.10 g of pure $CaCO_3$ similar to the samples. The factor is given as:-

$$f = \frac{W * T}{1.22 * V} \quad\text{...(3.1)}$$

Where: W = grams weighed of pure $CaCO_3$

T = temperature of measurement in K

V = ml produced CO_2

The above correction factor was used to calculate the % $CaCO_3$ (based on 1.7 g of dried fly ash) as follows:-

$$F = CR_1- (0.04) (CR_{20}-CR_1) \dots\dots\dots\dots\dots\dots\dots\dots\dots(3.2)$$

Where CR_1 = reading at 1 minute $* f$

CR_{20} = reading at 20 minutes$* f$

$$\% \ CaCO_3 = 0.232F \dots\dots\dots\dots\dots\dots\dots\dots\dots\dots\dots..(3.3)$$

3.3.7 Total Acid digestion

Acid digestion was carried out to determine total elemental content of the fresh ash and the carbonated residues.

3.3.7.1 Methodology

Aqua regia (a mixture of nitric acid and hydrochloric acid) was made by mixing HNO_3 and HCl in the ratios of 1:3. 200 mg of the powdered sample was weighed in to the teflon liner of a Parr bomb. A small volume of aqua regia (0.2 ml) was added as a wetting agent, which acts to prevent excessive reaction in the samples when HF is added. Following the aqua regia, 4 ml HF was added, the bomb was sealed tightly and heated in the oven at 110 °C for two hours. The samples were then allowed to cool after which excess HF in the digestate was neutralized by addition of 25 ml of saturated boric acid solution. The digestate was filtered through 0.45 μm membrane filter and the solution was diluted to 50 ml with ultra pure water. The solutions were acidified to pH less than two and analyzed using ICP-MS.

69

3.3.8 Geophysical mapping of the ash dumps

As discussed earlier, Secunda utilizes the wet ash disposal technique while Tutuka utilizes the dry disposal scenario. Geophysics mapping was carried out to determine the resistivity of the ash dumps, which in turn would give an indication of the interaction between the ash leachate and the water table.

3.3.8.1 Methodology

An Abem SAS 1000 terrameter and ES 464 switching unit were used for the field survey. Four multicore cables and stainless steel pegs were used with the "roll-along" surveying method. Measurement of the resistivity of the ground was carried out by transmitting a controlled current (I) between two electrodes pushed into the ground, while measuring the potential (V) between two other electrodes. Direct current (DC) or a very low frequency alternating current was used, thus the method is often called DC-resistivity. The resistance (R) was calculated using Ohm's law. All electrodes were inserted approximately 40 cm into this layer and moistened with a water and copper sulphate mixture to maximize input current into the subsurface. An input current of 500 milli-amperes was channeled into the subsurface during the measurements. This resulted in a data set of excellent quality (low noise) and a low root-mean-squared (RMS) error. The RES2Dinv version 3.52-inversion program was used to invert the measured data after being manually and mathematically filtered (Takahashi, 2006).

LUND imaging system with field cables and accessories and a Terrameter SAS 4000

Figure 3.2: Field cables, switching units and a terrameter SAS 4000

Ohm's law states that the current through a conductor between two points is directly proportional to the potential difference or voltage across the two points and inversely proportional to the resistance between them:-

$$I = V/R \dots\dots\dots\dots\dots\dots\dots\dots\dots\dots\dots\dots\dots\dots\dots\dots \ (3.4)$$

Where: - V= potential difference measured across the resistance in volts

I= current through the resistance in amperes

R= resistance of the conductor in ohms

3.3.9 Use of Piper diagrams for brine classification

Piper diagrams (Piper, 1944) are some of the tools used in the classification of waters. It is important to note that the program used to generate these plots named AqQa utilizes the major cations and anions to classify the waters. The piper diagrams are tri-linear with two simple triangular plots on the right and left side of a parallelogram (Figures 4.10 and 4.11). In the triangular plots, the axes should run from 0 to 100 on each of the three sides. In the right triangle, the axes increase in a counter-clockwise direction; the axis restarts to zero at each apex; in the left triangle, the axes increase in a clockwise direction; restarting at zero at each apex. For each sample, there are three variables to determine the plotting position in each triangular plot, for example the axes may be the three major cations (left) and anions (right) and the variables are the cation/anion composition of the

71

sample. Each of the three cation/anion variables, in milliequivalents, is divided by the sum of the three values, to produce a percent of total cations. For example, if Ca= 0.80 meq, Mg =0.26 meq, and Na+K = 0.89 meq, then % Ca = 41, % Mg = 13, and % Na+K = 46. The data points in the parallelogram are located by extending the points in the lower triangles to the point of intersection in the parallelogram. The axis values at the top and bottom of the parallelogram are 100; the axis values on the left and right side of the center field are zero.

3.3.10 Thermal Gravimetric Analysis

A METTLER TOLEDO TGA/SDTA 851e with sample robot and a TSO800 GC gas control unit was used.

3.3.10.1 Procedure

The required weight of the sample was loaded via sample robot on to the pan. Analysis was done with 30 ml reactive gas (Ar in this study) using a heating rate of 10 °C/min up to 900 °C. Nitrogen was used as the protective gas at a flow rate of 35 ml/min.

3.4 STATISTICALLY DESIGNED CARBONATION EXPERIMENTS

The statistical design of experiments (DOE) was employed in the study to optimize the carbonation conditions during FA/brine/CO_2 interaction. The input variables considered were pressure, temperature, particle size and S/L ratio. A D-Optimal design which allows one to choose any number of levels (Montgomery, 2009) for each categorical factor was chosen as the factors were at mixed levels. The following is the procedure of setting up a D-optimal design in the Design-Expert software:-

1) Select the number of factors and their levels.
2) Select the model that you want to fit with the Edit Model button (Quadratic is usually the default model).
3) Enter the names of the responses and click to continue, this is what happens internally:

a) Design-Expert creates an overall candidate point set (many possible runs that would work) depending on the model chosen.

b) Design-Expert chooses specific design points (the runs that the experimenter will do), including replicates.

c) Design-Expert does step (3b) several times (5 by default) and then compares the d-optimality value of the 5 designs created. It outputs the best of the 5 designs.

3.4.1 Justification for the chosen input parameters

In this study the input variables considered were particle size, S/L ratio, temperature and pressure while % $CaCO_3$ was the output variable. Both temperature and pressure were at two levels (30 °C and 90 °C; 1 Mpa and 4 Mpa), S/L ratio was at three levels (0.1, 0.5 and 1) while particle size was at four levels (bulk ash, <20 μm, 20 μm -150 μm and >150 μm). The design can therefore be referred to as a $4X3X2^2$, which simply translates to 1 factor at 4 levels, 1 factor at 3 levels and 2 factors at 2 levels. Table 3.2 shows the generated design using Design-Expert. The range of particle size was advised by relative amount of CaO in the different fractions that had been obtained through fractionation as described in section 3.2. The results of lime partition are present in Tables 4.1 and 4.2 as well as Figure 4.7 and the reader is referred to them. The intention was to compare the carbonation efficiency of the bulk ash and the fractionated ash. The 20 μm -150 μm particle size fraction had a fairly equal amount of CaO averaging out to 9.3 wt %. It was also interesting to evaluate the carbonation efficiency of the smallest particle size available i.e. <20 μm fraction. For the pressure, the interest was to observe the effect of low and moderate values thus 1 Mpa and 4 Mpa were investigated. At a temperature of 150 °C initially chosen, pressure build up was observed in the rector and this led to a back flow of the liquid when the gas valve was opened. This caused the regulator to malfunction and a temperature below the boiling point of water was thus settled on. In this case, 30 °C and 90 °C were settled upon. S/L ratios at low, medium and high values were chosen to investigate their effects on the carbonation efficiency. The D-optimal design

generated using Design Expert is given in Table 3.2 showing all the input variables, their units and their different levels as well as the input variable.

Table 3.2: The D-optimal design generated using Design-Expert 7 (<150 represent the 20 µm-150 µm particle size range)

	Factor 1	Factor 2	Factor 3	Factor 4	Response 1
Run No.	A:Pressure Mpa	B:Temperature °C	C:Particle size µm	D:S/L ratio g/ml	% CaCO₃ (wt %)
R1	1	90	<20	0.5	
R2	1	90	<150	0.5	
R3	4	90	Bulk	0.1	
R4	1	30	<20	0.5	
R5	4	90	>150	0.5	
R6	1	90	<150	1	
R7	1	90	>150	0.1	
R8	1	30	<150	0.1	
R9	4	90	<150	0.1	
R10	4	30	Bulk	0.5	
R11	4	90	<150	0.1	
R12	1	30	Bulk	0.1	
R13	4	30	<150	1	
R14	4	90	<20	1	
R15	4	90	>150	1	
R16	1	30	Bulk	1	
R17	1	30	<20	0.5	
R18	1	30	<20	0.1	
R19	1	30	>150	0.5	
R20	4	30	Bulk	1	
R21	4	90	<20	0.5	
R22	4	30	<20	1	
R23	1	30	Bulk	0.5	
R24	4	90	<20	0.1	
R25	4	30	>150	0.1	
R26	1	90	<150	0.1	
R27	1	90	Bulk	0.5	
R28	4	30	<150	0.5	
R29	1	30	>150	0.1	
R30	1	90	>150	1	
R31	4	90	Bulk	1	
R32	4	30	>150	1	

Notice that the response parameter (% CaCO$_3$) is empty as this is the design before the runs were carried out.

3.4.2 Procedure

The carbonation reactions were carried out in an autoclave reactor made of stainless steel and with a 600 ml volume capacity. The brine and FA were contained in a teflon liner which was immersed in the steel jacket. A schematic of the reactor is shown in Figure 3.3 while the reactor assembly is given in Figure 3.4.
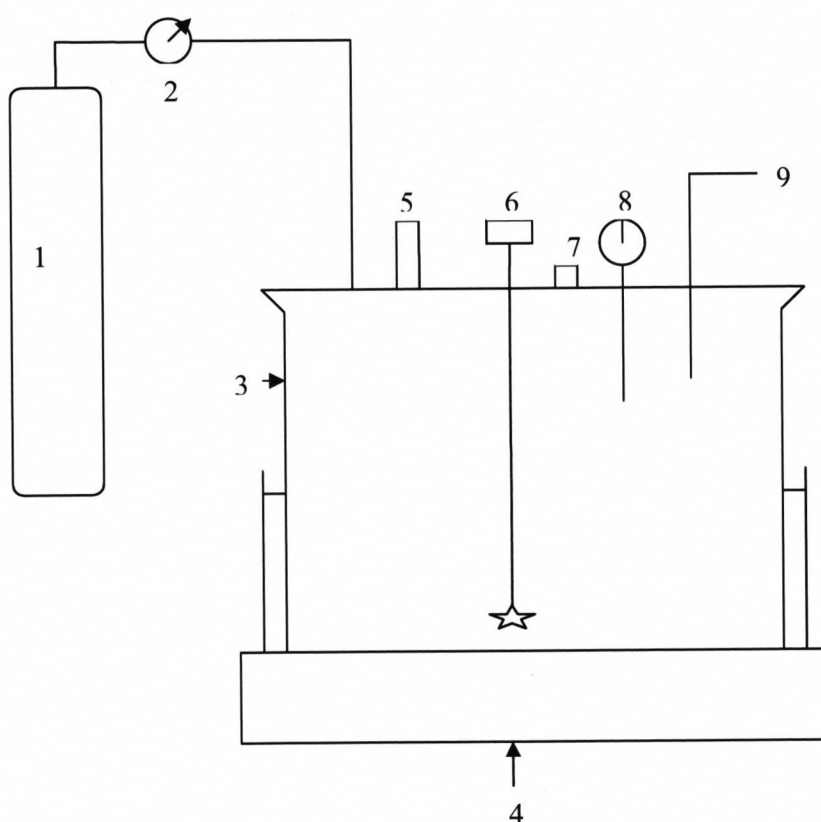
Figure 3.3: Schematic of the high pressure reactor

1) Carbon dioxide cylinder
2) Pressure regulator
3) Stainless steel reactor vessel (maximum temperature= 350 °C with a teflon liner, maximum pressure = 345 bars)
4) Heating jacket
5) Pressure relief valve
6) Stirrer powered by a magnetic drive
7) Thermocouple

8) Pressure gauge
9) Liquid sampling valve

Figure 3.4: The autoclave reactor used in the study and the assembly consisting of the controller, mount and gas cylinder (manufactured by Parr Instruments).

A 600 ml Parr high pressure/high temperature reactor (model series 4560, stainless steel, custom 1.5 in. internal diameter) was used to conduct reactions between FA, CO_2 and brine. A total of 32 experimental runs were conducted with specified levels of each variable as set out in Table 3.2. Two different temperatures of carbonation were used (30 °C and 90 °C) while the pressure was varied between 1 Mpa and 4 Mpa. The following fractions of the FA were used; < 20μm, 20 μm-150 μm, >150 μm and the bulk ash. To investigate the influence of solid/ liquid (S/L) ratio on carbonation, S/L ratios were varied between 0.1, 0.5 and 1. The dispersion (brine + FA) was placed inside the teflon liner in the pressure vessel and closed. Following the sealing of the pressure vessel, the body of the reactor was placed in the heater assembly and the thermocouple, magnetic stirrer drive system, and water coolant supply controlled by a solenoid valve were put in place. The gas supply connection for the CO_2 feed line was then attached. The system was then purged three times with CO_2 at 0.05 Mpa to ensure that all the air was expelled. After the final purge, the heating of the system began. When the specified temperature was reached, CO_2 (technical grade) was charged into the reactor to achieve the specified testing pressure. The brine/FA/CO_2 mixture was then stirred at 600 rpm for 2 hours to prevent any settling of solids during the experiments. At the end of the experiment, the reactor was removed from the heating system and was quenched in cold water. The reaction cell was

depressurized for 15 minutes during the water cooling period. Upon cooling to room temperature, the reactor was disassembled, and the solid product was separated by centrifugation (30 minutes at 6000 rpm), thereafter the supernatant solutions were decanted. Finally, the solid product was dried in an oven for 8 h at 90 °C. The supernatant solutions were filtered through a 0.2 μm pore membrane. The filtered solutions for cation analysis were immediately acidified to pH < 2 while those for anion analysis were stored as they were i.e. without acidification. The samples were stored in the fridge at 4 °C awaiting analysis. The concentration of the major elements, minor and trace elements was determined using ICP-MS. The anions were analyzed using IC. The pH was also measured in the filtered solutions prior to acidification.

Mineralogical and elemental characterization of the solid residues was done using XRD and XRF, while morphological analyses were done using SEM-EDS. The carbonate content of the solid residues was determined using quantitative XRD, Chittick tests and thermal gravimetric analysis.

The optimized input variables were then used to run the carbonation experiments replacing brine with ultra-pure water to provide a baseline for the carbonation experiments. Also studied during this experiment was the effect of time in the carbonation experiment. Since the carbonation had been carried out at a constant two hours, a value that had been derived from literature (Perez-Lopez et al., 2008), the time factor was studied for the leaching of CaO from FA as it is the rate determining reaction (Soong et al., 2006).

3.5 SECTION SUMMARY

Chapter three has clearly outlined all the analytical and wet analysis techniques used in the study. The results thus obtained will be discussed in the following sections where chapter four, will discuss the characterization of fresh FA and brine while chapter five will discuss the results of the statistically designed carbonation experiments.

CHAPTER FOUR

CHARACTERIZATION OF FLY ASH AND BRINES

4.1 INTRODUCTION

This chapter presents and discusses the results obtained from the physical, mineralogical and chemical characterization of fresh ash and brine effluents from the coal fired power plants. The FA and brine were later applied as the raw materials for the carbonation experiments. Different techniques such as SEM-EDS, XRD, XRF and TGA were used to characterize the FA and the carbonated residues as described in sections 3.3.1, 3.3.2, 3.3.3 and 3.3.10, while IC and ICP-MS were used to characterize brine and the carbonation leachates as described in sections 3.3.4 and 3.3.5.

4.2 PHYSICAL, CHEMICAL AND MINERALOGICAL COMPOSITIONS

Size fractionation of the fresh Tutuka and Secunda FA was carried out as specified in section 3.2, to check for differences in the composition of the different FA size fractions in terms of major, minor and trace elements. Mass % distribution by particle size within the chosen range (<20 μm to >150 μm) for the two FA types (Tutuka and Secunda) was calculated by weighing the FA on each sieve and dividing with the mass that had been used for the sieving, giving the following range as shown by Figure 4.1.
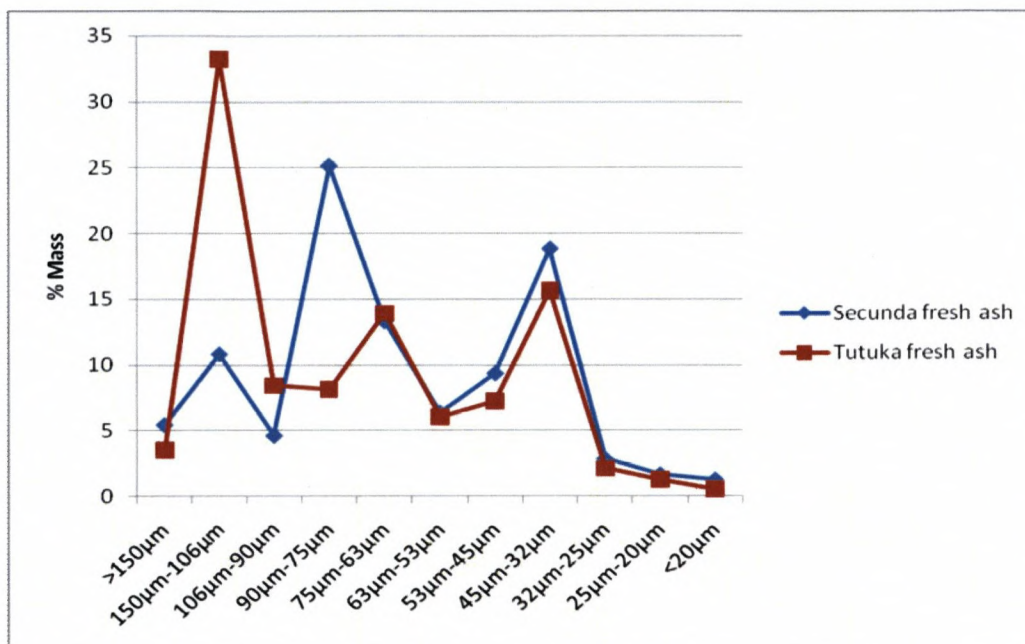
Figure 4.1: Size distribution of Secunda and Tutuka FA

The results of the particle size fractionation whose procedure is given in section 3.2 indicate that 78.53 % of the Secunda fly ash and 54.84 % of the Tutuka FA lie within the fraction below 75 μm (Figure 4.1). Thus Tutuka ash was found to be coarser than Secunda FA with the major fraction being over 90 μm in size. This was also reported by Foner et al., (1999) who found that 89.8 % of the South African FA lies within the fraction below 75 μm. A tri-modal distribution can also be observed over the size range selected. Goodarzi, (2006) observed that particles of FA emitted from stacks consisted of three size fractions, specifically $PM_{>10}$, PM_{10} and $PM_{2.5}$. The author further shows that $PM_{2.5}$ particles have a bimodal size distribution with mean diameters of 0.05μm and 2.50 μm and that volatile elements such as Cd, Pb and S are commonly enriched on the surface of these particles.

4.2.1 Morphological analysis by Scanning Electron Microscopy-Electron Dispersive Spectroscopy (SEM-EDS)

The morphology of FA was studied as described in section 3.3.1 to observe the difference in particle morphology between the fresh and the weathered ash. The

79

weathered ash samples were from Tutuka power plants which had been obtained by air coring. The fresh ash on the other hand had been collected from the precipitators/bag filters of Secunda power plant. The different morphologies are presented in Figure 4.2 below.
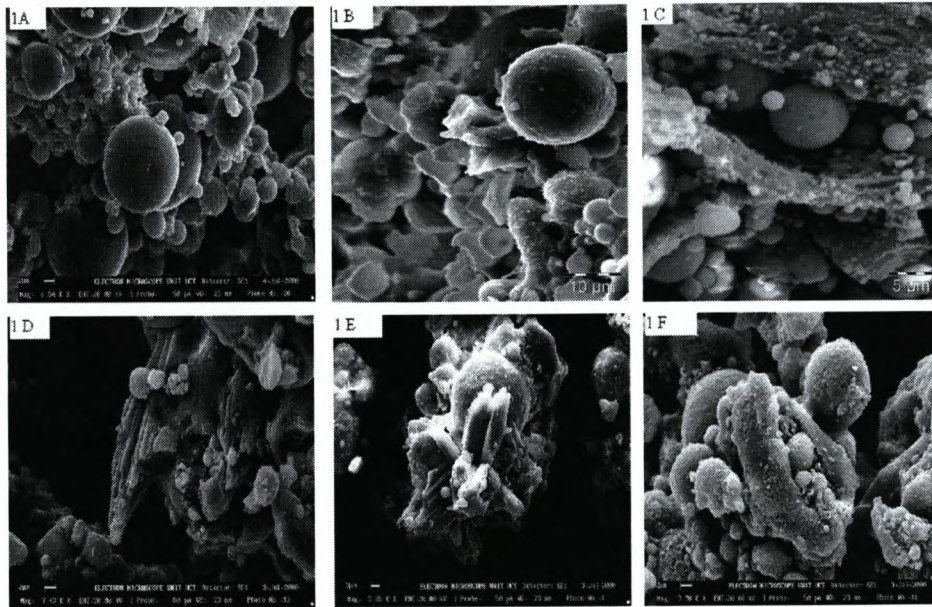
Figure 4.2: Scanning electron micrographs showing the surface morphology of fresh Secunda ashes (1A-1C) and weathered Tutuka fly ashes (1D-1F).

SEM images of Secunda FA (1A-1C of Figure 4.2) show that fresh FA particles are usually spherical in shape though some agglomeration can also be observed in 1C of Figure 4.2. According to Saikia et al., (2006), the spherical shape is an indication that the particles were formed under un-crowded freefall conditions and a relatively sudden cooling, which helps to maintain the spherical shape while the agglomerated nature of some particles is an indication that the particles were produced due to high temperature sintering reactions. This is further reported by Li et al., (2003). The outer surfaces of most of the FA particles are observed to be smooth 1A of Figure 4.2. Hollow spheres "cenospheres" are clearly visible in 1B of Figure 4.2 while plerospheres (hollow cavities containing numerous smaller spheres) can be seen in 1C of Figure 4.2. The weathered samples 1D to 1F of Figure 4.2 show the presence of rod-like structures of varying lengths and thickness. This altered morphology could be due to the presence of secondary

minerals phases such as calcite and gypsum which are formed during the weathering process. Major alteration reactions reported during weathering of FA are dissolution/precipitation of salts, glass corrosion, hydration and oxidation reactions of metals or metal oxides, slaking of lime and hardening reactions (cementation and carbonation). The reported alteration/weathering products are anhydrite, ettringite, calcite, iron oxides and hydroxides as well as gibbsite (Speiser et al., 2000).

Three morphologies have been reported in fresh FA: well-rounded solid spheres (as seen in 1A of Figure 4.2); well rounded hollow spheres (1B of Figure 4.2) with thin walls termed as cenospheres and plerospheres (1C of Figure 4.2). The fine fraction fly ash particles are typically well-rounded, solid spheres and the larger particles within the larger size fraction sub-samples contain a few particles up to 0.5 mm with cenospheres common and an occasional plerosphere. Some of the larger particles are vesicular (i.e. made up of small spherical or oval cavity produced by the presence of bubbles of gas or vapour). Pieterson (1993) attributes the origin of the vesicles to generation of gases and vapors such as CO, CO_2, SO_2 and H_2O. Remnants of unburned coal are often found as rounded, somewhat less spherical (irregularly shaped) vesicular grains. During combustion, minerals in coal become fluid at high temperature and are then cooled. In a pulverized coal fired boiler, the furnace operating temperatures are typically in excess of 1400 °C. At these temperatures the mineral matter within coal may oxidize, decompose, fuse, disintegrate or agglomerate. Rapid cooling in the post combustion zone results in the formation of spherical, amorphous (non-crystalline) particles. These spherical particles can be clearly observed in 1A of Figure 4.2. Expansion of trapped volatile matter can cause the particle to expand to form a hollow cenosphere as observed in 1B of Figure 4.2. These are filled with nitrogen or carbon dioxide and they give FA its light weight. Cenospheres vary in particle size from 20-200 μm and can compose up to 20 % by volume of the ash. Minerals with high melting points may remain relatively unchanged hence appearing as unburnt particles (Kutchko and Kim, 2006). Morphological analysis of FA is of importance as morphology has a bearing on the leachability of heavy

metals. Ramesh and Koziński (2001) in their study on morphology of FA and its relationship with heavy metal release found that the presence of a non-porous continuous outer surface and a dense particle interior may prevent heavy metal leachability from the FA.

It can be concluded that Secunda fresh FA is made up of spherical particles, cenospheres and plerospheres while the weathered Tutuka ashes are rich in secondary mineral phases. These may be phases such as anhydrite, gypsum and calcite.

4.2.2 Elemental analysis by X-Ray Fluorescence (XRF)

The elemental composition of fresh Secunda and Tutuka FA was determined as specified in section 3.3.3 and the results for the major elements for Secunda ash are presented in Table 4.1 while that for Tutuka are given in Table 4.2. Both the bulk fresh ash as well as the fractionated FA were analyzed separately in order to observe the enrichment of elements either in the bulk or in the different fractions. Furthermore, this information acted as a basis for the carbonation reactions as reactivity would be determined by the relative lime content of the ash used.

Table 4.1: XRF analysis results for major elements given as oxides in % w/w for fresh Secunda FA (values significant to 3 decimal points).

Majors (wt %)	Bulk	>150µm	150 µm-106 µm	106 µm-90 µm	90 µm-75 µm	75µm-63 µm	63 µm-53 µm	53µm-45 µm	45µm-32 µm	32 µm-25 µm	25 µm-20 µm	<20 µm
SiO_2	51.227	42.458	50.640	51.770	52.417	52.668	51.400	52.641	52.373	52.709	52.761	51.118
TiO_2	1.548	0.979	1.214	1.333	1.514	1.580	1.616	1.630	1.655	1.684	1.695	1.844
Al_2O_3	26.000	17.968	22.034	24.055	25.270	25.979	27.224	26.355	27.352	26.554	27.353	28.510
Fe_2O_3	2.430	1.984	3.472	2.628	2.756	2.426	2.419	2.280	2.394	2.243	2.245	2.572
MnO	0.061	0.041	0.058	0.062	0.064	0.062	0.063	0.060	0.059	0.065	0.061	0.064
MgO	2.439	1.662	2.342	2.513	2.714	2.534	2.569	2.451	2.499	2.480	2.472	2.624
CaO	9.198	5.894	9.014	9.671	10.286	9.484	9.591	9.261	9.129	8.768	8.498	8.634
Na_2O	0.457	0.146	0.281	0.287	0.355	0.385	0.384	0.466	0.537	0.582	0.558	0.688
K_2O	0.787	0.652	0.778	0.746	0.768	0.778	0.781	0.796	0.815	0.823	0.823	0.872
P_2O_5	0.698	0.438	0.542	0.576	0.691	0.718	0.747	0.755	0.770	0.781	0.777	0.878
SO_3	0.358	0.360	0.261	0.264	0.301	0.351	0.317	0.368	0.375	0.379	0.385	0.395
Cr_2O_3	0.033	0.022	0.029	0.031	0.033	0.034	0.036	0.040	0.038	0.040	0.041	0.041

Table 4.2: XRF analysis for major elements given as oxides in % w/w for fresh Tutuka FA(values significant to 3 decimal points).

Majors (wt %)	Bulk	>150µm	150 µm-106 µm	106 µm-90 µm	90 µm-75 µm	75 µm-63 µm	63 µm-53 µm	53 µm-45 µm	45 µm-32 µm	32 µm-25 µm	25 µm-20 µm	<20 µm
SiO_2	56.943	58.428	61.988	63.072	58.578	56.527	56.003	55.991	55.120	55.873	54.240	51.09
TiO_2	1.434	1.308	1.207	1.173	1.331	1.488	1.479	1.527	1.567	1.489	1.603	1.806
Al_2O_3	24.004	24.194	21.720	20.062	22.709	24.354	24.682	24.922	25.246	24.404	25.094	26.116
Fe_2O_3	5.369	3.932	4.604	5.140	5.066	5.065	5.421	5.090	5.885	5.635	6.439	7.547
MnO	0.062	0.055	0.059	0.061	0.061	0.064	0.072	0.063	0.071	0.068	0.067	0.075
MgO	1.954	1.573	1.681	1.818	1.980	1.968	2.023	1.968	2.053	1.941	2.129	2.391
CaO	6.617	4.616	5.372	6.121	6.839	6.865	6.855	6.726	6.795	6.624	6.725	7.425
Na_2O	0.246	0.162	0.114	0.092	0.148	0.243	0.217	0.239	0.224	0.300	0.349	0.377
K_2O	0.820	1.110	1.059	0.908	0.815	0.784	0.769	0.755	0.774	0.743	0.760	0.775
P_2O_5	0.303	0.219	0.219	0.227	0.265	0.333	0.309	0.333	0.353	0.331	0.365	0.443
SO_3	0.472	0.160	0.157	0.178	0.338	0.568	0.548	0.576	0.585	0.594	0.636	0.744
Cr_2O_3	0.038	0.032	0.030	0.023	0.033	0.038	0.040	0.037	0.040	0.046	0.043	0.052

The results presented in Tables 4.1 and 4.2 show that both Secunda and Tutuka FA contain SiO_2, Al_2O_3, Fe_2O_3 and CaO as the major oxides. The two ashes can therefore be classified as class F since the sum of the percentage composition of SiO_2, Al_2O_3 and Fe_2O_3 is greater than 70 % according to the American Society for Testing and Materials (ASTM 618-1993). Furthermore, the CaO content is lower than 10 % which is also a grading criteria for class F FA. The composition in ash of these four major oxides however varied between the two utilities. The lime content of Secunda FA (9.198 wt %) was greater than that for Tutuka (6.617 wt %). However it was observed that the fraction with the highest lime content in two ashes varied. In the Tutuka ash, the <20 μm fraction had the highest content of 7.425 wt % CaO while in the Secunda ash the 90 μm - 75 μm fraction had the highest content of CaO, 10.286 wt %. Reardon et al., (1995) reported that the basic oxides such as CaO and MgO play an important role in the leaching chemistry of FA and the pH values of its leachates. The higher lime content of Secunda FA thus implies higher pH values in the leachates than that of Tutuka FA. The pH values were 12.67-13.08 for Secunda FA while Tutuka's values ranged from 12.56 to 12.7. This was further confirmed by Fatoba (2007) who had observed that the electrical conductivity of Secunda leachate (7.93-10.46 mS/cm) was higher than that for Tutuka leachates (5.14-7.82 mS/cm). He attributed this to the higher concentrations of the highly soluble oxides present in Secunda FA. Among all the major elements, no clear cut trend of elements partition within the various particle size ranges was observed. Elemental partitioning would mean that the fractions with higher values of CaO and MgO will have higher carbonation efficiencies.

Below are graphs (Figures 4.3 and 4.4) showing the trace elements partition within the different particle size ranges for both Secunda and Tutuka FA. The data is tabulated in Appendices 4 and 5 respectively.
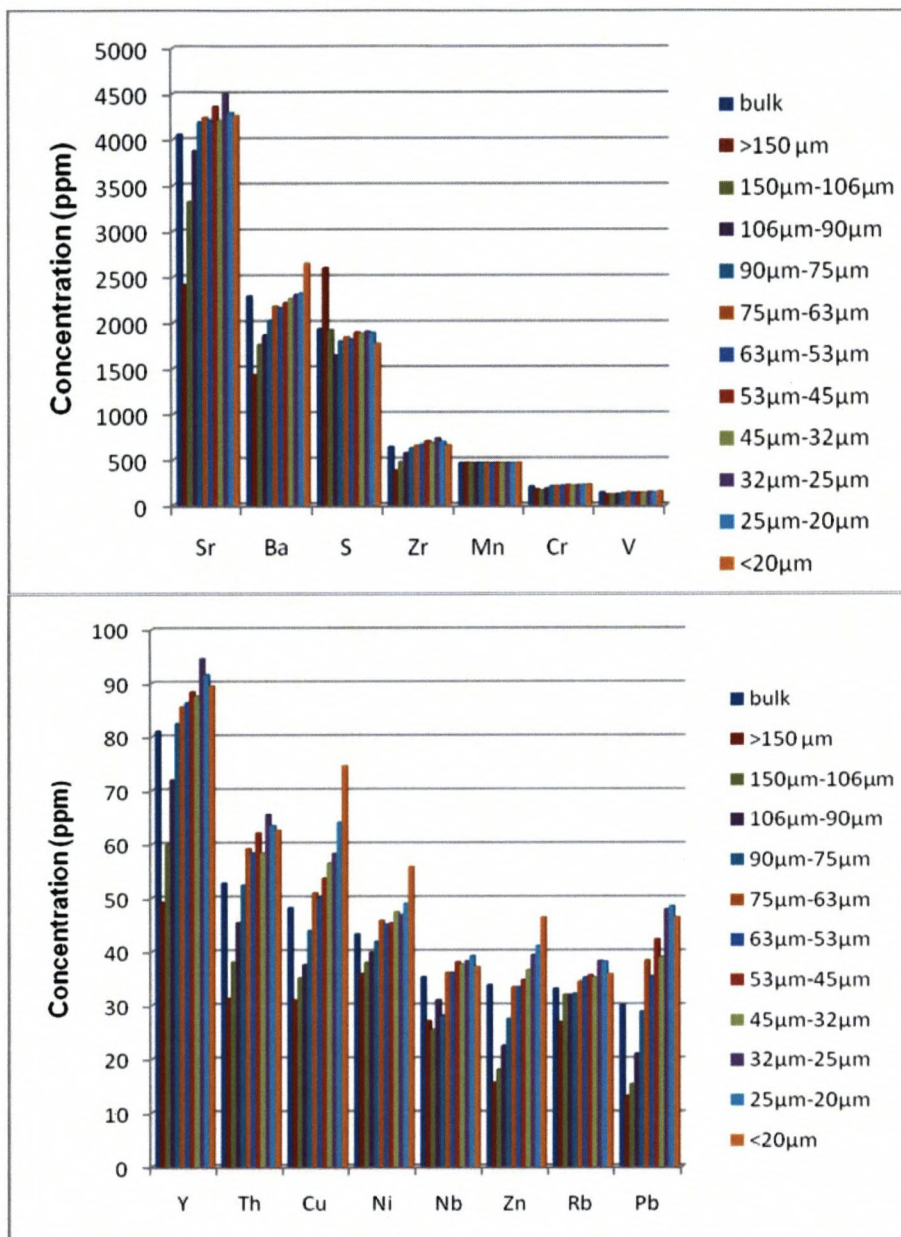
Figure 3: Trace element within the different particle size ranges for Secunda ash
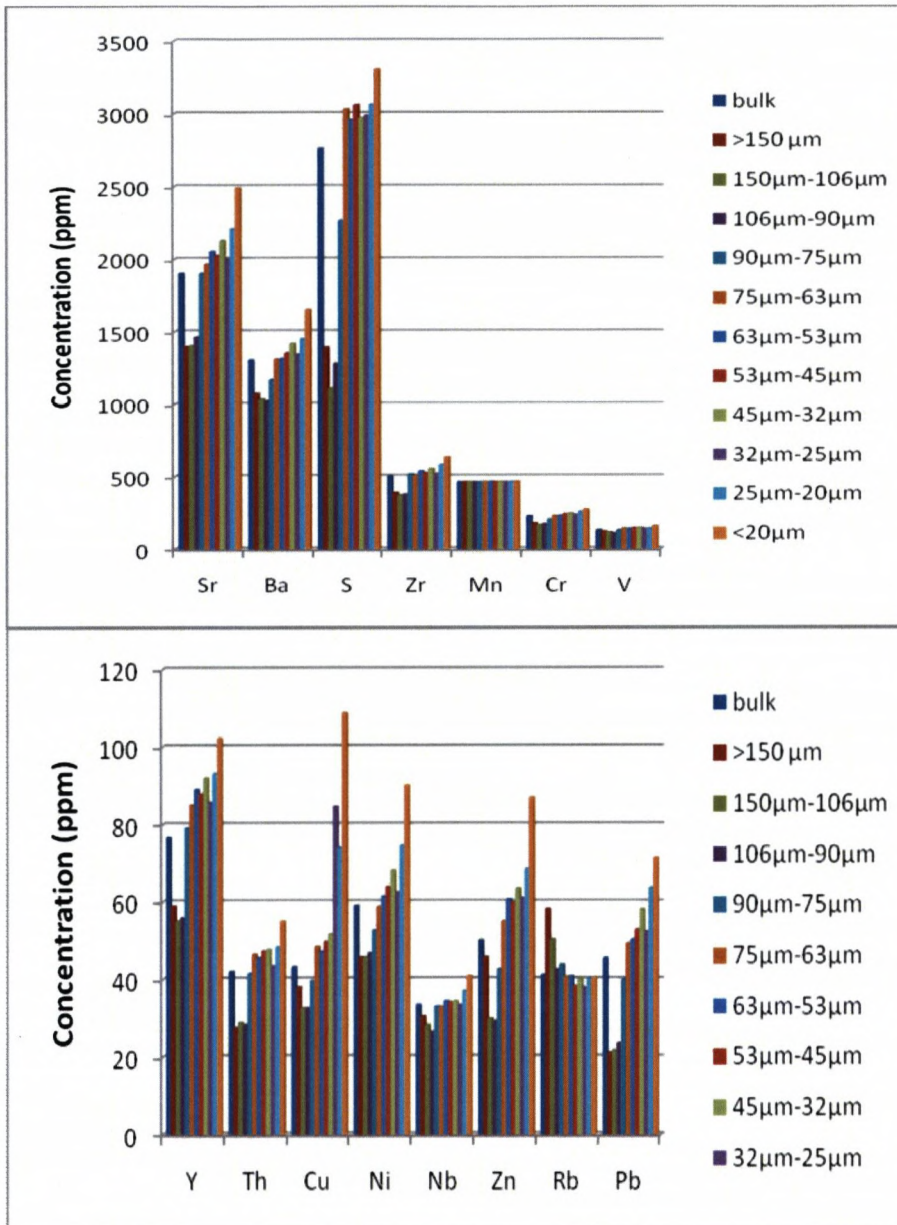
Figure 4.4: Trace element partition within the different particle size ranges for Tutuka ash

In both ashes S, Sr, Ba, Zr, Mn, Cr and V are the main traces present. Though an increasing trend is observed with decreasing particle size for S, Sr, Ba, Zr, Cr and V, Mn shows a constant trend throughout the chosen particle size range. The very high content of these traces seems to dwarf the other traces whose partition also follows the increasing trend with decreasing particle size. It is also evident that the bulk ash had lesser concentration of all the trace elements unlike the smaller

fractions. Based on the degree of concentration dependence on particle size, the elements can be categorized into three groups namely (a) elements showing a pronounced trend of increased concentration with decreasing particle size viz Sr, Ba, Zr, CR,V,Y, Cu and Pb in Secunda ash while in Tutuka FA it is S, Sr, Ba, Zr, Cr, V, Y, Ni, Zn, Pb, Cu and Th. (b) Elements showing limited concentration trends viz Rb and Nb in Tutuka FA and Nb, Zn, Rb, Ni, Th and S in Secunda FA and (c) those elements showing no concentration trends viz Mn in both Tutuka and Secunda FA. The variations in concentration of the oxides and trace elements can be attributed to the difference in the source and type of coals burned in the two stations and the operating conditions of the two plants. This can further vary the mineralogy and chemical compositions of the two FA.

Elements showing greatest concentration dependence with particle size are generally associated with elemental forms that boil or sublime at coal combustion temperatures. Fine particles with their large ratio of surface area to mass preferentially concentrate these elements (Sarkar et al., 2006). Volatilization of the elements at the high combustion temperatures (1400-1600 °C) followed by the condensation on particle surface is the probable mechanism for concentration enhancement. Several studies have noted that the most salient features of FA are the gradation effects of particle size on elemental concentration. Klein et al., (1995); Kaakinen et al., (1975); Davison et al., (1974), observed that As, Cd, Cu, Ga, Mo, Pb, S, Sb, Se, Ti and Zn tend to increase in concentration with decreasing fly ash particle size. The most volatile elements which are the last to condense are partitioned to the smaller particles. Eary et al., (1990) observed that the chalcophillic elements (As, Cd, Cu, Pb, Hg, Se, V, and Zn) which tend to be present as sulphide minerals or associated with the organic fraction in coal, are more strongly volatilized during combustion and tend to become more enriched on smaller particle surfaces than elements associated with silicate and oxide minerals in coal. The less volatile elements (Al, Ba, Ca, Ce, Co, Eu, Fe, Hf, La, Mg, Rb, Sc, Si, Sm, Sr, Ta, Th and Ti) show little tendency to partition according to particle size. There are also elements such as Be, Cr, K, Na, Ni and U which exhibit an intermediate behavior. Other researchers such as Campbell et al.,

(1978); Lee et al., (1975) reported similar effects of particle size on elemental concentrations.

A higher concentration of the trace elements is observed in the Tutuka FA as compared to Secunda FA. This could be explained in terms of its sulphur content which is higher than that of Secunda. Ainsworth and Rai (1987) observed that the concentrations of some trace elements are higher in FA from bituminous coal than other coal types, which is attributed to the sulphide content of the coal. According to Goodarzi, (2006) the volatile elements such as Cd, Pb and S are commonly enriched on the surface of particulate matter 2.5 ($PM_{2.5}$). He suggested that the size of a particle is important because its surface may act as a site for deposition/condensation of volatile elements since the smaller the particle diameter, the greater the surface area relative to volume available for the adsorption of liquid and gaseous materials and that distribution of all elements increase with decreasing particle size. Bosch (1990) investigated some FA from South Africa coal burning power stations and noted that there was a tendency for higher concentration of trace elements in FA to be associated with small particle sizes. The study of the enrichment of trace elements on smaller FA particles has received special attention because (i) they are less efficiently collected by existing control technologies (ii) they have a relatively long atmospheric residence time and (iii) upon inhalation they are efficiently deposited in and slowly removed from the pulmonary region of the respiratory tract (Tarazona et al., 1996). Furthermore elements enriched at the FA surface are likely to be leached during the weathering of ashes disposed of in landfills. The explanation proposed for the observed enrichment trend is that relatively volatile elements vaporize in the high temperature combustion zone under conventional boiler conditions and later condense on the surface of pre-existing ash particles as the combustion gases are cooled.

From the above results it can be concluded that the smaller the FA particle size, the more leachable toxic trace elements present. Furthermore these particles are expected to be most reactive due to the high surface area to volume ratio. This

would thus mean that the trace species therein are more bio-available and prone to leaching in case of rain water percolation which could in turn lead to surface and ground water contamination. Additionally, leaching of Tutuka FA would be more detrimental due to the higher concentration of trace elements when compared to Secunda FA.

4.2.3 Mineralogical analysis by X-Ray Diffraction (XRD)

Phase characterization was done using XRD as described in section 3.3.2. The following diffraction patterns (Figure 4.5) showed that the two FA consist of mullite and quartz as the major crystalline phases. Lime, magnetite and hematite were also observed but with lower peak intensities.
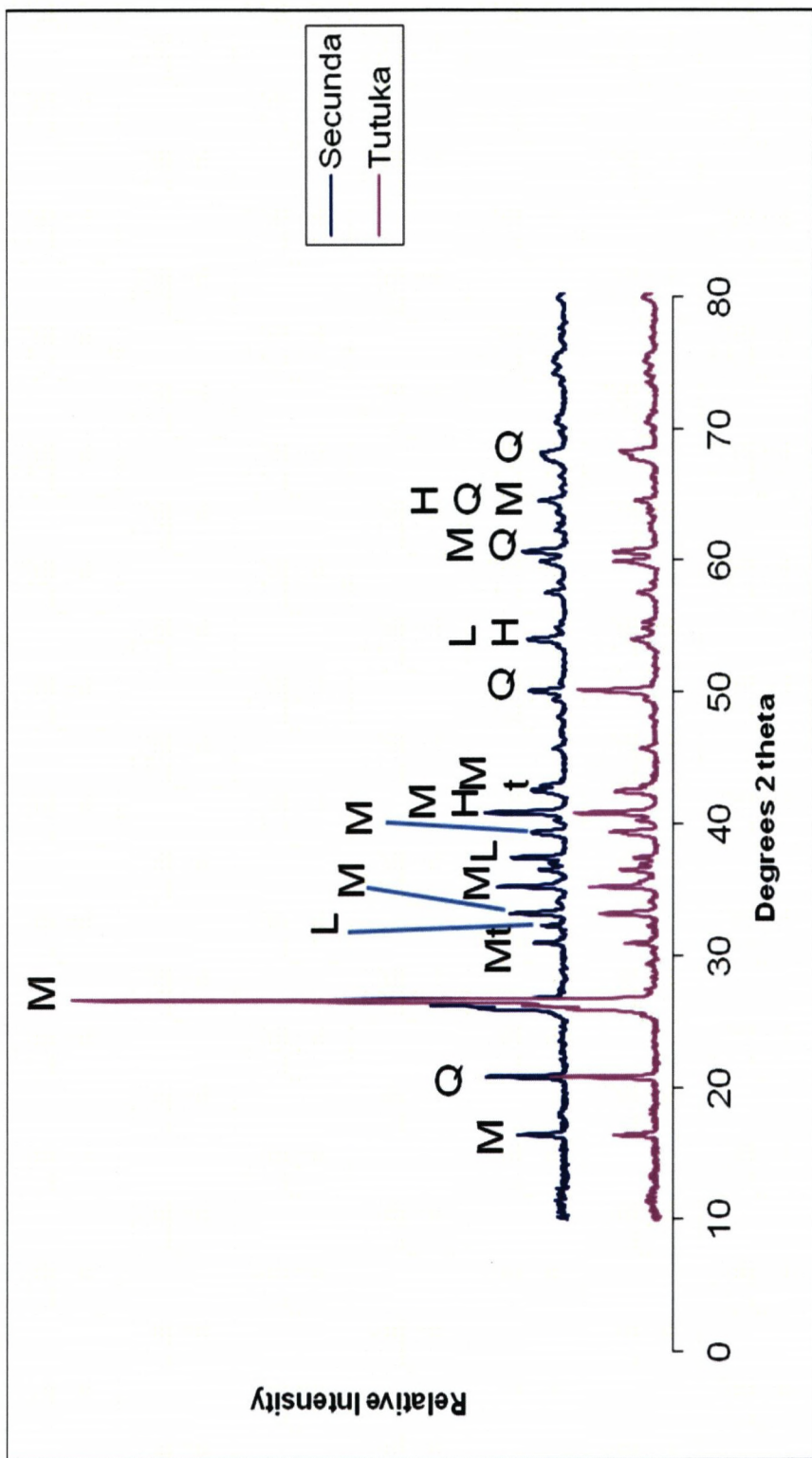
Figure 4.5: XRD spectra of fresh Secunda and Tutuka ashes showing the major phases; mullite (M), quartz (Q), lime (L), hematite (H) and magnetite(Mt).

The mineralogy of the two FA is similar with major phases observed being mullite, quartz, lime, hematite and magnetite. The XRD spectra agree with the results of XRF analysis (Tables 4.1 and 4.2) which showed high percentages of the oxides of Si, Ca, Fe and Al since these elements are the major components of the mineral phases observed in the XRD. However one notes that qualitatitive XRD is not such a powerful tool compared to XRF as one cannot infer on the relative amounts present for each element. This is only possible with quantitative XRD. Figure 4.6 below shows the partition of the crystalline phases between the bulk ash and the lowest size fraction attained i.e. <20 μm as determined by quantitative XRD.
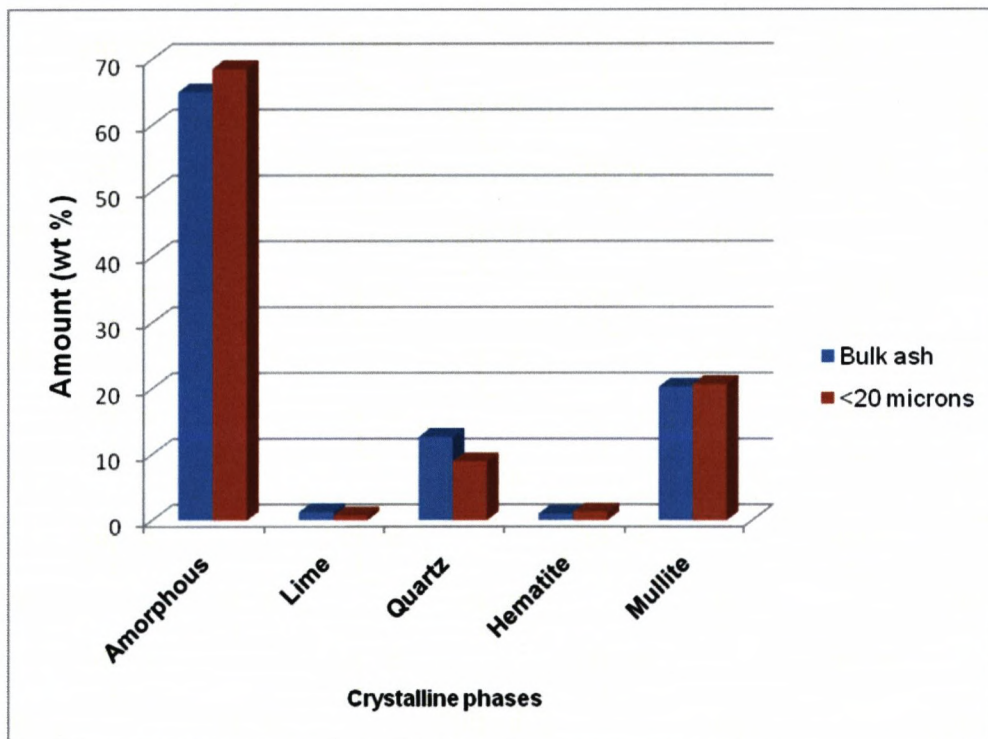
Figure 4.6: Major crystalline phases partition between the bulk ash and the <20 microns.

The bulk ash is richer in quartz and lime while the <20 μm ash fraction is enriched in the amorphous, hematite and mullite phases (Figure 4.6). The higher lime content of the bulk ash would imply greater buffering capacity as well as carbonation efficiency. According to Matsunaga et al., (2002), crystallinity

increases with increasing particle size for precipitator FA while the reverse is true for cenospheres. According to them, the dependence of crystallinity on the size of precipitator FA particle size is probably due to the differences in cooling rates between small and large FA particles. The cooling rate in smaller particles is likely to be faster due to higher surface to volume ratio. If transient time is similar for all particle sizes, then the small particles are quenched into the glassy phase while the interior of the large particles cool much more slowly allowing time for crystallization to take place. Therefore, the large particles will have a much higher crystalline to glassy ratio.

Below is a plot of the variation of CaO content within the different particle size ranges as determined by XRF (Figure 4.7).
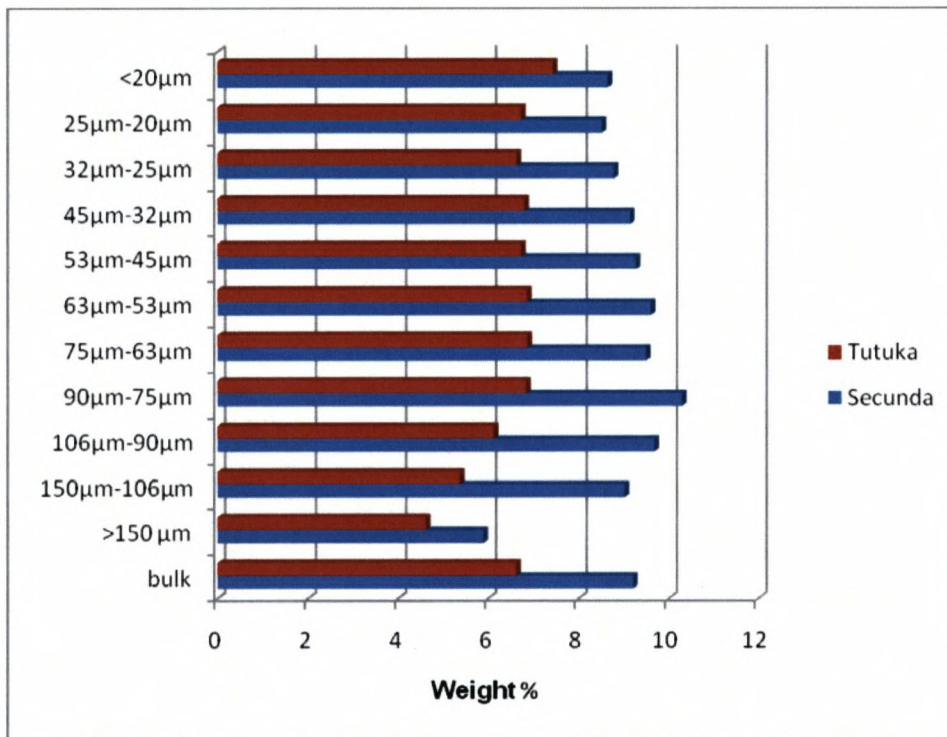
Figure 4: Variation of the CaO content with particle size

From Figure 4.7 it is apparent that the CaO content for Tutuka FA increases with decreasing particle size in the > 150 to <20 microns range. This is however not clear with Secunda FA and the highest content is observed in the 75-95 microns range. When it comes to the bulk ash, Secunda has a higher CaO content

92

compared to Tutuka FA. This would imply not only a higher buffering capacity from the available CaO but also a higher carbonation efficiency for bulk Secunda ash as opposed to bulk Tutuka ash. Grigorios et al., (2009), in their studies observed that in the >150 μm fraction, the percentage content of CaO and SO_3 is relatively low while the components of the difficult to crush materials (SiO_2, AlO_3) occur in significant quantities. They further observed that in the <75 μm there is substantial presence of CaO because of the easy to crush limestone minerals that occur in the feed coal. Additionally, the thermal disruption of calcite explains the significant occurrence of free lime. Their observations are in agreement with this study for Secunda FA.

4.3 RESISTIVE TOMOGRAPHY

Resistive tomography was carried out according to the procedure outlined in section 3.3.8 to investigate how the two ash disposal techniques i.e. dry and wet ash disposal are likely to affect the underlying bedrock and the leaching potential thereof. Figures 4.8 and 4.9 below show the resistive tomograms for Secunda and Tutuka ash dumps.
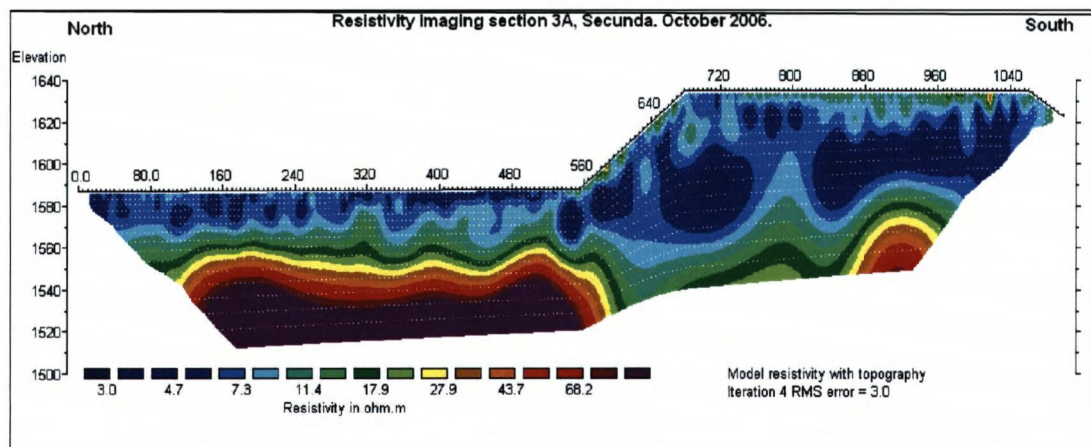
Figure 5: Resistivity tomogram of Secunda ash dump

It is assumed that the site is underlain by a Karoo dolerite and that no ash was dumped north of the existing dump in the past. Modeled resistivity between 3 and 10 Ohm (approximately) (Figure 4.8) can be associated with highly weathered dolerite (clay) as well as ash. This is clearly visible on the profile where the

boundary of the ash dump is visible. The red–brown contours are associated with less weathered to fresh dolerite. Between 560 and 880 meters, the red brown contours are not present, this implies that the ash leachate is in direct contact with the bed rock and hence there is massive potential for ground water pollution.
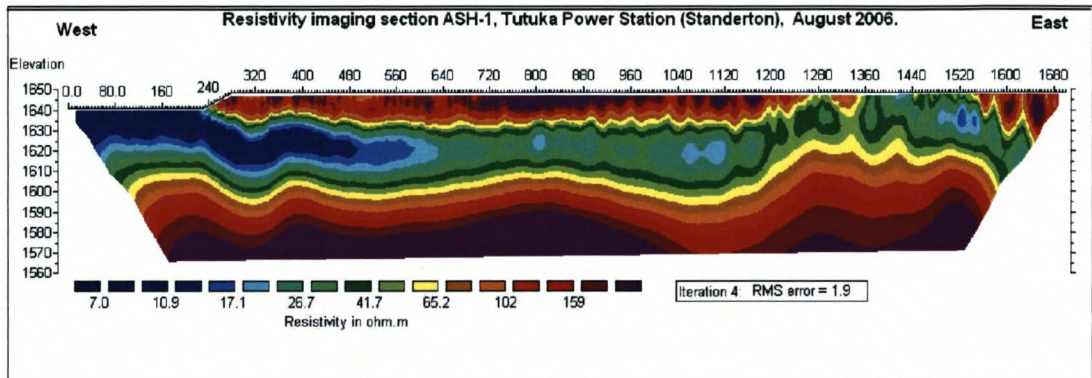
Figure 4.9: Resistivity tomogram of Tutuka ash dump

Contrary to the Secunda tomogram, the bed rock is clearly visible in the Tutuka tomogram (red-brown contours) and it is evident that disposal is taking place at the western side between 240 and 80 meters. The area is highly conductive, which is from brine irrigation for the dust suppression operations and sluicing of the dump to prevent wind erosion. There is no direct contact of the ash leachate with the ground water systems due to the presence of the bed rock and therefore one can conclude from the above tomograms that the dry disposal technique is less harmful in terms of potential ground water pollution as opposed to the wet disposal technique.

4.4 BRINE CONCENTRATIONS IN TUTUKA AND SECUNDA

The brines were analyzed as described in sections 3.3.4 and 3.3.5. The results for the major cations and anions are presented in Tables 4.3 and 4.4 below. Their analysis was necessitated by the need to understand their composition as they formed part of the reactants to be used in the carbonation reactions. Moreover the brines are used either to transport the ash (in the case of Secunda) or to condition the ash and for dust suppression (in the case of Tutuka).

Table 4.3: Major, minor and trace cations and anions concentration in Tutuka brines. (* means element not detected)

	RO brine (ppm)	RO permeate (ppm)	Brine after contact with ash (ppm)	VC brine (ppm)	VC permeate (ppm)
Na	4315	137.09	4358.62	23581.62	2.12
K	104.1	3.38	120.93	581.32	0.04
Ca	101.76	1.97	503.16	557.04	0.16
Mg	158.73	2.25	1.28	658.08	0.04
Cl	2036	115.12	2071.17	11147.1	0.34
SO_4	9488.91	132.47	7058.05	36464.5	3.06
NO_3	8.565	1.563	9.95	37.45	*
PO_4	4.690	0.1	19.9	24.9	*
Al	0.044	0.003	0.807	0.627	0.007
As	0.007	*	0.016	0.034	*
Ba	0.055	0.005	0.558	0.509	0.032
Cd	*	*	0.055	0.063	*
Co	0.015	*	0.007	0.048	*
Cr	0.014	0.001	0.217	0.260	*
Cu	0.067	0.005	0.006	1.079	*
Fe	0.051	0.019	2.507	3.304	0.003
Mn	0.082	0.005	0.032	0.285	*
Mo	0.039	0.001	0.132	0.235	*
Ni	0.116	0.003	0.546	0.670	*
Pb	*	*	0.030	0.042	*
Se	0.004	*	0.005	0.019	*
Sr	3.030	0.051	5.626	16.714	*
V	0.016	*	0.196	0.116	*
Zn	0.100	0.012	0.186	1.246	0.002

The vapour compressor (VC) brine has a higher salt load compared to both the reverse osmosis (RO) brine and the brine/ fly ash make–up. The reason being that VC is used to concentrate the RO brine further before disposal on the ash dumps. The VC permeate has a lesser salt and ions load compared to the RO permeate implying that the VC stage is the polishing stage. This has been reported elsewhere by Petrik et al., (2007).

Table 4.4: Major and trace cations and anions in Secunda brines. (* means element not detected)

	TRO feed water (ppm)	TRO brine (ppm)	TRO permeate (ppm)	EDR feed water (ppm)	SRO brine (ppm)	SRO Permeate (ppm)
Na	1720.29	2487.29	100.34	5599.95	1477.45	1049.95
K	189.65	254.59	14	69.82	131.35	744.99
Ca	616.56	823.36	17.25	1204.62	1160.12	165.41
Mg	22.31	8.24	0.16	673.16	2.29	61.65
Cl	1110.87	1643.78	103.71	969.38	822.62	600.95
SO$_4$	3339.65	4364.38	99.65	12145.45	2407.13	24.5
NO$_3$	9.95	9.95	1.996	24.95	0.959	24.95
PO$_4$	19.9	19.9	0.1	49.9	*	49.9
Al	0.519	0.851	0.18	1.524	0.077	16.599
As	0.022	0.034	*	0.019	*	0.637
Ba	0.34	0.496	0.009	0.45	0.004	16.949
Cd	0.054	0.054	*	0.12	*	0.126
Co	0.006	0.007	*	0.013	*	0.036
Cr	0.227	0.292	0.005	0.415	0.002	0.502
Cu	0.062	0.022	0.003	0.652	0.01	4.144
Fe	3.228	2.911	0.014	6.446	*	60.381
Mn	0.039	0.041	*	0.167	*	2.177
Mo	0.626	0.939	0.02	0.036	0.009	0.062
Ni	0.147	0.168	0.002	0.216	*	0.269
Pb	0.099	0.141	*	0.069	*	49.9
Se	0.073	0.129	0.004	0.01	0.002	0.167
Sr	19.912	27.387	0.571	27.255	0.267	0.595
V	0.046	0.054	*	0.058	*	0.087
Zn	0.371	0.297	0.03	0.652	0.01	4.144

The feed water for tubular reverse osmosis (TRO) has a lower concentration of all the major contaminants as compared to the brine, on the other hand the concentration reduces even further in the permeate from the TRO systems. The spiral reverse osmosis (SRO) permeate is observed to have a higher concentration of both K and Mg compared to the brine. This implies that the two cations are concentrated by the SRO system. According to El-Manharawy and Hafezb (2003), chloride ions control the solubility of carbonate and sulphate ions to a great extent over the range of salinity from <200 mg/l and up to 65000 mg/l. They went ahead and summarized this as follows:- Low Cl$^-$ water types have higher bicarbonate with low SO$_4^{2-}$. Moderate Cl$^-$ water types are low in bicarbonate with relatively high SO$_4^{2-}$. High Cl$^-$ waters are depleted in bicarbonate and enriched with SO$_4^{2-}$.

Their observation is quite evident in Tables 4.3 and 4.4, for instance comparing the brine from the two stations one observes the following: - The Cl^- content of RO brine from Tutuka is 2036 ppm while the SO_4^{2-} content of the same brine is 9488.91 ppm. On the other hand the Cl^- content of SRO brine from Secunda is 822.617 ppm while the SO_4^{2-} content is 2407.133 ppm. Looking at the TRO brine from Secunda, one observes that the Cl^- content is 1643.78 ppm while the SO_4^{2-} content is 4364.38 ppm. Clearly, the SO_4^{2-} content increases with increasing chloride content. Also evident is the fact that the Na, K and Mg contents are inversely proportional to increasing chloride while sulphates increase with increasing chloride concentration.

4.4.1 Brine Classifications

The classification of Tutuka and Secunda brines were carried out using the data in Tables 4.3 and 4.4 and the graphical presentations of the classification are given in Figures 4.10 and 4.11 respectively. This is possible using AqQa software which generates piper diagrams for classification as described in section 3.3.9.
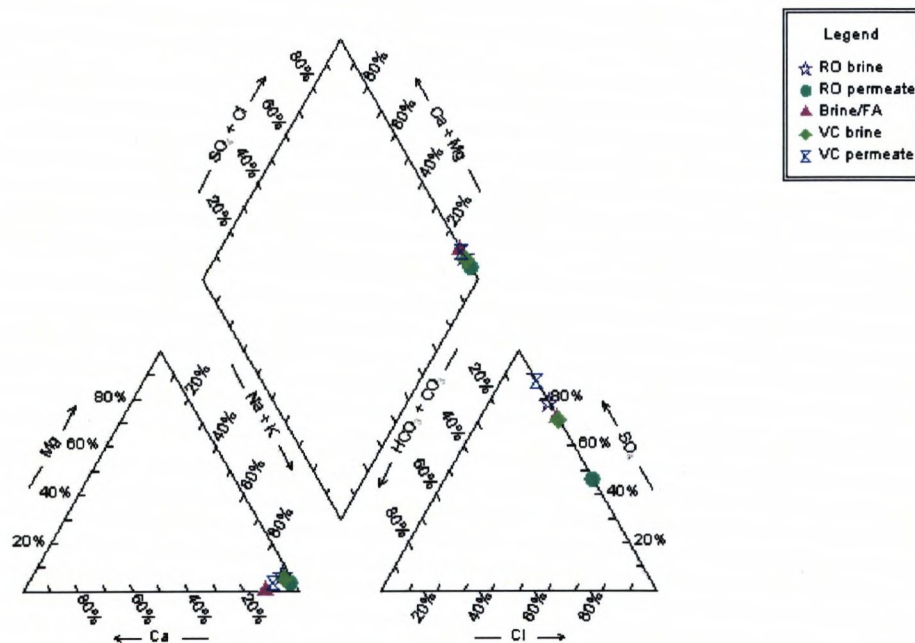
Figure 4.10: Piper diagram of Tutuka brines comparing the RO brine, RO permeate, brine in contact with ash (brine/FA), VC brine and VC permeate.

From Figure 4.10, the RO brine at Tutuka can be classified as a $Na\text{-}SO_4$, RO permeate is a Na-Cl type brine. Brine in contact with ash is a $Na\text{-}SO_4$ brine, the VC brine is a $Na\text{-}SO_4$ type brine while the VC permeate is a $NaHCO_3$ type brine. It is important to note that the brine solutions used for carbonation experiments (section 3.4.2) were the RO brines from Tutuka.
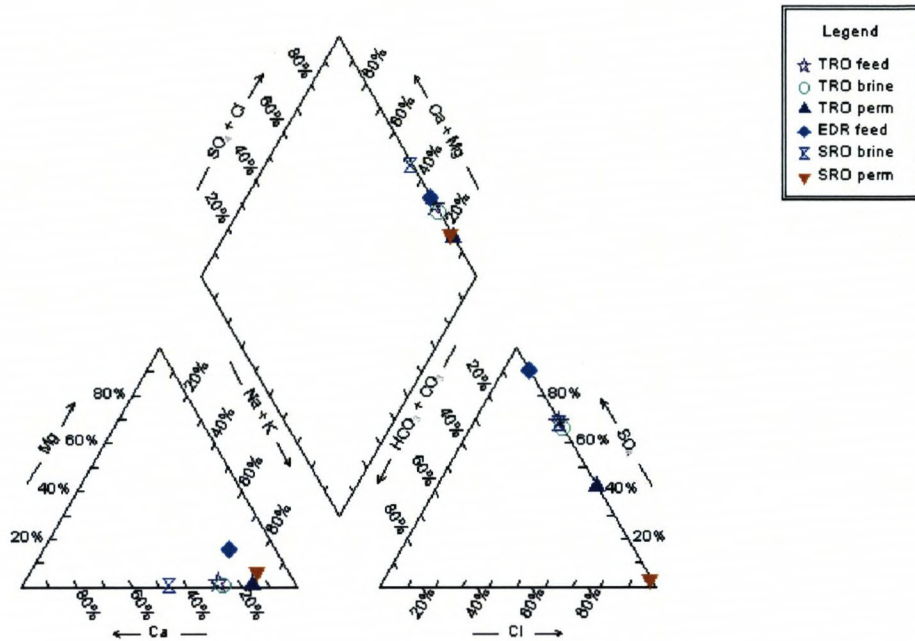
Figure 4.11: Piper diagram for Secunda brines comparing the TRO feed water, TRO brine, TRO permeate, EDR feed water, SRO brine and SRO permeate.

In Figure 4.11, it is shown that the Secunda TRO brine, TRO feed, SRO brine and EDR feed water are all $Na\text{-}SO_4$ types while the TRO permeate and SRO permeate are Na-Cl type waters. El-Manharawy and Hafezb (2003) observed that for high chloride brines, carbonate fouling is rare while sulphate-fouling potential is extremely high. This implies that the high chloride content impinges on the carbonate precipitation while facilitating rapid sulphate precipitation. This could be an important aspect in the carbonation experiments depending on which brine type is used to perform such investigations.

Figure 4.12 below compares the raw brine with brine that has come into contact with ash at Tutuka. This was done to investigate how the major cations and anions are expected to interact with the ash.
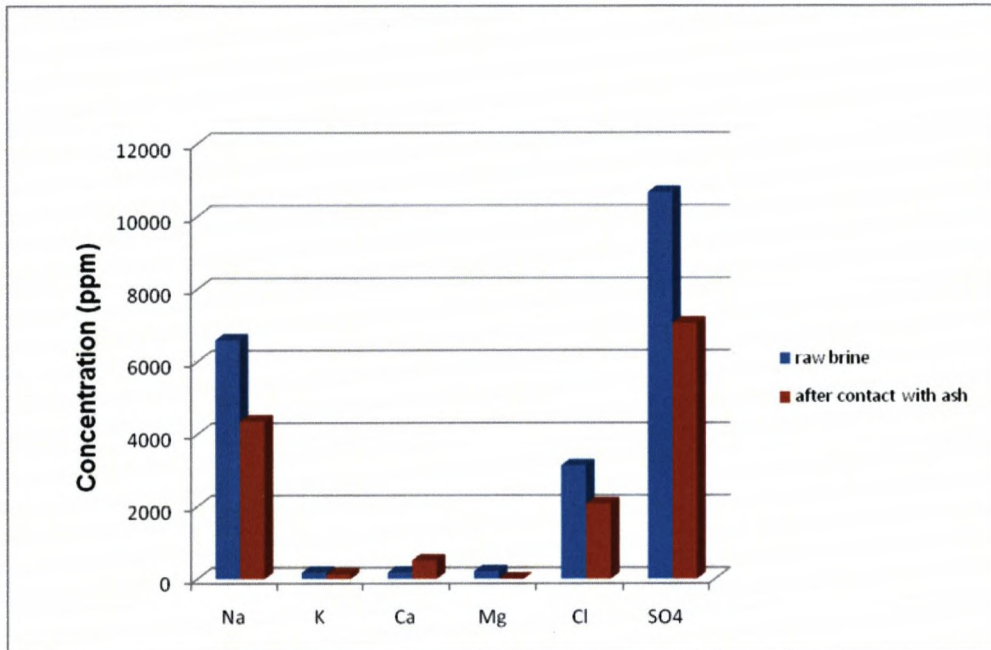
Figure 4.12: Comparison of raw brine and brine after contact with Secunda FA

A comparison of the raw brine and the brine after contacting FA shows a reduction of all the ions in the raw brine with the exception of calcium indicating that the brine components can be trapped within the ash matrix or precipitate as salts on the surface of FA particles. FA is known to be alkaline in nature due to the high content of CaO. The CaO thus acts to increase the brine pH as was observed where the brine pH was 8.48 but after ash addition the pH rose to a value of 11.55. Presence of oxides (CaO and MgO etc) as well as silicates such as $CaSiO_3$ which react rapidly with aqueous media leads to the rapid pH increase (Reddy et al., 1994). Mooketsi et al., (2007) observed that contacting of brine with FA leads to irreversible retention of brine species in the FA matrix, which could lead to an environmentally safe brine disposal option. Accordingly to the authors, brine treated ash residues have improved leachate quality in terms of overall TDS as well as EC, Na, K, Ca, Cl and SO_4 mainly due to the added CaO from fly ash. They postulated that added CaO reacts with the SO_4^{2-} species present

in brine forming insoluble $CaSO_4$ which consumes SO_4 thus reducing the labile form of SO_4 species like Na_2SO_4 in the brine.

4.5 SECTION SUMMARY

The main findings from this chapter are: morphologies of the fresh un-carbonated FA are made up of spherical particles as well as the presence of cenospheres and plerospheres. Secunda FA had the highest % CaO (9.198 %), compared to Tutuka's 6.617 %. It was thus decided that Secunda FA be applied for the carbonation experiments as it would lead to higher carbonation efficiency than Tutuka FA.

Comparison of the bulk Secunda ash and the < 20 μm fraction indicated that the bulk ash had a higher CaO content than the <20 μm fraction. This variation would further be investigated during the carbonation experiments to ascertain whether the bulk ash would have a higher carbonation potential than the < 20 μm fraction.

Wet ash disposal technique used in Secunda has a higher potential for ground water contamination compared to the dry ash disposal technique used in Tutuka. Both Tutuka and Secunda RO brines were $NaSO_4$ type and hence their speciation would be expected to be similar during the carbonation process. However due to the availability of Tutuka RO brine in large quantities as opposed to Secunda RO brine and the other waste waters that had been sampled in small quantities for analysis meant that Tutuka RO brine was utilized in the carbonation process. From this point on, the reader should thus keep in mind that Secunda FA and Tutuka RO brine were carbonated as described in section 3.4.2.

Results of the statistically designed carbonation experiments as well as the effects of carbonation on the FA and brine elemental composition will be discussed in detail in chapter five.

CHAPTER FIVE

CARBONATION OF FLY ASH – BRINE – DISPERSIONS

5.1 INTRODUCTION

This chapter presents and discusses the results obtained from the FA + brine carbonation experiments designed using the Design Expert software as described in section 3.4. The simulated carbonation experiments were carried out according to the procedure in section 3.4.2 to ascertain the ash and brine's capacity to sequester CO_2. Also considered was the effect of carbonation on brine effluent leachate quality as well as its effect on the elemental composition of the FA residues. The input parameters evaluated in the carbonation experiments were particle size (<20 μm, 20 μm-150 μm, > 150 μm and the bulk ash), temperature (30 °C and 90 °C), pressure (1 Mpa and 4 Mpa) and S/L ratio (0.1, 0.5 and 1). Justification for the choice of the different levels chosen is given in section 3.4.1. Sample number descriptions can be found in Table 5.1.

Table 5.1: Input variables for the carbonation experiments (<150 represents the 20 μm-150 μm particle size range)

Run No.	Factor 1 A:Pressure Mpa	Factor 2 B:Temperature °C	Factor 3 C:Particle size μm	Factor 4 D:S/L ratio g/ml
R1	1	90	<20	0.5
R2	1	90	<150	0.5
R3	4	90	Bulk	0.1
R4	1	30	<20	0.5
R5	4	90	>150	0.5
R6	1	90	<150	1
R7	1	90	>150	0.1
R8	1	30	<150	0.1
R9	4	90	<150	0.1
R10	4	30	Bulk	0.5
R11	4	90	<150	0.1
R12	1	30	Bulk	0.1
R13	4	30	<150	1
R14	4	90	<20	1
R15	4	90	>150	1
R16	1	30	Bulk	1
R17	1	30	<20	0.5
R18	1	30	<20	0.1
R19	1	30	>150	0.5
R20	4	30	Bulk	1
R21	4	90	<20	0.5
R22	4	30	<20	1
R23	1	30	Bulk	0.5
R24	4	90	<20	0.1
R25	4	30	>150	0.1
R26	1	90	<150	0.1
R27	1	90	Bulk	0.5
R28	4	30	<150	0.5
R29	1	30	>150	0.1
R30	1	90	>150	1
R31	4	90	Bulk	1
R32	4	30	>150	1

5.2 D-OPTIMAL DESIGN ANALYSIS

Table 5.2 below shows the statistically generated experiments with the input variables and the output factor chosen to monitor the response which in this study was the degree of carbonation as determined by XRD and Chittick analysis. At this point it is important to know that Runs R15, R30 and R32 could not be performed due to the formation of too thick a slurry that could not be agitated. The above three runs were using the >150 μm ash fraction at a S/L ratio of 1. Furthermore no leachate could be obtained from these runs at the end of the experiment and this was important for evaluation of the carbonation effect on the brine effluent quality. Table 5.2 gives the statistically designed experiments showing the input factors and the response factor as determined by Chittick tests and quantitative XRD

Table 5.2: Statistically designed experiments showing the input factors and the response factor as determined by Chittick tests and quantitative XRD (<150 represents the 20 µm-150 µm particle size range).

Run no.	Factor 1 A: Pressure (Mpa)	Factor 2 B:Temperature (°C)	Factor 3 C:Particle size (µm)	Factor 4 D: S/L ratio (g/ml)	Chittick test CaCO$_3$ (wt %)	XRD CaCO$_3$ (wt %)
R1	1	90	<20	0.5	4.92	4.25
R2	1	90	<150	0.5	5.64	8.14
R3	4	90	Bulk	0.1	5.85	5.28
R4	1	30	<20	0.5	4.31	3.99
R5	4	90	>150	0.5	4.69	4.38
R6	1	90	<150	1	5.64	6
R7	1	90	>150	0.1	4.34	3.8
R8	1	30	<150	0.1	4.74	5.22
R9	4	90	<150	0.1	6	5.32
R10	4	30	Bulk	0.5	5.52	4.86
R11	4	90	<150	0.1	6.16	5.32
R12	1	30	Bulk	0.1	4.57	4.96
R13	4	30	<150	1	5.1	5.1
R14	4	90	<20	1	5.14	3.38
R16	1	30	Bulk	1	4.23	3.58
R17	1	30	<20	0.5	4.17	3.16
R18	1	30	<20	0.1	3.38	3.58
R19	1	30	>150	0.5	3.5	2.63
R20	4	30	Bulk	1	4.11	4.08
R21	4	90	<20	0.5	4.62	4.18
R22	4	30	<20	1	4.69	3.3
R23	1	30	Bulk	0.5	4.73	4.64
R24	4	90	<20	0.1	4.96	3.26
R25	4	30	>150	0.1	2.81	0.77
R26	1	90	<150	0.1	6.22	6.4
R27	1	90	Bulk	0.5	5.41	6.96
R28	4	30	<150	0.5	5.68	6.07
R29	1	30	>150	0.1	2.75	1.21
R31	4	90	Bulk	1	6.5	4.99

From Table 5.2 it is evident that for Chittick tests, Run R31 which was carried out at 4 Mpa, 90 °C, S/L ratio of 1 using bulk ash gave the highest % CaCO$_3$ yield of 6.5 % while Run R29, carried out at 30 °C, 1 Mpa, > 150 µm at a S/L ratio of 0.1 gave the lowest % CaCO$_3$ yield of 2.75 %. On the other hand from XRD quantification, Run R2 carried out at 1 Mpa, 90 °C, 20 µm-150 µm at a S/L ratio

of 0.5 resulted in the highest % CaCO$_3$ yield of 8.14 % while Run R25 carried out at 4 Mpa, 30 °C, > 150 µm at a S/L ratio of 0.1 gave the lowest % CaCO$_3$ yield of 0.77 %. These discrepancies will be discussed further in the following sections clearly indicating which results were chosen for the statistical analysis and why.

The following sequence was used in the analysis of the D-optimal design:-

1) Estimation of factors effects so as to gain information regarding which factors and interactions may be important.

2) Formation of the model with both main effects and the arising interactions.

3) Statistical testing using the analysis of variance (ANOVA) to test the significance of not only the main effects but also the interactions.

4) Refining the model by eliminating the non-significant variables from the full model.

5) Analysis of the residuals to check for model adequacy.

6) Finally, interpretation of the results graphically for both the main effects and the interactions.

5.3 CHARACTERIZATION OF THE CARBONATED SOLID RESIDUES

5.3.1 Scanning Electron Microscopy

The solid residues carbonated at 90 °C, 4 Mpa, S/L ratio of 1 using the bulk ash were chosen for the characterization using scanning electron microscopy as these conditions had been observed to lead to the highest % of CaCO$_3$ yield by Chittick tests. The sample preparation and equipment setup was as described in section 3.3.1. Figure 5.1 shows the micrographs of the un-carbonated FA while Figure 5.2 shows the micrographs for carbonated solid residues.
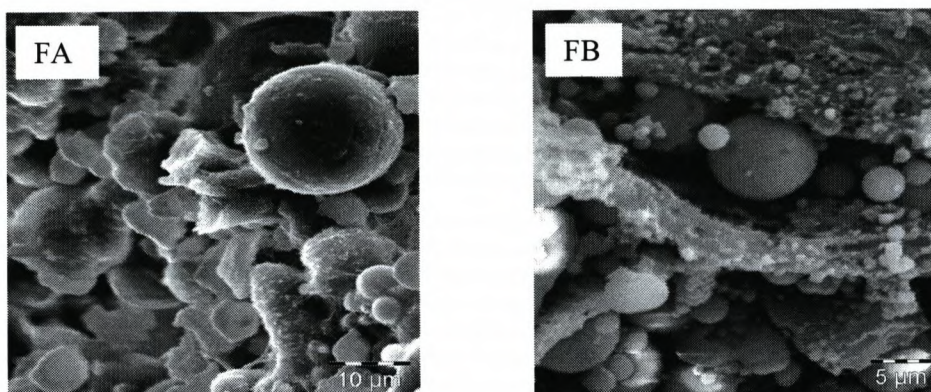
Figure 5.1: Scanning electron micrographs of fresh un-carbonated ash.

Needle-like particles
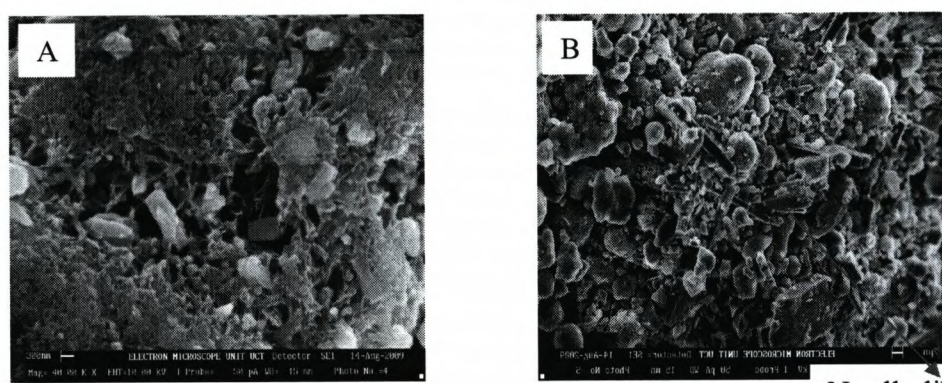
Figure 5.2: SEM micrographs of carbonated FA (Bulk ash, 90 °C, 4 Mpa and S/L ratio of 1).

Micrographs of un-carbonated FA show presence of spherical particles (FA of Figure 5.1), cenospheres (FA of Figure 5.1) and plerospheres (FB of Figure 5.1). The carbonated FA however shows "cubic-like" structure of calcite (A of Figure 5.2), while in Figure 5.2 (B) "needle-like" structures of aragonite are observed. Carbonation thus leads to transformation of the ash morphology due to formation of secondary phases such as calcite and aragonite. Similar morphologies of carbonated FA have been reported by several authors (Perez- Lopez et al., 2008; Montes-Hernandez et al., 2009; Fernandez et al., 2004) who identified calcite as the main polymorph of $CaCO_3$ formed during the carbonation process. However one finds that scanning electron microscopy at best can only give qualitative data and thus cannot be used to quantify the amount of $CaCO_3$ formed in the carbonation process. Other characterization techniques such as quantitative XRD,

Chittick tests and thermal gravimetric analysis were carried out as described in sections 3.3.2.3, 3.3.6 and 3.3.10 respectively to quantify the CaCO$_3$. The results obtained are presented in the following sections.

5.3.2 X-ray diffractometry

Both qualitative and quantitative XRD were carried out to identify the phase transformation due to carbonation as well as to quantify the different phases present in the carbonated solid residues. Sample preparation and equipment setup are described in sections 3.3.2 and 3.3.2.3 respectively.
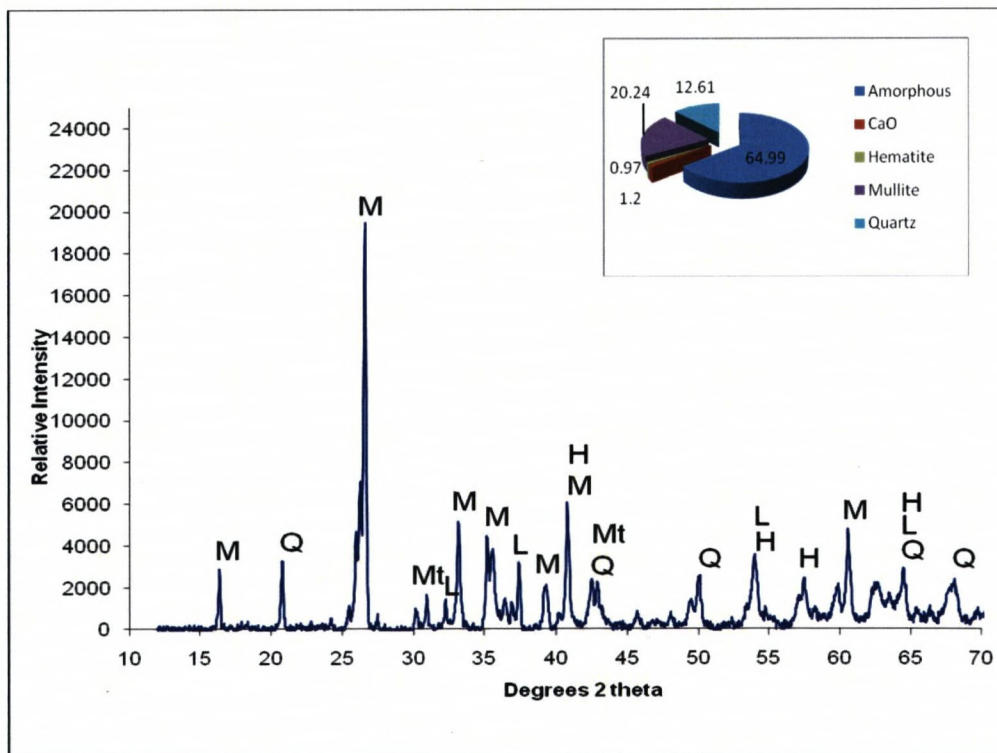
Figure 5.3: Phase identification and quantification in the pre-carbonated ash; M (mullite), Q (quartz), Mt (magnetite), L(lime), H (hematite)
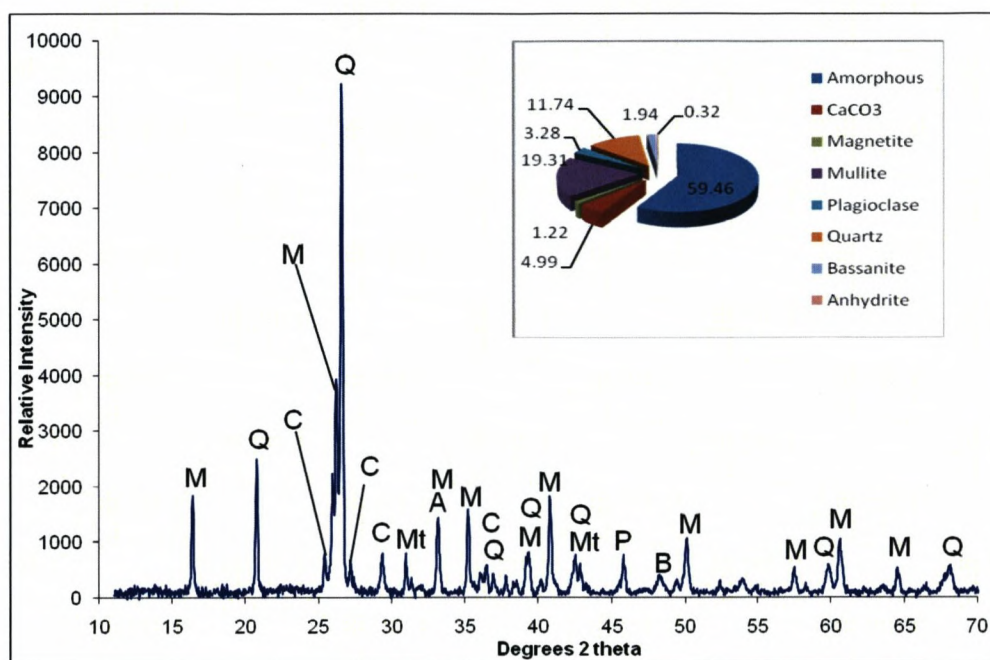
Figure 5.4: Phases identification and quantification in the post-carbonated FA (90 °C, 4 Mpa, bulk ash at a S/L ratio of 1); M (mullite), Q (quartz), C (calcite), A (anhydrite), P (plagioclase), B (bassanite), Mt (magnetite).

The CaO fraction was present in the pre-carbonated ash (Figure 5.3), but in the post-carbonated ash, the presence of $CaCO_3$ can be observed (Figure 5.4) thus XRD confirmed the conversion of CaO to $CaCO_3$ during the carbonation process.

5.3.3 Quantification using X-ray Diffractometry

After carbonation of FA and brine under the different conditions given in Table 3.2, the residues were characterized using quantitative XRD as described earlier in section 3.3.2.3. This was done to determine the % $CaCO_3$ formed which had been set as the response factor in the formulation of the statistical design. The obtained results are tabulated in Table 5.2 and are graphically presented in Figure 5.5. The mass % results for calcite and aragonite phases, the two polymorphs of $CaCO_3$ identified in the carbonated ash by XRD were used to plot the % $CaCO_3$ yield for each carbonation condition (Figure 5.5).

108
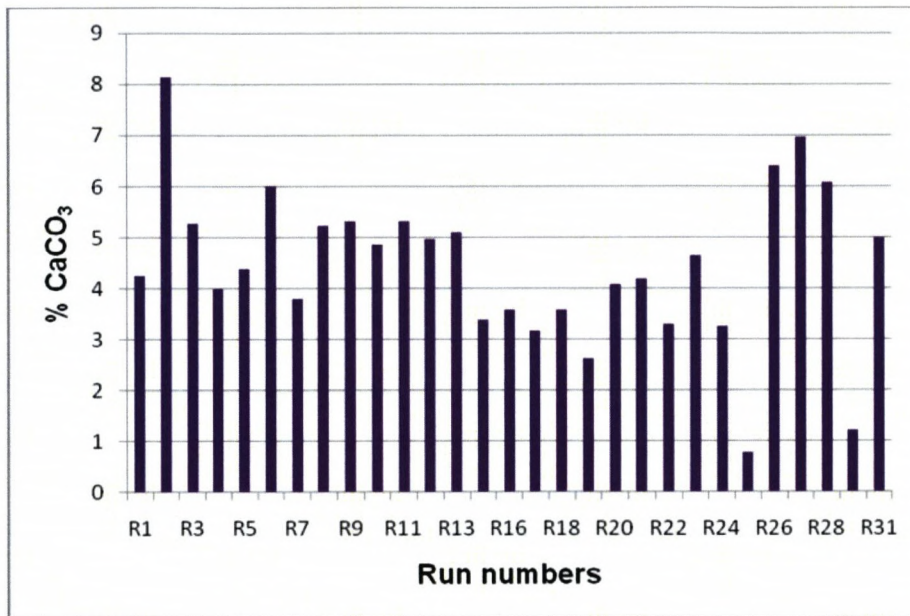
Figure 5.5: Graph showing the % CaCO$_3$ yield for each run for the carbonated fresh Secunda FA as determined by quantitative XRD.

Rendek et al., (2006) suggested that calcite is the predominant phase formed during carbonation, a phenomenon also observed in this study. Figure 24 shows that the conditions applied for Run R2 which were 1 Mpa, 90 °C, 20 µm-150 µm and a S/L ratio of 0.5 resulted in a high value of 8.14 % while Run 25, which was performed using the condition (4 Mpa, 30 °C, > 150 µm at a S/L ratio of 0.1) resulted in a low value of 0.77 % CaCO$_3$ being formed.

5.3.4 Chittick test analysis

Chittick tests were carried out as described in section 3.3.6 to ascertain the % CaCO$_3$ formed due to carbonation after characterization using quantitative XRD. The results obtained are given in Table 5.2 and plotted in Figure 5.6. The amount of CO$_2$ evolved was converted to % CaCO$_3$ using the equations provided in section 3.3.6.
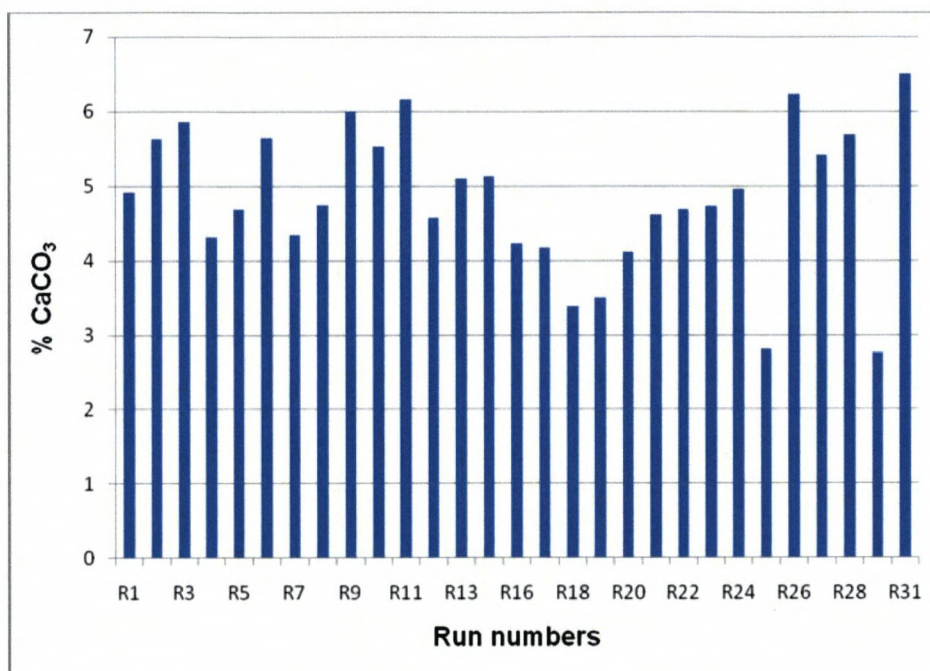
Figure 5.6: % CaCO$_3$ yield for each run for the carbonated fresh Secunda FA as determined by Chittick tests.

Chittick tests show that each condition applied resulted in different degrees of carbonation of the ash. Ash and brine carbonated under the following conditions in the case of Run R31, 4 Mpa, 90 °C, bulk ash and a S/L ratio of 1 resulted in 6.5 % CaCO$_3$. On the other hand, Run R29 was carbonated at 1Mpa, 30 °C, > 150μm ash fraction and a S/L ratio of 0.1 and these conditions resulted in the lowest amount of CO$_2$ being encapsulated as CaCO$_3$ (2.75 %).

5.3.5 Comparison of quantitative XRD and Chittick test

A comparison of the mass % of CaCO$_3$ yield determined by quantitative XRD and by Chittick tests was drawn up to correlate the two methods in quantifying the mass % of CaCO$_3$ formed in the carbonation process. The correlation between the two methods is given in Figure 5.7.

110
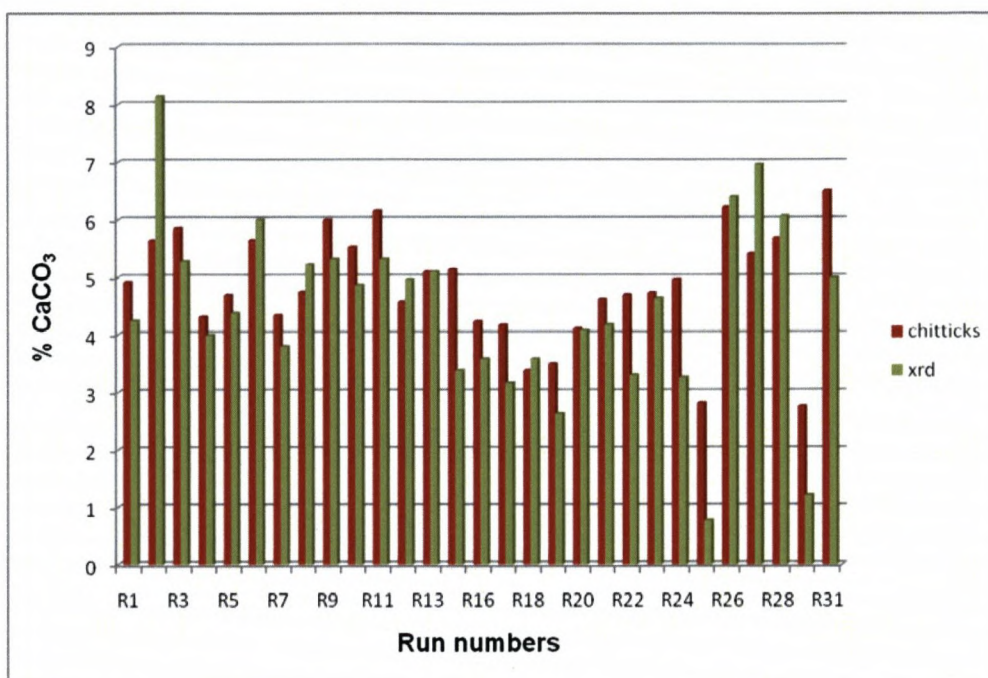
Figure 5.7: Correlation of mass % $CaCO_3$ yield determined by quantitative XRD and Chittick test

As is evident from Figure 5.7, the mass % of $CaCO_3$ could be determined by both methods as correlation was observed except for runs R2, R14, R24, R25, R27 and R29. Statistical testing was carried out to determine whether Chittick tests gave a better estimate of the % $CaCO_3$ than XRD. It was hypothesized that Chittick test gave a greater % $CaCO_3$ yield than XRD. The null hypothesis was thus set to $H_o = X_1 \leq X_2$ where:- X_1 represents Chittick test, X_2 represents XRD and H_o signifies the null hypothesis. The alternative hypothesis which should be the complement of the null hypothesis was taken to be $H_a = X_1 > X_2$ where: - Ha is the alternative hypothesis while X_1 and X_2 are Chittick test and XRD respectively. Since the alternative hypothesis contains the < inequality, a one-tailed prediction was used as would have been the case if the alternative hypothesis contained the > inequality (Hinton, 1995). However if the alternative hypothesis contains the ≠ sign, the prediction would have been a two-tailed prediction (Hinton, 1995). Student t-test statistic was applied to test the hypothesis that Chittick test gave a higher % $CaCO_3$ yield. Table 5.3 gives the values required to fit into the formula for t-test given below.

111

$$t = \cfrac{\mu_1 - \mu_2}{\sqrt{\cfrac{\Sigma d^2 - \cfrac{(\Sigma d)^2}{N}}{N(N-1)}}} \quad \dots\dots\dots\dots\dots\dots\dots\dots\dots\dots\dots\dots\dots\dots\dots\dots\dots \text{(5.1)}$$

Where: - μ_1 and μ_2 are the means of the two data sets (μ_1 is the mean of X_1 and μ_2 is the mean of X_2), d is the difference between the two data sets and N is the sample size. Table 5.3 gives the data applied in the t-test formula.

Table 5.3: Data for student t-test of quantitative XRD and Chittick test

Run no.	Chittick Test (X_1)	XRD (X_2)	Difference (d)	Squared d (d^2)
R1	4.92	4.25	0.67	0.45
R2	5.64	8.14	-2.5	6.25
R3	5.85	5.28	0.57	0.32
R4	4.31	3.99	0.32	0.10
R5	4.69	4.38	0.31	0.10
R6	5.64	6	-0.36	0.13
R7	4.34	3.8	0.54	0.29
R8	4.74	5.22	-0.48	0.23
R9	6.00	5.32	0.68	0.46
R10	5.52	4.86	0.66	0.44
R11	6.16	5.32	0.84	0.71
R12	4.57	4.96	-0.39	0.15
R13	5.10	5.1	0	0
R14	5.14	3.38	1.76	3.10
R16	4.23	3.58	0.65	0.42
R17	4.17	3.16	1.01	1.02
R18	3.38	3.58	-0.2	0.04
R19	3.50	2.63	0.87	0.76
R20	4.11	4.08	0.03	0
R21	4.62	4.18	0.44	0.19
R22	4.69	3.3	1.39	1.93
R23	4.73	4.64	0.09	0.01
R24	4.96	3.26	1.7	2.89
R25	2.81	0.77	2.04	4.16
R26	6.22	6.4	-0.18	0.03
R27	5.41	6.96	-1.55	2.40
R28	5.68	6.07	-0.39	0.15
R29	2.75	1.21	1.54	2.37
R31	6.50	4.99	1.51	2.28
N=29	μ_1=4.84	μ_2=4.44	Σd= 11.57 $(\Sigma d)^2$=133.86	Σd^2=31.38

both Chittick test and XRD. The Pearson correlation coefficient which is obtained by dividing the covariance of the two methods with the products of their standard deviations gave a value of 0.799 which is indicative of a relatively high degree of correlation. The concordance correlation coefficient is essentially supposed to be 1 for high correlation and the value of 0.682 obtained in this study means that most of the points are relatively far from the identity line (where X=Y in this case the line is 2,2- 7,7) when the values from Chittick test are plotted against those of XRD as shown in Figure 5.8 below.
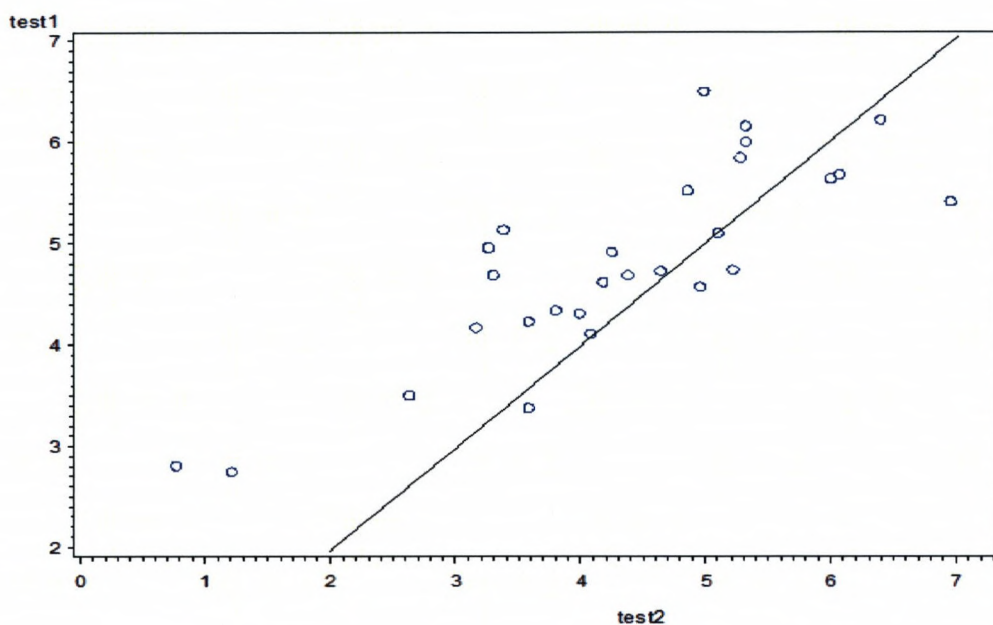
Figure 5.8: Plot of the concordance correlation coefficient for Chittick test and XRD (test 1 is Chittick test while test 2 is XRD)

From Figure 5.8, one notices that majority of the points lie above the identity line which means that test 1 (Chittick test in this case) gives higher values for the % $CaCO_3$ yield, further confirming the observations from the t- test.

5.3.6 Thermal Gravimetric Analysis

Thermal gravimetric analysis was carried out as described in section 3.3.10. Only three samples with the highest % $CaCO_3$ as determined by quantitative XRD and similarly only three samples with highest % $CaCO_3$ yield as determined by

Inserting the figures into the t formula one gets:

$$t = \frac{4.84 - 4.44}{\sqrt{\frac{31.38 - \frac{133.86}{29}}{29(29-1)}}} = 2.198 \dots\dots\dots\dots\dots\dots\dots\dots\dots\dots\dots\dots\dots\dots\ (5.2)$$

The degrees of freedom (df) for a related t-test is always (N-1), so df in this study = 28. At the p = 0.05 level of significance (i.e. 95 % confidence interval), it was found from the t distribution tables (Hinton, 1995) that t= 1.701, df = 28 for a one-tailed test. The calculated value of t of 2.198 was greater than the table value of 1.701. The null hypothesis was thus rejected and it was concluded that Chittick analysis gave a higher % $CaCO_3$ yield.

Further a measure of agreement or concordance by using the concordance correlation coefficient was also tested as described by Lin, (1989). The concordance correlation coefficient is a measure of scatter of the data points around the identity line (the X=Y line) (rather than around the least squares regression line as it would be for the ordinary correlation coefficient). The following statistics were obtained using SAS statistical program in testing for the concordance correlation coefficient (Table 5.4).

Table 5.4: Concordance correlation coefficient data

n1	n2	N	Mean1	Mean2	Std1	Std2	Pearson	Concordance Correlation
29	29	29	4.84	4.44	0.95	1.53	0.799	0.682

Concordance Corr Lower 95% CL	Concordance Corr Upper 95% CL	Location Shift	Scale Shift	Bias Correction
0.497	0.808	0.331	0.621	0.854

In the analysis of concordance correlation coefficient, Chittick test was set as test 1 and XRD as test 2. Thus n1 and n2 are the sample sizes for Chittick and XRD; N is the average sample size, mean 1 and mean 2 give the values of the means for

Chittick test were further analyzed using thermal gravimetric analysis due to cost constrains. Samples chosen were Runs R11, R26 and R31 for Chitticks and Runs R2, R27 and R28 for XRD. Thermal gravimetric analysis was carried out to confirm the statistic testing carried out on the two analysis methods. A summary of the results is given in Table 5.5.

Table 5: Comparison of % $CaCO_3$ determined by three different techniques

Run number	% $CaCO_3$ by TGA	% $CaCO_3$ by XRD	% $CaCO_3$ by Chittick Tests
R2	5.13	8.14	5.64
R11	5.43	5.32	6.16
R26	6.00	6.40	6.22
R27	4.71	6.96	5.41
R28	5.60	6.07	5.68
R31	6.27	4.99	6.50

Generally the values of % $CaCO_3$ obtained from the thermal gravimetric analysis were lower than those obtained for both Chittick tests and quantitative XRD analysis. This may be due to the small quantities and possibly in-homogeneity of samples that are used during the TGA analysis compared to the other analytical techniques. However there is a closer correlation between TGA and the Chittick test than between TGA and XRD. Discrepancies in XRD and Chittick tests are expected because, XRD detects only the crystalline phases and some of the CO_2 might have gone to the amorphous phase which XRD cannot detect. Furthermore, some of the Ca cations from both FA and brine go to form other phases such as bassanite and plagioclase thus depleting the available Ca cations for carbonation. Silicon standard addition in the quantitative XRD could also lead to interference hence leading to an overestimate or underestimate of the % $CaCO_3$ formed. Chittick tests on the other hand are a form of titration and thus all the encapsulated CO_2 is expected to be released within the time limit of the experiment in addition to using a high concentration of the HCl acid (6N). The results obtained using the Chittick tests were thus applied in the Design of Experiments to interpret the data.

Having tested the results from both Chittick test and XRD using t-test, concordance correlation coefficient and carrying out the TGA test for the best three samples from each of the methods (Chittick test and XRD), it was concluded that the two methods were correlating but that Chittick test gave a higher yield of the $CaCO_3$ and thus the results from Chittick test were confidently applied in the statistical analysis of the D-optimal design. The reader is thus reminded that the following statistical analysis of the design is based on the results from Chittick tests.

5.4 STATISTICAL ANALYSIS OF THE DESIGN

After putting in the input variables (pressure, temperature, particle size and S/L ratio at their different levels) and the response factor in this case % $CaCO_3$ yield, the software generated a summary of the model (Table 5.6) which describes the type of design chosen, number of runs generated, the various factors, their names, units used, type of factors (in this case, categoric), number of levels of each factor (2 for temperature and pressure, 3 for the S/L ratio and 4 for the particle size). The justification for the choice of factors and their levels is given in section 3.4.1.

Categorical factors are factors for which the levels cannot be arranged in order of magnitude. In this case, we are interested in the relationship of % $CaCO_3$ with varying levels of the input parameters (temperature, pressure, particle size and S/L ratio) (Mead, 1991).

Table 5.6: Design summary

Study Type:	Factorial					
Initial Design	D-optimal		Point Exchange		Runs	32
Center Points	0				Blocks	No Blocks
Design Model	2FI					

Factor	Name	Units	Type	Low Actual	High Actual	Levels
A	Pressure	Mpa	Categoric	1	4	2
B	Temperature	°C	Categoric	30	90	2
C	Particle size	μm	Categoric	<20	Bulk	4
D	S/L ratio	g/ml	Categoric	0.1	1	3

Response name	Units	Observations	Analysis	Minimum	Maximum	Mean	Std. Dev	Ratio	Transformation	Model
% $CaCO_3$	wt %	29	Factorial	2.75	6.5	4.84069	0.950658	2.36364	None	2FI

117

5.4.1 Factor effect estimation

Estimation of factor effects is done by evaluating the percentage contribution of each input factor (namely temperature, pressure, S/L ratio and particle size) as well as the interactions of these input factors. The percentage contribution determines which terms are larger contributors than others (Design Expert 7.1 User's manual, 2001). Table 5.7 below gives the contribution of the main effects and the interactions arising. In order to evaluate the contribution of various effects, a tentative percentage contribution of each model term to the total sum of squares is generated by the software as given in Table 5.7.

Table 5.7: Estimation of the factor effect

	Term	Sum Square	MeanSquare	F Value	% Contribution
Model	A-Pressure	2.27669	2.27669	0.0049	8.68676
Model	B-Temperature	8.27049	8.27049	0.0014	31.5562
Model	C-Particle size	11.6495	3.88318	0.0029	44.449
Model	D-S/L ratio	0.533621	0.26681	0.0406	2.03604
Model	AB	0.00407797	0.00407797	0.6090	0.0155596
Model	AC	0.265754	0.0885848	0.1152	1.01399
Model	AD	0.167835	0.0839177	0.1187	0.640378
Model	BC	0.547924	0.182641	0.0588	2.09061
Model	BD	1.14584	0.572918	0.0193	4.37195
Model	CD	0.300636	0.0601272	0.1657	1.14708
Aliased	ABC	0.52314	0.26157	0.0414	1.99605
Aliased	ABD	0.500634	0.500634	0.0218	1.91018
Aliased	ACD	Aliased			
Aliased	BCD	Aliased			
Aliased	ABCD	Aliased			
Error	Lack Of Fit	0			
Error	Pure Error	0.0226			0.0862306
	Residuals	0.0226	0.0113		

The Sum of Squares (SS) for a term is the amount of information that can be attributed to the term as it changes (Design Expert 7.1 User's manual, 2001). Model terms are all the terms that are included in making the model. Aliased factors on the other hand are factors that cannot be uniquely estimated and thus their estimated effect is the linear combination of all the aliased terms. For

118

instance aliased "ABC" term means A is aliased within B which is aliased within C and the estimate of ABC is a linear combination of A, B and C. On the other hand the F value acts as a test for comparing the model variance with residual (error) variance. The percentage contribution can be used to estimate the importance of each model term. One notes that the factor with considerable contribution were the main factors A (pressure), B (temperature), C (particle size), D (S/L ratio); interactions of BC and BD. These factors were thus used to test the model significance using ANOVA as described below.

5.4.2 Estimation of model significance

In order to determine the significance of the model as well as the factor effects, analysis of variance (ANOVA) is carried out on the model. ANOVA has two main functions, first, it provides a subdivision of the total variation between experimental units into separate components, each component representing a different source of variation, thus the relative importance of the different sources can be assessed. Secondly, it gives an estimate of the underlying variation between units which provides a basis for inferences about the effects of the applied treatments (Mead, 1991).

Table 5.8: Analysis of variance (ANOVA) for the model

Source	Sum of Squares (SS)	Degrees of freedom (df)	Mean Square (MS)	F value	p-value Prob>F
Model	24.48	12	2.04	18.87	<0.0001
A-Pressure	0.51	1	0.51	4.76	0.0444
B-Temperature	6.43	1	6.43	59.46	<0.0001
C-Particle size	9.86	3	3.29	30.40	<0.0001
D-S/L ratio	0.49	2	0.25	2.28	0.1342
BC	0.54	3	0.18	1.66	0.2152
BD	1.13	2	0.57	5.25	0.0177
Residual	1.73	16	0.11		
Lack of Fit	1.71	14	0.12	10.79	0.0879
Pure Error	0.023	2	0.011		
Cor Total	26.21	28			

The Sum of Squares (SS) for a term is the amount of information that can be attributed to the term as it changes (Design Expert 7.1 User's manual, 2001). The degrees of freedom (df) for a main effect is the number of levels of the factor minus one, while that for interaction is the product of the number of degrees of freedom associated with individual components of the interaction. The mean Square (MS) is given by dividing:-

$$\text{SS}_{model} \div \text{df}_{model} = 24.48 \div 12 = 2.04 \dots\dots\dots\dots\dots\dots\dots\dots\dots\dots\dots\dots\dots\dots\dots\dots\dots(5.3)$$

On the other hand the F value acts as a test for comparing the model variance with residual (error) variance. Prob> F is the probability value that is associated with the F Value for any term. It is the probability of getting an F Value of this size if the term did not have an effect on the response.

In general, a term that has a probability (Prob>F) value less than 0.05 would be considered a significant effect. A probability value greater than 0.10 is generally regarded as not significant (Design Expert 7.1 User's manual, 2001). One can therefore conclude that the variables A, B, C and BD are significant model terms. A significant lack of fit means the runs replicate well and therefore their variance is small (Design Expert 7.1 User's manual, 2001). The Lack of Fit should not be significant as the idea is to have a model that fits. The Lack of Fit value of 10.79 indicates that there is a 8.79 % chance that a "Lack of Fit" this large can be due to noise. The Model F-value of 18.87 implies the model is significant. There is only a 0.01 % chance that a "Model F-Value" this large could occur due to noise. The residual mean square (MS) is the estimate of variance around the model. This value gives any deviation not explained by the model.

In addition to ANOVA, the software generates the statistics for ANOVA which explains the model behavior. This statistical analysis is given in Table 5.9.

Table 5.9: Statistics for the ANOVA analysis

Standard deviation	0.33	R-Squared (R^2)	0.9340
Mean	4.84	Adjusted R^2	0.8845
Coefficient of variance (C.V) %	6.79	Predicted R^2	0.7833
PRESS	5.68	Adequate Presicion	15.814

Standard deviation is the root square of the error mean square. The quantity R – squared measures the proportion of total variability in the data (Montgomery, 2009). It is calculated as:-

$$R^2 = SS_{model} \div SS_{total} = 24.48 \div 26.21 = 0.9340 \dots\dots\dots\dots\dots\dots\dots\dots\dots\dots(5.4)$$

The value of 0.9340 obtained above (Table 5.9) means the model explains 93.40 % of the variability obtained in the % $CaCO_3$. The coefficient of variation (C.V) measures the unexplained or residual variability in the data as a percentage of the mean of the response variable, % $CaCO_3$ in this case. The adjusted R-squared (R^2 Adj) is a statistic adjusted for the number of parameters in the model relative to the number of points in the design. The adjusted R^2 basically plateaus when insignificant terms are added to the model, while the R^2 predicted decreases in the event of too many insignificant terms. The predicted R^2 value of 0.7833 (Table 5.9 above) indicates that the model can explain 78.33 % of the variability in new data. Ideally the adjusted and predicted r-squared values should be within 0.2 of each other (Design Expert User's manual, 2001). This criteria is fulfilled in the current model (Adjusted R^2- Predicted R^2 = 0.8845 – 0.7833 = 0.1012). Adequate Precision measures the signal to noise ratio. A ratio greater than 4 is desirable. The design's ratio of 15.814 indicates an adequate signal hence the model can be used to navigate the design space. The predicted Error Sum of Squares (PRESS) is a measure of how well the model will predict in a new experiment. A model with a small value of PRESS indicates that the model is likely to be a good predictor (Montgomery, 2009). A value of 5.68 (Table 5.9), thus indicates that this model will   be   a   good   predictor   in   a   new   experiment.

5.4.3 Diagnostics checking

Diagnostics checking is analysis of the input data, both the input and output variables to check for outlying data points. It includes a host of plots that graphically represent the data thus making it easy to identify outliers. The plots include normal probability plot (Figure 5.9), residual versus predicted plot (Figure 5.10), residuals versus run plot (Figure 5.11), predicted versus actual plot (Figure 5.12), Box-Cox plot for power transformation (Figure 5.13), leverage versus run plot (Figure 5.14) and the Cook's distance plot (Figure 5.15). Random orientation is desired for all the plots which would imply independence of the data points.

The normal probability plot (Figure 5.9) indicates whether the residuals follow a normal distribution in which case the points will follow a straight line (Montgomery, 2009). Some scatter can be expected with normal data, however an "S-shaped" curve would indicate that a transformation of the response may provide a better analysis. A straight line is observed in this study, thus no transformation is required. A plot of the normal probability is given in Figure 5.9 below.
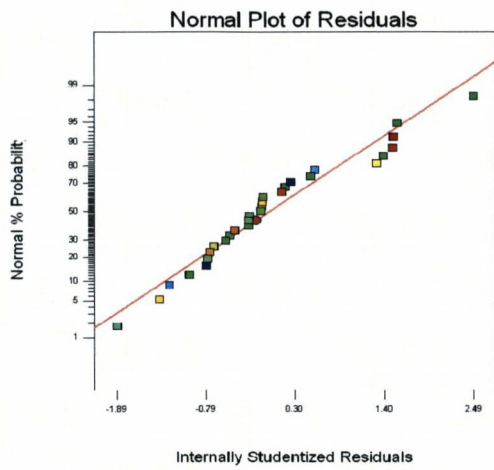
Figure 5.9: Normal probability plot of residuals
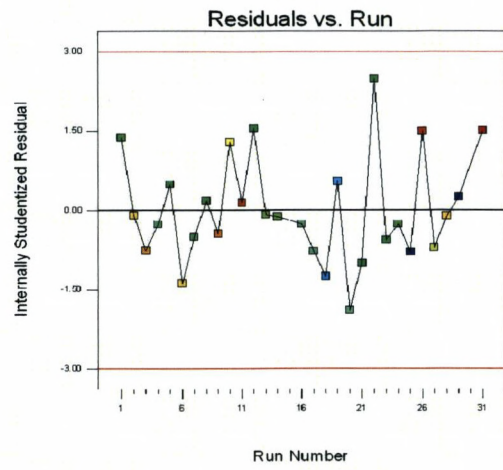
Figure 5.11: Plot of Residuals versus Runs
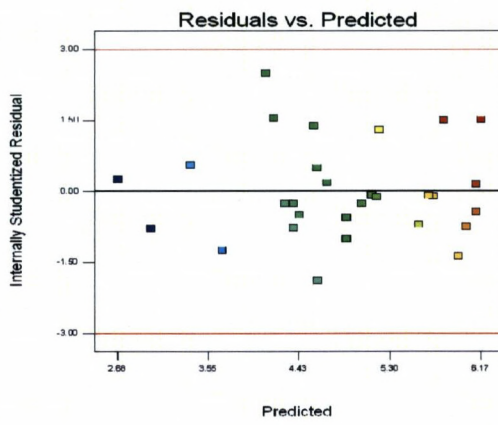
Figure 5.10: Plot of Residuals versus Predicted
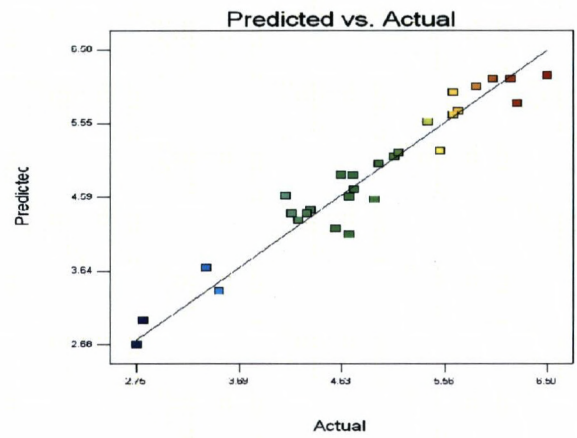
Figure 5.12: Plot of Predicted versus Actual

123

The plot of normal probability (Figure 5.9), given above should not indicate any pattern, in other words, there should be normal distribution of the data. In this study the plot followed the ideal situation, which should be a straight line. This is done to ascertain the predictability of the data (Mead, 1991). On the normal probability curve (Figure 5.9), internally studentized residuals mean the residual has been divided by the estimated standard deviation of each particular residual. It measures the number of standard deviations separating the actual and predicted values.

The plot of Residuals versus Predicted (Figure 5.10) tests the assumption of constant variance. Ideally the plot should be a random scatter as is seen in Figure 5.10 with no definite pattern (Montgomery, 2009). A straight line thus in this case implies that the variance is constant in the residuals.

The Residuals versus Run (Figure 5.11) plots the residuals against the experimental run order. It internally checks for lurking variables that may have influenced the response factor during the experiment. The plot should also be a random scatter as seen in Figure 5.11 meaning that the residuals are random.

The Actual versus Predicted (Figure 5.12) is a graph of the actual response values versus the predicted response values. It helps to detect a value or group of values that are not easily predicted by the model. A straight line is ideal as is the case in Figure 31 above (Design Expert 7.1 User's manual, 2001).

The Box-Cox plot of power transforms was developed to help in identifying the best power law transformation to apply in a model (Montgomery, 2009). Figure 5.13 below shows this plot:-
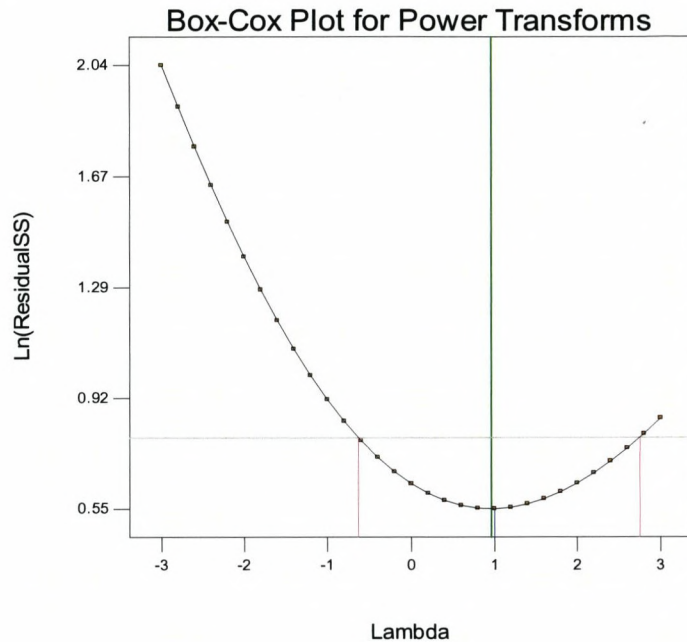
Figure 5.13: Box-Cox plot for power transforms

The red lines (Figure 5.13) indicate the 95 % confidence interval surrounding the lambda value. The blue line shows the current transformation, in this case it points to a value of 1 for lambda which symbolizes the power applied to the response values (% $CaCO_3$). A lambda of 1 indicates no transformation is required (Montgomery, 2009). The green line indicates the best lambda value, in this case 0.96.

A recommended transformation is given based on the best lambda value. If the 95 % confidence interval around the lambda value includes one, then the software does not recommend a specific transformation as is in this case.

Leverage of a point varies from 0 to 1 and indicates how much an individual design point influences the model's predicted values (Virgil and McLean, 1974). A plot of leverage versus run is given in Figure 5.14.
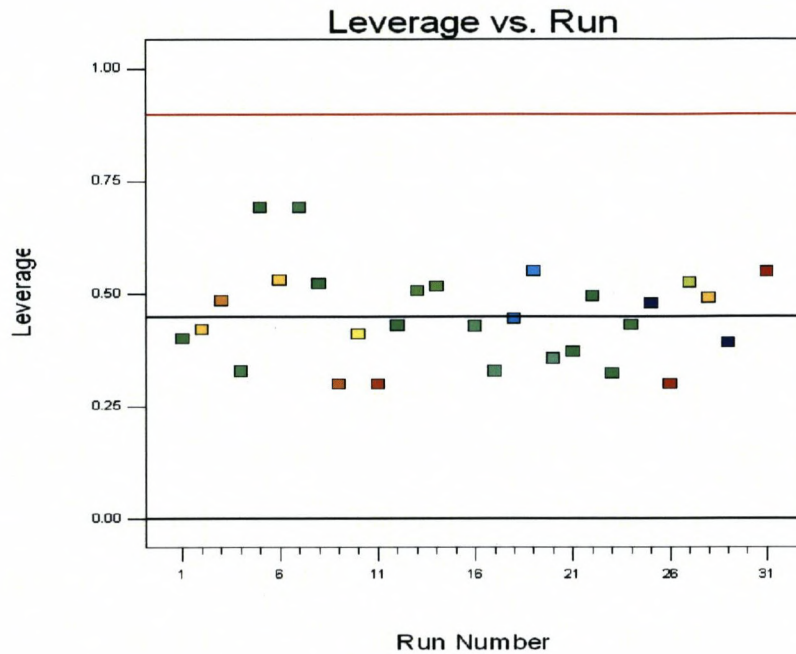
Figure 5.14: Plot of Leverage versus Run

Leverage is a measure of how each point influences the model fit. Leverage points are those, if any, made at extreme values of the independent variables such that the lack of neighbouring observations means that the fitted regression model will pass close to that particular observation (Everitt, 2002). A leverage of 1 means the predicted value at that particular case, will exactly equal the observed value of the experiment in other words the residual will be zero (Montgomery, 2009). Ideally, a clustering of points should appear close to zero but definitely less than 1. In Figure 5.14 above clustering is observed between the 0.25 and 0.75 mark, which is allowed as all the points are below 1.

Cook's distance (D_i) is a measure of how much the regression would change if a data point is omitted from analysis or deleted. A plot of Cook's distance is given in Figure 5.15 below.
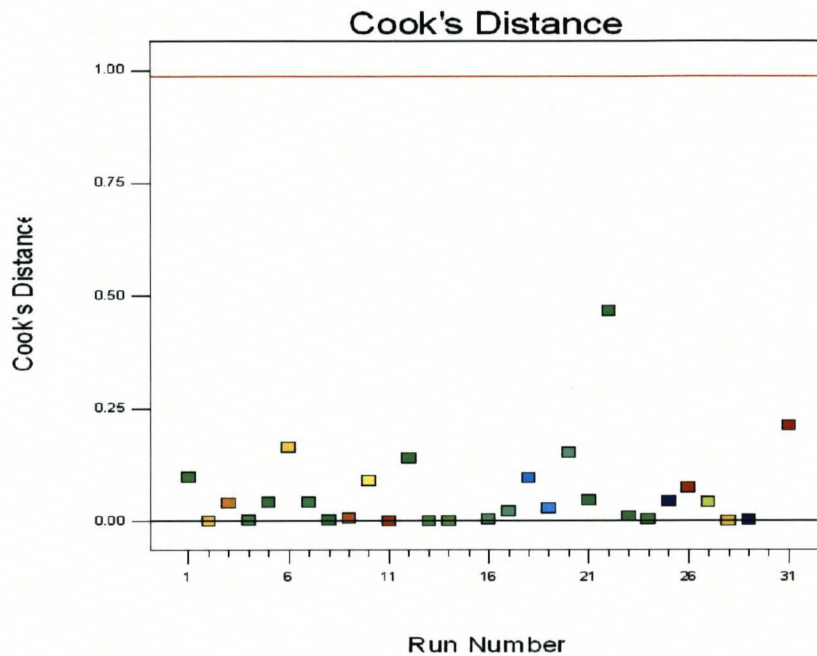
Figure 5.15: Plot of Cook's distance

Relatively large values are associated with cases with high leverage and large studentized residuals (a measure of how many standard deviation the actual value deviates from the predicted value after deleting the point in question). Cases with large D_i relative to other cases are due to large residuals or outliers which may affect the accuracy of the outcome and regression is not guaranteed. Points with a Cook's distance of 1 or more call for closer examination (Montgomery, 2009). On the other hand if the value of Cook's distance is substantially less than 1, deleting any case will not change the estimates of the regression coefficients very much. It is desired that there be strong clustering near the zero point (Montgomery, 2009), this is observed in Figure 5.15 above. This confirms lack of outliers and all the data points are thus within range of each other.

Having checked for outliers and thus confirmed that the residual checks were within permissible limits, the model was confirmed to be valid and could thus be confidently used to interpret the results.

5.5 INTERPRETATION OF RESULTS

Interpretation of a main effect involves comparison between levels (both high and low) of a single factor e.g. temperature, averaging over levels of all the other factors (pressure, particle size and S/L ratio in this case). Interpretations of interactions on the other hand involve comparison between levels of one factor over different levels of the other factor. For instance AB (A= pressure and B= temperature) interaction will involve determining the behavior of pressure at all the levels of temperature and vice versa. To interpret the results, the order of interpretation should be as follows; main effects first, followed by two factor interactions, three factor interactions and so on (Mead, 1991). Generally in cases where the two factor effects and higher order interactions appear negligible, then the results of the experiment should be interpreted in terms of the main effect mean responses only, ignoring the mean responses of the combination of levels for the variables chosen. Likewise if a two factor interaction is clearly important, then the interpretation of the effects of these two factors should normally be based on the mean responses for the combination of levels of the variables chosen for those two factors (Mead, 1991).

5.5.1 Analysis of the main effects upon carbonation

The main effects of the variables upon the degree of carbonation in this case will be temperature, pressure, particle size and S/L ratio. From ANOVA analysis (Table 5.8) one realizes that A (pressure), B (temperature), C (particle size) main effects are significant. Factor D (S/L ratio) is not significant but it is added to make the model hierarchical. After observation of the behavior of the main effects with different factor combination, only the trends were chosen for presentation to reduce the amount of graphs possible. Where different trends were observed for the same main effect, the graphs showing all the different trends will be presented in this section. Pressure, temperature and particle size were observed to behave similarly in that their effect on the % $CaCO_3$ formed was higher at higher values. The visual interpretation is usually in the form of line graphs as shown below in Figures 5.16 to 5.20. One should look out for the effect of the input variable (be it

128

pressure, temperature, particle size or S/L ratio) on the % CaCO3 as the input variable varies across the chosen levels. The Y-axis gives the % CaCO3 for all the plots (Figures 5.16 to 5.20), while the X-axis shows the different levels of the chosen input variable, for instance in the case of temperature the levels will be 30 ºC and 90 ºC.
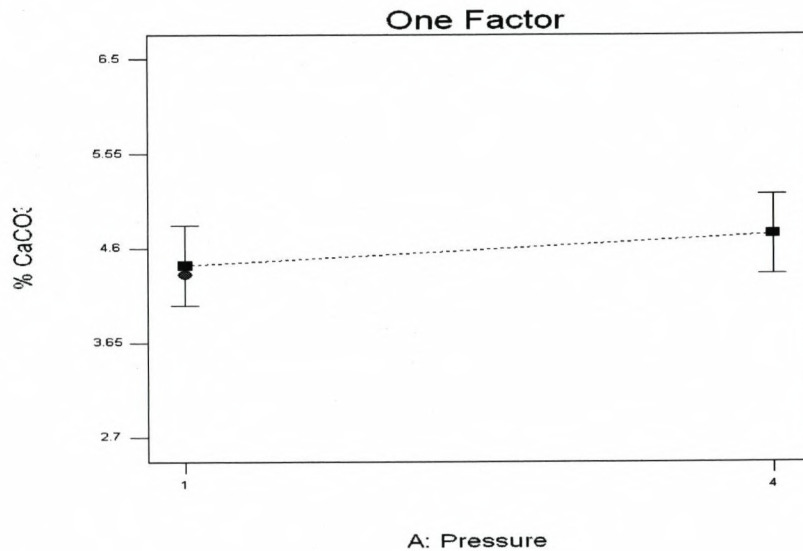
Figure 5.16: Main effect of pressure for all factor combinations

Variation of the other factors (i.e. temperature, particle size and S/L ratio) had the same effect on the pressure as shown above (Figure 5.16). This means that at all levels of temperature, particle size and S/L ratio, the % CaCO3 increased slightly as the pressure was increased from 1 Mpa to 4 Mpa. Thus only one plot is given. Pressure can therefore be said not to have an overly significance on carbonation and hence the output (% CaCO3). Reddy et al., (1994) in their studies on carbonation of alkaline FA observed that higher pressure values were not significant in the carbonation process. Rendek et al., (2006) also reported that the CO_2 pressure does not affect the carbonation equilibrium, from a thermodynamic point of view but only influences the kinetics of the process. Other researchers such as Soong et al., (2004), Chiquet et al. (2007) and Montes-Hernandez et al., (2009), also reported that increase in pressure does not have a high significance on the % CaCO3 formation. This study is thus in agreement with what has been proposed in literature.
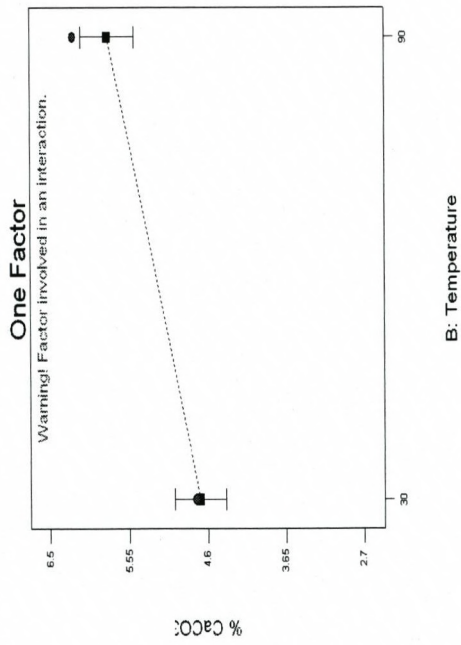
Figure 5.17: Main effect of temperature for all factor combinations
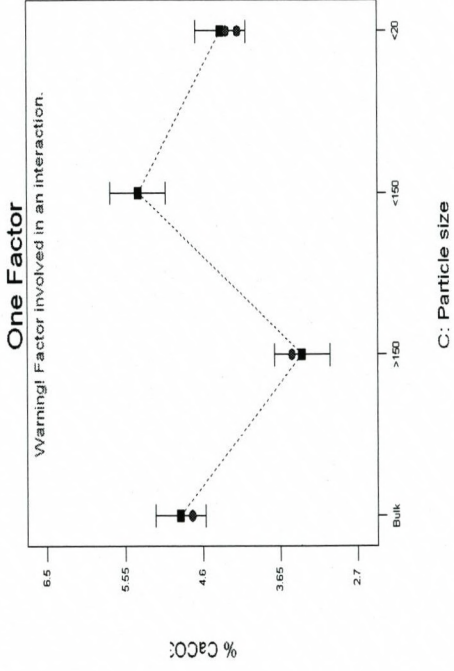
Figure 5.18: Main effect of particle size for all factor combinations
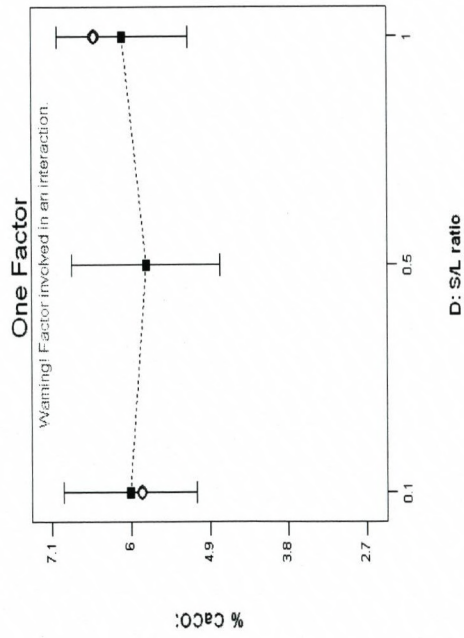
Figure 5.19: Main effect of S/L ratio at low temperature (30 °C)
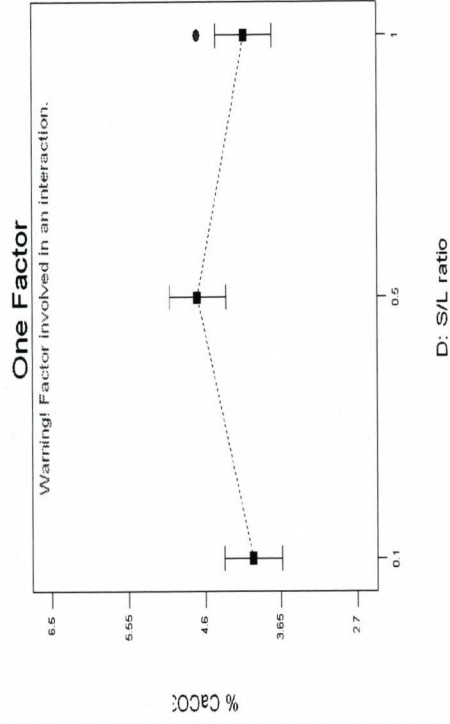
Figure 5.20: Main effect of S/L ratio at high temperature (90 °C)

For Figures 5.17 to 5.20, a warning is displayed on the graphs. This is generated by the software to inform one that the main effect being investigated is also involved in an interaction. Caution is thus called for, when interpreting the main effects, as some of them are involved in interactions as displayed in the warning signs above some graphs. One therefore needs to look at the interactions in order to make a comprehensive conclusion about the contribution of the effect of a particular variable towards the formation of $CaCO_3$ through carbonation.

Figure 5.17 shows the effect of temperature on the amount of $CaCO_3$ formed during carbonation. It is clear that as the temperature increases from 30 °C to 90 °C, the % $CaCO_3$ formed increases considerably. This signifies the importance of temperature in the carbonation process. Li et al., (2007) reported a similar observation and concluded that high temperatures improve the reaction kinetics hence increasing the carbonation efficiency.

In Figure 5.18 the effect of particle size on the formation of $CaCO_3$ is given. One is reminded that four particle sizes were considered as outlined in section 3.4.1. These were bulk ash, > 150 μm, 20 μm-150 μm and the <20 μm fractions. The 20 μm-150 μm fraction is observed to have the highest effect on the % $CaCO_3$. The bulk ash has the next highest contribution to % $CaCO_3$ formation followed by the <20 μm fraction. The >150 μm fraction however, is the least favourable for carbonation as it led to the lowest % $CaCO_3$ output (Figure 5.18). These observations correlate with the XRF analysis done on the un-carbonated Secunda fly ash (Table 4.1) where it was observed that the 20 μm-150 μm particle size range had the highest CaO (averaging at 9.3 %) while the >150 μm particle size fraction had the lowest CaO of 5.894 %. CaO in the FA is the main source of the Ca^{2+} though the Ca^{2+} in brine also contributes towards the total Ca cations available for carbonation. Fernandez et al., (2004) evaluated the effect of particle size in the carbonation of MSWI ash and observed that carbonation was higher with smaller particle sizes. They attributed this observation to the higher CaO content of the smaller particle sizes, homogeneity of the particle sizes as well as the higher surface area of these particles.

131

Figures 5.19 and 5.20 give the effect of S/L ratio at low and high temperature respectively. At low temperatures (30 ºC), a S/L ratio of 1 gives a higher amount of $CaCO_3$ arising due to carbonation (Figure 5.19). On the other hand at high temperatures (90 ºC) the S/L ratio of 0.5 gave the highest % $CaCO_3$ formation compared to a S/L ratio of 0.1 or 1 (Figure 5.20). This implies that the S/L ratio is temperature dependent. A low S/L ratio and high temperature will lead to higher carbonation efficiency as will a high S/L ratio at low temperature. This would be attributed to the increased kinetics at high temperatures, hence low S/L ratio will suffice and vice versa. Li et al., (2007) in their study on the effect of S/L ratio on the carbonation of MSWI ash obtained an optimum value of 3. According to them, as water is the medium of dissolution, ionization and transportation of CO_2, very low or very high liquid ratios will retard the reaction. Hydration and dissolution of CO_2 occurs in the presence of water as well as the dissolution of Ca^{2+} ions from the solid phase which reacts with the carbonate ions to form $CaCO_3$. In low S/L ratios, the gas permeability is high and the gas can effectively diffuse into the material. Increase of the liquid content seals off the pores in the ash thus inhibiting the reaction (Li et al., 2007).

5.5.2 Interpretation of interactions between the input variables

A factor interaction is the variation between the mean for different levels of one factor over different levels of the other factor. Two factor interactions should be examined first, then three factor interactions and so on (Mead, 1991). The reader is reminded that only BC (temperature and particle size interaction) and BD (temperature and S/L ratio interaction) factor interactions were found to be significant (Table 5.8). Only general trends are reported here in order to reduce the number of graphs to be discussed. Observation of the BC interaction at all the levels of the different factors yielded a similar trend which is presented by Figure 5.21.

132
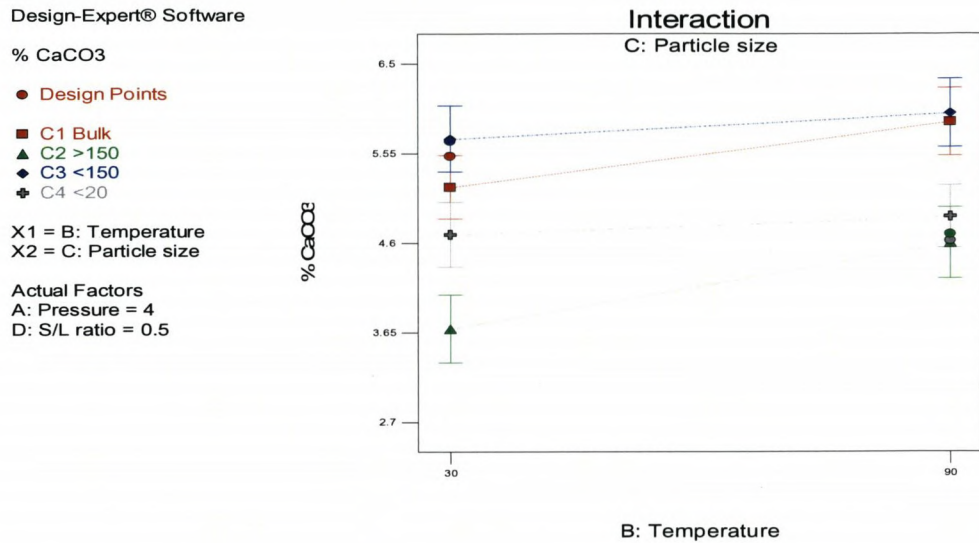
Figure 5.21: Interaction effect of BC for all factor combinations (<150 represent the 20 µm-150 µm particle size range)

The "I-Beam" symbols on the plot given in Figure 5.21 depict the 95 % least significant difference (LSD) interval for the plotted points (Design Expert 7.1 User's manual, 2001). The points that have non-overlapping intervals are significantly different. In other words if the lines describing the simple main effects are not parallel, then the possibility of an interaction exists. As can be seen in Figure 5.21, the lines for 20 µm-150 µm and the < 20 µm (blue and grey lines respectively) are almost parallel and straight. However, the lines for bulk ash and > 150 µm fraction (red line and green line respectively) show an increasing % $CaCO_3$ with increasing temperature. In other words, high temperatures are recommended for these two larger particle fractions while on the hand temperature will have little effect on the smaller particle size fraction i.e. the 20 µm-150 µm and <20 µm fractions. Hence for effective carbonation without high energy inputs, it would be necessary to use the smaller size fractions of FA.

The interaction of temperature and S/L ratio (BD interaction) investigates the effect of the different temperatures at each S/L employed and is given in Figure 5.22 below.
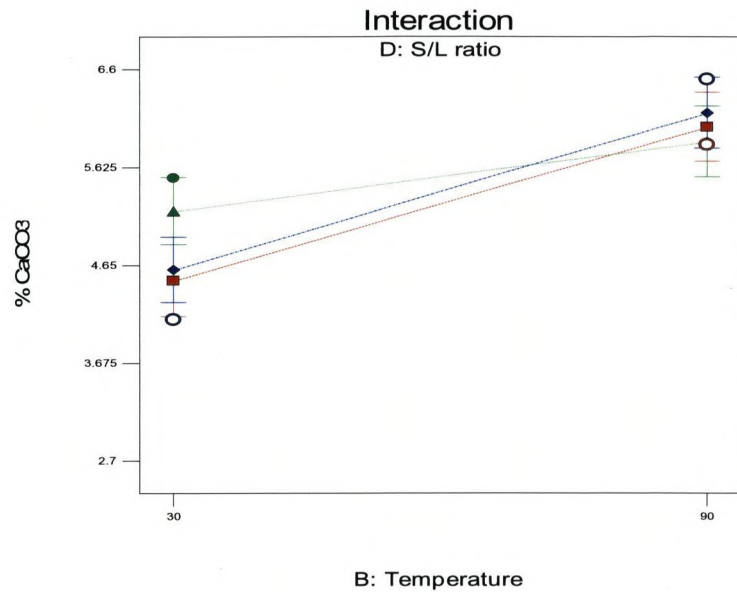
Figure 5.22: Interaction effect of BD for all factor combinations

Overlapping of the lines on the high temperature side depicts lack of interaction between temperature and all the S/L ratios used. This is due to the fact that only the points that have non-overlapping intervals are significantly different but in Figure 41 all the S/L ratios overlap at the high temperature (90 °C). However one observes that on the lower temperature side (30 °C), S/L ratio of 0.1 and 0.5 interact with temperature. The 0.5 ratio will however give a higher % $CaCO_3$. This is contrary to what was observed in Figures 5.19 and 5.20 where a S/L ratio of 1 was observed to have a higher effect on the amount of $CaCO_3$ at 30 °C and a S/L ratio of 0.5 optimum at 90 °C. As it had been pointed out earlier, main effects that are involved in interactions cannot be relied upon solely to investigate their effect on the carbonation efficiency. The interaction plots are more robust and hence one would therefore consider experimenting at low temperature using a S/L ratio of 0.5 i.e. relying on the interaction plots.

5.6 CARBONATION EFFICIENCY OF SECUNDA FLY ASH

The carbonation efficiency of Secunda FA used in this study was calculated to determine and establish how much CO_2 the FA could sequester. The pressure drop

was established by subtracting the final pressure of the system from the initial pressure of CO_2 charged into the reactor. The pressure drops from the carbonation experiments is given in Table 21 for each run.

Table 5.10: Pressure drop due to carbonation for each run

Run no.	Initial pressure (Mpa)	Final pressure (Mpa)	Pressure drop due to carbonation (Mpa)
R1	1	0.48	0.52
R2	1	0	1
R3	4	0.55	3.45
R4	1	0.55	0.45
R5	4	1.03	2.97
R6	1	0.14	0.86
R7	1	0.17	0.83
R8	1	0.48	0.52
R9	4	0.76	3.24
R10	4	1.52	2.48
R11	4	0.69	3.31
R12	1	0.34	0.66
R13	4	1.24	2.76
R14	4	0.59	3.41
R16	1	0.28	0.72
R17	1	0	1
R18	1	0.07	0.93
R19	1	0.31	0.69
R20	4	0.34	3.66
R21	4	0.83	3.17
R22	4	0.21	3.79
R23	1	0	1
R24	4	0.38	3.62
R25	4	0.14	3.86
R26	1	0.07	0.93
R27	1	0.07	0.93
R28	4	0.14	3.86
R29	1	0.14	0.86
R31	4	0.83	3.17

For pure oxides (e.g. CaO and $Ca(OH)_2$, the theoretical extent of carbonation is a function of basic stoichiometry (Hutzinger et al., 2009):

$$CaO_{(s)} + CO_{2(aq)} \rightarrow CaCO_{3(s)} \dots\dots\dots\dots\dots\dots\dots\dots\dots\dots\dots\dots\dots\dots\dots\dots\dots(5.5)$$
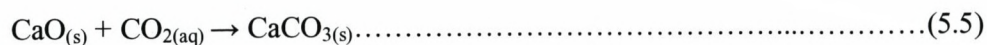
Using the simple equation of mass = moles * molar mass, and bearing in mind that the molar ratio is 1:1, it follows that every ton of CaO can potentially sequester up to 0.799 tons of CO_2. For wastes such as FA, the theoretical extent of carbonation can also be calculated as a function of stoichiometry, though in this case the extent of carbonation will also depend on the availability of the oxides for reaction. Theoretically the maximum CO_2 uptake capacity can be calculated as a function of the chemical composition of the original material in this case FA, using the Stenoir formula (Fernandez et al., 2004):

$$CO_2 \ (\%) = 0.785 * (\% \ CaO - 0.7 \ \% \ SO_3) + 1.09 \ \% \ Na_2O + 0.93 \ \% \ K_2O$$
....(5.6)

Using the data in Table 8 for the different oxides present in the fresh Secunda ash, the formula becomes:

$$\% \ CO_2 = 0.785 \ (9.198 - 0.7* 0.358) + 1.09* 0.457 + 0.93*0.787 = 8.254 \ \% \ ...(5.7)$$

This means that theoretically, assuming all available oxides react to form carbonates, the sequestration capacity of Secunda fly ash is 8.254 % i.e. for every 1 ton of FA, 0.083 tons of CO_2 can be sequestered.

Knowing the pressure drop due to carbonation, the amount of CO_2 consumed by carbonate precipitation can be calculated using the ideal gas law (Perez-Lopez et al., 2008; Montes-Hernandez et al., 2009) as follows:

$$n_{CO2} = \frac{P_{carbonation\_pressure\_drop}V}{RT}$$
....(5.8)

Where V is the reactor volume occupied with gas. The teflon liner used together with the steel jacket was not a tight fit and hence the volume of gas in this case

136

will be, the volume of the steel jacket – volume of the teflon liner – the volume occupied by the solid and liquid mixture in the teflon (calculated using the formula of the volume of a cylinder to a value of 149.87 cm^3). The teflon volume was calculated by a simple displacement experiment where the volume displaced by the teflon was taken to be its volume (observed to be 200 cm^3). The volume of the steel jacket was calculated from the equation for the volume of a cylinder i.e V = $\pi r^2 h$, (r = radius of the jacket (3.15 cm), h = height of the steel jacket (15 cm) which gave a value of 467.65 cm^3. V thus is given by 467.65 cm^3 – 200 cm^3 – 149.87 cm^3 = 117.78 cm^3 which converts to 0.118 L.

T is the temperature of reaction in $^{\circ}$K (363 $^{\circ}$K), n_{CO2} are the moles of CO_2 and R is the gas constant (0.08314472 L.bar/$^{\circ}$K.mol). One should note that the pressure drop observed was converted from Mpa to bars for use in this equation.

Applying the conditions of Run R31 (bulk ash, 90 $^{\circ}$C, S/L ratio of 1 at 40 bars), which was observed to have the highest % $CaCO_3$ as established by the Chittick tests and whose pressure drop was observed to be 3.17 Mpa or 31.7 bars, a value of 0.124 moles of CO_2 was obtained. Taking into account the number of moles obtained above and the fact that the FA contains 9.2 wt % of CaO as was determined by XRF (Table 8), the carbonation efficiency (CE) can be calculated by the following expression (Perez-Lopez et al., 2008; Montes-Hernandez et al., 2009):

$$CE = \frac{n_{CO2} * M_{CO2}}{\frac{W_{CaO}}{M_{CaO}} * M_{CO2}} * 100 \dots\dots\dots\dots\dots\dots\dots\dots\dots\dots\dots\dots\dots\dots\dots\dots\dots\dots\dots\dots(5.9)$$

Where n_{CO_2} is the number of moles consumed, calculated by equation 5.8 above, M_{CO_2} is the molar mass of CO_2 (44.01 g/mol), W_{CaO} is the starting mass of the CaO in the reactor (9.2 g) and M_{CaO} is the molar mass of CaO (56.077 g/mol).

Applying equation 5.9 above and the information given, the carbonation efficiency for Secunda FA was thus calculated to be 75.54% after two hours of carbonation at 90 °C, 4 Mpa (40 bars), S/L ratio of 1 using the bulk ash. Theoretically one ton of FA containing 9.2 % of CaO could sequester 0.083 tons of CO_2. With this experimental protocol and bearing in mind the carbonation efficiency (75.54 %), 1 ton of fly ash can thus sequester 0.062 tons of CO_2.

Montes-Hernandez et al., (2009) in their study on the carbonation of FA obtained an efficiency of 82 % after 18 hours of carbonation at 30 °C. However the sequestration potential of their ash was lower than our FA (0.026 tons of CO_2 per ton of fly ash as opposed to our value of 0.062 tons of CO_2 per ton of FA). This is attributable to two factors, firstly, the FA used in this study had a higher CaO content as opposed to theirs (9.2 % as opposed to 4.1 % of CaO) and secondly, they used water for the carbonation experiments unlike brine used in this study. This confirms that brine contributes additional Ca^{2+} for the carbonation process.

5.7 COMPARISON OF ULTRAPURE WATER AND BRINE AS THE FLY ASH DISPERSION MEDIA IN THE CARBONATION EXPERIMENTS.

Carbonation was also carried out for Run R31 (at 4 Mpa, 90 °C, using bulk ash at a S/L ratio of 1 as these conditions had been observed to lead to the highest % $CaCO_3$ yield) using ultra pure water in place of brine to investigate the contribution of the components in the brine solutions to the carbonation efficiency. Table 22 gives a comparison of the aqueous extract (or leachate) recovered after carbonation using either ultra-pure water or Tutuka brine solutions. Analysis of the raw brine solutions as given in sections 3.3.4 and 3.3.5 while the concentrations of the various brine components are given in Table 10.

Table 22 below compares the concentration of the raw brine, leachates obtained after carbonation using ultra-pure water and the leachates from brine carbonation.

Table 5.11: Concentrations of the raw brine, leachates obtained after carbonation using brine and ultra-pure water (NA means not analyzed; * means not detected)

Element	Raw brine (ppm)	Run 31 (water) (ppm)	Run 31 (brine) (ppm)
K	104.1	23.532	9.75
Al	0.044	0.063	*
As	0.007	0.003	*
B	NA	64.039	2.72
Ca	101.76	26.851	25.5
Co	0.015	*	0.002
Cr	0.014	0.010	0.001
Cu	0.067	0.044	*
Fe	0.051	0.030	*
Mg	158.73	103.238	1.522
Mn	0.082	*	*
Mo	0.039	1.204	0.069
Na	4315	58.048	3201
Ni	0.116	0.112	*
Se	0.004	0.094	*
Sr	3.030	2.019	*
V	0.016	4.559	0.15
Zn	0.100	0.140	*

One notices in Table 5.11 that majority of the trace elements have a higher concentration in the water leachates than in the brine leachates except for Na. The Na content of the brine leachates is very high (3201 ppm) compared to the water leachates (58.05 ppm). From Tutuka brine classification (Figure 4.10) it had been noted that the brine samples used are $NaSO_4$ rich solutions hence the high Na content as opposed to the Na content of the water/FA leachates. Magnesium content of the water leachates is higher than that for the brine leachates, 103.24 ppm and 1.522 ppm respectively. This signifies that Mg in brine takes part in the carbonation, though magnesite was not identified using XRD, maybe due to very low quantities being formed. The observation of lower concentrations of the various elements in the brine carbonated leachates can be attributed to the co-precipitation of the brine components with $CaCO_3$ as was suggested by Mooketsi et al., (2007).

139

Quantification of the solid residues obtained after carbonation using water and brine for Run R31 was carried out to evaluate the effect of the liquid media used for FA dispersion on the relative amounts of the phases formed. Figure 5.23 below shows the variation in the relative amounts of the phases quantified from the water and brine carbonation experiments.
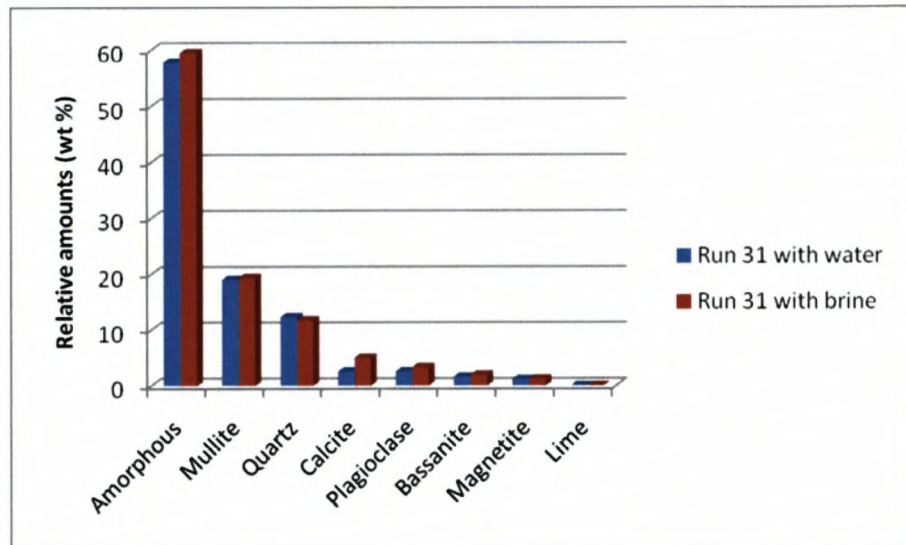
Figure 5.23: Quantification of the phases present in the carbonation solid residues

The most important phenomena to note is that, the calcite formation is higher in the brine carbonated residues as opposed to the water carbonated residues. This is due to the fact that brine contributes additional Ca^{2+} that takes part in the carbonation as was suggested by Soong et al., (2006). Also evident is the fact that no lime was present in both the water and brine residues. The explanation for this would be that the lime in the brine reactions was used to raise the brine pH for carbonation to occur (Soong et al., 2006), on the other hand the lime in the water reactions hydrolyses to the hydroxide form that later transforms to $CaCO_3$.

5.8 EFFECT OF TIME ON THE CARBONATION PROCESS

It has been reported in literature that the maximum carbonation time is 2 hours (Perez-Lopez et al., 2008) and hence this time factor was applied in this study. However it is necessary to bear in mind that the rate determining step for the

carbonation process is the leaching of Ca^{2+} and its subsequent conversion to the hydroxide (Soong et al., 2004):

$$CaO + H_2O \rightarrow Ca(OH)_2 \ldots\ldots\ldots\ldots\ldots\ldots\ldots\ldots\ldots\ldots\ldots\ldots\ldots\ldots\ldots\ldots\ldots\ldots\ldots(5.10)$$
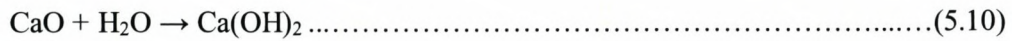
The effect of time on the leaching of Ca^{2+} from FA was thus investigated in order to observe the leaching trend with time by agitating the FA with ultra-pure water at varying time intervals. A S/L ratio of 1 was used and the time limit considered ranged from 30 minutes to 2 hours 30 minutes. The results are presented in Figure 5.24.
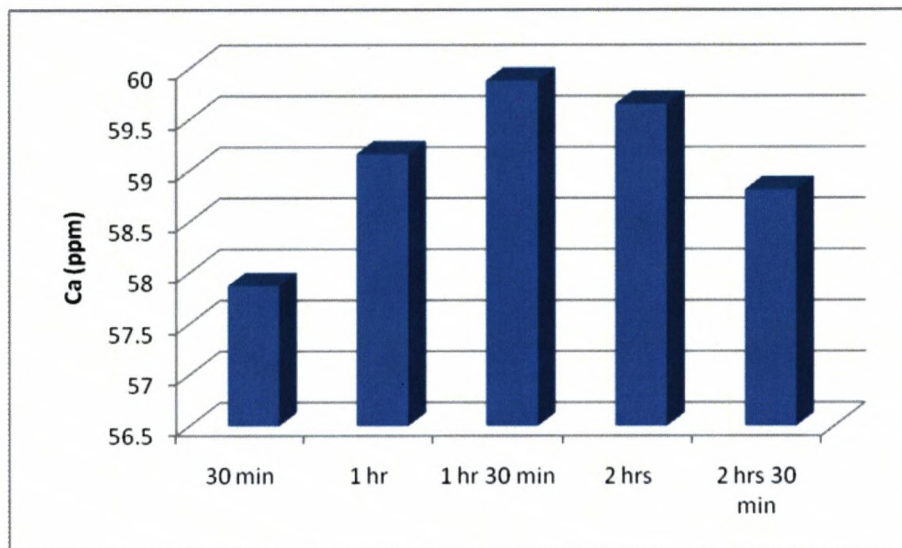
Figure 5.24: Effect of time on the leaching of Ca $^{2+}$ from FA

It is clear that the maximum leaching of Ca^{2+} occurred after the 1 hour 30 minutes time duration because by this point all the free lime had out. This confirms what had been obtained from literature and thus the time factor of two hours used for the carbonation procedure in this study was confirmed to be suitable.

5.9 EFFECT OF CARBONATION ON THE BRINE QUALITY

An investigation of the effect of carbonation on the quality of the brine used as dispersion media and the FA was carried out by comparing the elemental composition of the brine before carbonation with that of the leachates obtained

after carbonation. Brine and the leachate analysis were done using both IC and ICP-MS as described in sections 3.3.4 and 3.3.5 respectively. The leachates of Run R31 (carbonated at a pressure of 4 Mpa, 90 °C, S/L ratio of 1 using the bulk ash) are used to illustrate the % removal obtained while the results from the other runs are tabulated in Appendices 1 and 2. Table 5.12 below presents the elemental composition of the brine before and after carbonation for Run R31 whose conditions were observed to have resulted in the highest degree of carbonation using Chittick tests (Table 5.12).

Table 5.12: Elemental concentrations of the raw brine and the carbonation leachates (* means not detected).

Elements	Brine (ppm)	Carbonation leachates (ppm)	Reduction/ Increase (%)
Ca	101.2	25.5	74.80
Na	4488.4	3201	28.68
Mg	76.6	1.522	98.01
Fe	0.053	*	100
Al	0.023	*	100
Mn	0.076	*	100
K	57.065	9.75	82.91
Co	0.007	0.002	71.43
Cr	0.006	0.001	83.33
Cu	0.101	*	100
Mo	0.019	0.069	72.46
V	0.009	0.15	94
Zn	0.053	*	100
Pb	0.001	*	100
Ni	0.056	*	100
As	0.004	*	100
B	1.410	2.72	48.16
Ba	0.031	0.008	74.19
Ti	0.001	*	100
Sr	2.9	*	100
Se	0.002	*	100
Si	7.375	*	100
Cl	2036	2193	7.16
NO$_3$	8.565	*	100
SO$_4$	9488	7511	20.83

Table 5.12 above show the % reduction or increase of the brine elements after carbonation. The values highlighted in red are indicative of the elements whose

142

concentration increased after carbonation i.e. Mo, V, B and Cl. For elements such as Fe, Al, Mn, Cu, Zn, Pb, Ni, As, Ti, Sr, Se, Si and NO_3 hundred percent removal was achieved by carbonation. Bearing in mind that the brine had been classified as $NaSO_4$ waters (Figure 4.10), one observes that Na reduction was achieved up to 28.68 % while $SO4^{2-}$ reduction was 20.83 %. The Na reduction could be due to the formation of plagioclase ($NaAlSi_3O_8$-$CaAl_2Si_2O_8$), a phase only observed in the carbonated fly ash. SO_4^{2-} on the other hand is due to formation of anhydrite ($CaSO_4$) and bassanite ($2CaSO_4.H_2O$) upon carbonation. Mooketsi et al., (2007) concluded that the decrease in SO_4^{2-} concentration is a result of reaction between sulphates in brine and CaO to form the insoluble anhydrite. These phases thus consume some of the Na and SO_4^{2-} from the brine hence the reduction in their concentration in the carbonation leachates. It has been reported that B, V and Mo leach out of fly ash with time (Jankowski et al., 2006) due to formation of oxyanions that are soluble at the high pH values attained during the carbonation process (Kim et al., 2009). Elements such as Pb and Zn co-precipitate with $CaCO_3$ due to the predominance of $PbCO_3$ at pH 6-9 and $ZnOH_2$ at pH 9-11 (Ecke, 2003; Ecke et al., 2002). Other co-precipitating elements are Cd, Cr and Cu and their reduction in the carbonated leachates could be due to these co-precipitation reactions. Rendek et al., (2006) concurs that indeed carbonation leads to a reduced mobility of the above elements. It has been reported that the Cl content of the carbonated leachates is reduced due to the formation of NaCl (Mooketsi et al., 2007). The Cl content of the brine leachates increased slightly (7.16 %) during carbonation, a phenomena that could not be explained since the Na content did decrease as expected. It can thus be concluded that the carbonation process does lead to cleaner effluents compared to the original brine solutions through complexation and co-precipitation with the ash components during the carbonation process hence the reduction in concentrations.

5.10 EFFECT OF CARBONATION ON THE ELEMENTAL COMPOSITION OF FLY ASH

Total acid digestion was carried out as described in section 3.3.7 in order to evaluate the elemental concentration of the fresh un-carbonated ash and the

carbonated solid residues for Run R31 whose applied carbonation conditions were observed to give the highest % $CaCO_3$ yield. The results are tabulated in Table 5.13.

Table 5.13: Elemental concentration of the fresh ash and the carbonation solid residues (Run R31).

Elements	Fresh ash (mg/kg)	Carbonation Residues (mg/kg)
Ca	97.15	68.49
Na	21.68	31.71
Mg	12.44	10.72
Fe	146.73	112.6
Al	739.64	678.4
Li	0.87	0.70
Mn	5.24	1.82
K	42.07	40.49
Co	0.024	0.03
Cr	2.08	1.90
Cu	0.91	0.59
Mo	0.21	0.19
V	1.41	1.08
Zn	0.98	0.18
Pb	0.20	0.10
Ni	1.62	1.41
P	32.2	27.40
As	0.14	0.25
B	5374.7	5326
Be	0.06	0.06
Cd	0.02	0.02
Ba	3.65	2.96
Ti	73.00	66.52
Sr	9.69	8.03

The elemental concentration of all the elements was higher in the fresh ash than in the carbonated solid residues except for Na, As and Co (highlighted in red). The B, Mo and V reduction after carbonation can be associated with the observed increase of these elements in the carbonation leachates (Table 5.13) due to leaching from fly ash as was suggested by Jankowski et al., (2006). Reduction in Ca concentration is expected as it not only takes part in the formation of $CaCO_3$ but also phases such as plagioclase ($NaAlSi_3O_8$-$CaAl_2Si_2O_8$), anhydrite ($CaSO_4$) and bassanite ($2CaSO_4.H_2O$) that were identified using XRD (Figure 5.4). A

possible reason for the decrease in the concentration of leachable metal contaminants (e.g. Pb, Zn, Cr and Mn) is probably due to the precipitation of metal carbonates which are more insoluble than oxides and/or hydroxides (Reddy et al., 1994). Carbonation thus has the potential to reduce the concentration of certain leachable inorganic contaminants present in the FA matrix thereby minimizing the risk of these elements contaminating various aspects of the environment such as ground water.

5.11 SUMMARY OF THE STATISTICAL ANALYSIS

The carbonated residues had additional crystalline phases of calcite, aragonite, anhydrite, plagioclase and bassanite as determined by XRD. Carbonation of FA and brine mixtures led to formation of calcite and aragonite, the two polymorphs of $CaCO_3$ that are able to sequester CO_2 via carbonation reactions.

Run R31 carried out at 4 Mpa, 90 °C, using bulk ash and a S/L ratio of 1 gave the highest % $CaCO_3$ yield (6.5 %) as determined by Chittick test while quantitative XRD gave Run R2 conducted at 1 M pa, 90 °C, using the 20 μm- 150 μm particle size range at a S/L ratio of 0.5 as the one with highest % $CaCO_3$ (8.14%).

From statistical testing using t-test and concordance correlation coefficient as well as TGA analysis, Chittick test analysis was found to be the most suitable method for determining the % $CaCO_3$ hence the Chittick results were used to statistically analyze the significance of the input factors (temperature, pressure, S/L ratio and particle size).

ANOVA analysis, gave the main effects of pressure, temperature and particle size as significant together with the interactions of temperature and S/L ratio as well as the interaction of temperature and particle size. The model was also found to be statistically significant and could explain 93.40 % of the variability in the % $CaCO_3$ data.

Diagnostic plots were observed to follow the ideal situation. The model however could not be used to optimize the levels of the variables applied as the three points

that had been left out during the analysis due to the ineffective mixing, had an effect on the analysis and could lead to misleading optimization figures.

Pressure had a slight influence on the % $CaCO_3$ while the effect of temperature was pronounced.

The particle size range of 20 μm – 150 μm enhanced the degree of carbonation that could be achieved. This was closely followed by the bulk ash while the >150 μm particle fraction had the least influence on the % $CaCO_3$. The effect of S/L ratio was temperature dependent. At low temperature a S/L ratio of 1 resulted in the highest % $CaCO_3$ formation. On the other hand at high temperature, the ratio of 0.5 resulted in the highest % $CaCO_3$ formation. The temperature dependence of the S/L ratio could also be explained in terms of the higher % contribution value observed for the temperature- particle size interaction. In the temperature-particle size interaction, both the bulk ash and the >150 μm fractions gave higher values of % $CaCO_3$ formation at high temperature.

Overall the two most important parameters in the carbonation of FA and brine were found to be particle size and temperature. Other studies have shown the importance of temperature in carbonation of either MSWI ash or FA while pressure has been shown to be an insignificant variable. The observations in this study thus confirm the literature observations. The effect of particle size was observed to be highest at smaller particle sizes due to the higher surface area to volume ratio hence better contact. For the S/L ratio, very low or very high values were observed to inhibit carbonation. High temperatures were shown to favour carbonation reactions as the reaction kinetics were enhanced while the particle size range of 20 μm -150 μm was found to enhance carbonation . On average, this particle size range had a CaO content of 9.3 % compared to the bulk ash's CaO content of 9.198 %, further confirming that CaO was enriched in the smaller ash particles fraction. Secunda FA was observed to have a carbonation of 75.537 % and thus one ton of the FA could sequester 0.062 tons of CO_2. Elemental concentrations of both FA and brine solutions were observed to reduce after carbonation.

CHAPTER SIX

This chapter summarizes the major findings of this work and to what extent the stated objectives were achieved. Recommendations for further work are also given.

6.1 GENERAL CONCLUSIONS

The study has demonstrated the feasibility of CO_2 sequestration using the South African, class F FA together with the typical brine solutions derived from the water treatment circuits of coal fired power plants. FA from both Secunda and Tutuka power plants were classified as class F based on their CaO content as well as the content of silica, alumina and ferric oxide. The two FA from Tutuka and Secunda were found to be different in terms of elemental and mineralogical composition. Due to the higher CaO content of the Secunda FA (9.198 %) compared to Tutuka's 6.617 %, the former was selected for use in the carbonation experiments. Fresh ash was observed to have mullite, quartz, magnetite, hematite and lime as the main phases while carbonated residues and additional phases of bassanite, plagioclase, anhydrite, aragonite and calcite.

The RO brines from both Tutuka and Secunda were classified as $NaSO_4$ types while their permeates were classified as NaCl water types.

Secunda fresh FA that was used in this study was observed to have a carbonation efficiency of 75.537 % demonstrating the potential for applying the waste ash in reducing the CO_2 emissions from the power plants. Calcite was produced as the major mineral carbonation product from the brine and FA dispersions with small amounts of aragonite.

Theoretically one ton of Secunda FA containing 9.198 % of CaO could sequester 0.083 tons of CO_2. With the optimized protocol developed in this study bearing in mind that the carbonation efficiency is 75.537%, 1 ton of Secunda FA could sequester 0.062 tons of CO_2 therefore 16 tons of FA are required for sequestration

147

of a ton of CO_2. This would translate to 0.65 % of CO_2 produced per annum at Secunda plant being sequestered in the FA/brine dispersions.

The brine components are significantly reduced after carbonation (at 90 °C, 4 Mpa, at a S/L ratio of 1 using the bulk ash) and this could be attributed to co-precipitation due to supersaturated conditions arising during the mineral carbonation reaction thus leading to cleaner effluents after the carbonation process. Percentage reductions for the major cations and anions are as follows: Ca (74.80 %), Na (28.68 %), Mg (98.01 %), K (82.91 %), SO4 (20.83 %) Cl concentration however was observed to increase by a value of 7.16 %.

It was also observed that carbonation using brine resulted in higher carbonation efficiency than carbonation using water as the Ca^{2+} component in the brine contribute towards the Ca^{2+} concentration.

The optimum carbonation conditions identified in the study were pressure of 4 Mpa, temperature of 90 °C, S/L ratio of 1 when using the bulk ash.

The application of statistical design in carrying out the experiments resulted in a clear understanding of the transformations and the relationships of the applied input parameters. Two main advantages were achieved using this statistical approach; first, the number of experimental combinations was greatly reduced compared to studying the factors one at a time. Considering the same cost and time expenditure, the statistical approach was found to be robust in generating the desired data. Secondly, it was possible to investigate the effect of each parameter as well as the arising interactions, which would not have been possible with one factor at a time approach.

6.1.1 Advantages of mineral carbonation to South African power utilities

This study showed that it would be feasible to utilize the two "waste products" i.e. FA and brine together in the sequestration of CO_2. This would lower the treatment

cost for these waste waters and lead to brine stabilization in form of mineral carbonates.

Application of bulk ash would mean that there would be no additional cost for fractionation of the ash which is an added advantage.

Bearing in mind that some CO_2 source points such as Secunda already produce pressurized and purified CO_2 emissions, these streams could be applied for carbonation as they do not require further purification or pressurization, thereby contributing towards cost reduction for CO_2 sequestration.

Though utilization of waste fly ash and brine to reduce CO_2 emissions will not lead to significant carbon credits and hence carbon trading, these wastes are available in huge amounts and in close proximity to the emission sites, hence transportation cost are lowered.

Considering that most of the brine components are stabilized within the ash matrix after carbonation, this process could be maximized and applied for brine clean-up thus reducing the cost of chemicals as FA and CO_2 are already considered as waste streams.

6.2 RECOMMENDATIONS

It would be valuable to investigate the carbonation efficiency of FA and brine streams from other South African power plants as the overall mineral carbonation process is expected to result in differing degrees of carbonation, depending on the operating conditions applied in the different coal combustion power plants and the ash composition which varies from site to site.

Due to the complexity of the applied design and the fact that three experiments that could not be carried out due to difficulty in mixing were left out, point prediction was not possible; it is recommended that a simpler design be applied to study the effects of the input parameters. This could be applied in a pilot scale to evaluate the economics of the process. Furthermore for the > 150 μm fraction, a

S/L ratio lower than 1 can be applied to study the effect of a S/L ratio other than 0.5 that was possible in this study.

Elemental and chemical studies of the weathered ash are recommended, in order to evaluate the differences with the fresh ash.

A leaching protocol should be applied to evaluate the long term stability of immobilized metals due to the carbonation process.

Since CO_2 serves as a reactant in the carbonation process, its use to purge the reactor could underestimate the CO_2 sequestered and should be replaced with an inert gas such as argon since argon is denser than air and thus can be used to rid the reactor of air.

A one way valve pressure regulator should be used with the high pressure reactor to prevent the contents of the reactor from flushing back into the inlet.

REFERENCES

Abufayed A.A. & El Ghuel M.K. (2001), "Desalination process application in Libya", *Desalination,* vol. 138, pp. 47-53.

Adriano, D.C., Page, A.L., Elseewi, A.A., Chang, A.C. & Straughan, I. (1980), "Utilization and disposal of fly ash and other coal residues in terrestrial ecosystems", *Journal of Environmental Quality,* vol. 9, no. 3, pp. 333-344.

Ahmed, M., Arakel, A., Hoey, D. & Coleman, M. (2001), "Integrated power, water and salt generation: a discussion paper", *Desalination,* vol. 134, no. 1-3, pp. 37-45.

Ahmed, M., Shayya, W.H., Hoey, D. & Al-Handaly, J. (2001), "Brine disposal from reverse osmosis desalination plants in Oman and the United Arab Emirates", *Desalination,* vol. 133, no. 2, pp. 135-147.

Ainsworth, C.C. & Rai, D. (1987), Chemical characterization of fossil fuel combustion wastes, Department of Energy, USA.

Aitken, R.L., Campbell, D.J. & Bell, L.C. (1984), "Properties of Australian fly ashes relevant to their agronomic utilization", *Austaralian Journal of Soil Research,* vol. 22, no. 4, pp. 443-453.

American Society for Testing and Materials (1993), *ASTM 618:* Standard speciation for fly ash and raw or calcined natural pozzolan for uses as a mineral admixture in Portland cement concrete, American Society for Testing and Materials, Philadelphia, Pennsylvania.

Amrhein, C., Haghania, G.h., Kim, T.S., Mosher, P.A., Gagajena, R.C., Amarios, T. & Torre, L. (1996), "Synthesis and properties of zeolites from coal fly ash", *Environmental Science and Technology,* vol. 30, no. 3, pp. 735-742.

151

Anthony, E.J., Jia, L., Woods, J., Roque, W. & Burwell, S. (2000), "Pacification of high calcic residues using carbon dioxide", *Waste Management,* vol. 20, no. 1, pp. 1-13.

Arenillas A, Smith K.M, Drage T.C and Snape C.E (2005), "CO_2 capture using some fly ash derived carbon materials", *Fuel,* vol. 84, pp. 2204-2210.

Bachu, S. (2008), "CO_2 storage in geological media; role, means, status and barriers to deployment", *Progress in Energy and Combustion Sciences,* vol. 34, pp. 254-273.

Bekkum, V.H., Flanigen, E.M. & Jansen, J.C. (1991), Introduction to zeolite science and practice, Elsevier Science, Netherlands.

Boccaccini, A.R., Petitmermet, M. & Wintermantel, E. (1997), "Glass ceramics form municipal incinerator fly ash", *American Ceramic Society Bulletin,* vol. 76, pp. 75-78.

Bolt, N. & Snel, A. (1986), "Environmental aspects of fly ash application in the Netherlands", Kema Scientific and Technical Reports, The Netherlands.

Bosch, G.L. (1990), "The mineralogy and chemistry of pulverized fuel ash produced by three South African coal burning power stations", Unpublished Msc Thesis, University of Cape Town.

Bouchekima, B., Gros, B., Ouahes, R. & Diboun, M. (2001), "Brakish water desalination with heat recovery", *Desalination,* vol. 138, no. 1-3, pp. 147-155.

Bourouni, K., Chaibi, M.T. & Tadrist, L. (2001), "Water desalination by humidification and dehumidification of air: State of the art", *Desalination,* vol. 137, no. 1-3, pp. 167-176.

Breck, D.W. (1984), "Zeolites molecular sieves, structure, chemistry and use", Kruger publishing, University of Michigan, USA.

Bristow, A., Pridmore, A., Tight, M., May, T., Berkhout, F. & Harris, M. (2004), "How can we reduce carbon emissions from transport?" Tyndall Centre Technical Report, London.

Buckley, C.A., Simpson, A.E., Kerr, C.A. & Schutte, C.F. (1987), "Treatment and disposal of waste brine solutions", *Desalination,* vol. 67, pp. 431-438.

Buhrmann, F., Van der Walt, M., Hanekan, D. & Finlayson, F. (1999), "Treatment of industrial wastewater for reuse", *Desalination,* vol. 124, pp. 263-269.

Cairns, S. & Newson, C. (2006), "Predict and decide: Aviation, Climate Change and UK Policy Report"., Environmental Change Institute, Oxford University.

Campbell, J.A., Laul, J.C., Nielson, K.K. & Smith, R.D. (1978), "Separation and chemical characterization of finely-sized fly ash particles", *Analytical Chemistry,* vol. 50, no. 8, pp. 1032-1042.

Carlson, C.L. & Adriano, D.C. (1993), "Environmental impacts of coal combustion residues", *Journal of Environmental Quality,* vol. 22, pp. 227-247.

Chae, S.R., Hwang, E.J. & Shin, H.S. (2006), "Single cell protein production of *Euglena gracilis* and carbon dioxide fixation in an innovative photo-bioreactor", *Bioresource Technology,* vol. 97, pp. 322-329.

Chang, A.C., Lund, L.J., Page, A.L. & Warneke, J.E. (1977), "Physical properties of fly ash amended soils", *Journal of Environmental Quality,* vol. 6, pp. 267-270.

Chapman, L. (2007), "Transport and climate change: A review", *Journal of Transport Geography,* vol. 15, pp. 354-367.

Chiquet, P., Daridon, J., Broseta, D. & Thibeau, S. (2007), "CO_2/water interfacial tensions under pressure and temperature conditions of CO_2 geological storage", *Energy Conversion & Management,* vol. 48, pp. 736-744.

Cioffi, R., Pernice, P., Aronne, A., Catauro, M. & Quattroni, G. (1994), "Glass-ceramics from fly ash with added Li_2O", *Journal of the European Ceramic Society,* vol. 13, no. 2, pp. 143-148.

Czarnecki, J. & Sestak, J. (2000), "Practical thermogravimetry.", *Journal of Thermal Analysis and Calorimetry,* vol. 60, pp. 759-778.

Davison, R.l., Natusch, D.F.S., Wallace, J.R. & Evans, C.A.J. (1974), "Trace elements in fly ash: Dependence of concentration on particle size", *Environmental Science and Technology,* vol. 8, no. 13, pp. 1107-1113.

Design-Expert 7.1 User's manual guide, (2001), "Factorial designs tutorial" DX7-03A, Revised on 15th April 2007.

Dreimanis, A. (1962), "Quantitative gasometric determination of calcite and dolomite by using Chittick apparatus", *Journal of Sedimentary Petrology,* vol. 32, pp. 520-529.

Eary, L.E., Rai, D., Mattigod, S.V. & Ainsworth, C.C. (1990), "Geochemical factors controlling the mobilization of inorganic constituents from fossil fuel combustion residues II, Review of the minor elements", *Journal of Environmental Quality,* vol. 19, pp. 202-214.

Eaton, A.D., Clescere, L.S., Greenberg, A.E. & Franson, M.A.H. (1995), "Standard methods for the examination of water and wastewaters", 19th edition, American Public Health Association, Washington DC.

Ecke, H. (2003), "Sequestration of metals in carbonated municipal solid waste incineration (MSWI) fly ash", *Waste Management,* vol. 23, pp. 631-640.

Ecke, H., Menad, N. & Lagerkvist, A. (2003), "Carbonation of MSWI fly ash and the impact on the metal mobility", *Journal of Environmental Engineering,* vol. 129, no. 5, pp. 435-440.

154

Ecke, H., Menad, N. & Lagerkvist, A. (2002), "Treatment oriented characterization of dry scrubber residue from municipal solid waste (MSWI)", *Journal of Materials Cycles and Waste Management,* vol. 4, no. 2, pp. 117-126.

El-Manharawy, S. & Hafezb, A. (2003), "A new chemical classification system of natural waters for desalination and other industrial uses", *Desalination,* vol. 156, pp. 163-180.

Eloneva, Sanni., Teir, Sebastian., Salminen, Justin., Fogelholm, Carl-Johan. & Zevenhoven, Ron. (2008), "Fixation of CO2 by carbonating calcium derived from blast furnace slag", *Energy,* vol.33, pp. 1461-1467.

El Saie, Ali., M.H., Ali El Saie, Y.M.H. & El Gabry, H. (2002), "Techno-economic study for combined cycle power generation with desalination plants at Sharm El Sheikh,", *Desalination,* vol. 153, no. 1-3, pp. 191-198.

Engelbrecht, A., Golding, A. & Hietkamp, S. (2004), "The potential for sequestration of CO_2 in South Africa", Council for Scientific and Industrial Research (CSIR), South Africa.

Eskom Environmental Report (2006), "Reducing water consumption".

Eskom Fact Sheet GFS.0011, (2006) (sourced from www.eskom.co.za on 27th July 2008).

Eskom Research Report, (2001).

Eskom Environmental Report, (2000).

Everitt, B.S. (2002), Cambridge Dictionary of Statistics, Cambridge University Press, ISBN 0-521-81099.

Fatoba, O.O. (2007), "Chemical composition and leaching behaviour of some South African fly ashes", Unpublished Msc Thesis, University of the Western Cape.

155

Fernandez, M.B., Li, X., Simons, S.J.R., Hills, C.D. & Carey, P.J. (2004), "Investigation of accelerated carbonation for the stabilization of MSW incinerator ashes and the sequestration of CO_2 ", *Green Chemistry,* vol. 6, pp. 428-436.

Ferreira, C., Ribeiro, A. & Ottosen, L. (2003), "Possible applications for municipal solid waste fly ash", *Journal of Hazardous Materials,* vol. 96, no. 2-3, pp. 201-216.

Figueroa, D.J., Fout, T., Plasynki, S., McIlvried, H. & Srivastava, D.R. (2008), "Advances in CO_2 capture technology, The US Department of Energy's carbon sequestration program", *International Journal of Greenhouse Gas Control,* vol. 2, pp. 9-20.

Fisher, G.L., Chang, D.P.Y. & Brummer, M. (1976), "Fly ash collected from electrostatic precipitators; microcrystalline structures and mystery of the spheres", *Science,* vol. 192, no. 4239, pp. 553-555.

Foner, H.A., Robl, T.L., Hower, J.C. & Graham, U.M. (1999), "Characterization of fly ash from Israel with reference to its possible utilization", *Fuel,* vol. 78, no. 2, pp. 215-223.

Freyssinet, P., Piantone, P., Azaroual, M., Itard, Y., Clozel-Leloup, B., Guyonnet, D. & Baubron, J.C. (2002), "Chemical changes and leachate mass balance of municipal solid waste bottom ash submitted to weathering", *Waste Management,* vol. 22, no. 2, pp. 159-172.

Furr, A.K., Parkinson, T.F., Gutenmann, W.H., Pakkala, I.S. & Lisk, D.J. (1978), "Elemental content of vegetables, grains and forages field grown on fly ash amended soil", *Journal of Agriculture and Food Chemistry,* vol. 26, no. 2, pp. 357-359.

Gangloff, W.J., Ghodrati, M., Sims, J.T. & Vasilas, B.J. (2000), "Impact of fly ash amendment and incorporation method on hydraulic properties of a sandy soil", *Water, Air and Soil Pollution,* vol. 119, pp. 231-245.

Ginster, M. & Matjie, H.R. (2004), "Beneficial utilization of Sasol coal gasification ash", Sasol Technology, Sasolburg.

Gitari, W.M. (2006), "Treatment of acid mine drainage with fly ash: removal of major contaminants and trace elements", *Journal of Environmental Science and Health,* vol. A41, no. 8, pp. 1729-1747.

Gitari, W.M., Petrik, L.F., Etchebers, O., Key, D.L., Iwuoha, E. & Okujeni, C. (2008), "Passive neutralization of acid mine drainage by fly ash and its derivatives: A column leaching study", *Fuel,* vol. 87, no. 8-9, pp. 1637-1650.

Glordano, M.P., Behel, D.A., Lawrence, J.E., Jr., Solleau, J.M., Jr. & Bradford, N.B. (1983), "Mobility in soil and plant availability of metals derived from incinerated municipal refuse", *Environmental Science and Technology,* vol. 17, pp. 193-198.

Goff, F., Guthrie, G. & Lackner, K.S. (1998), "Carbon dioxide sequestration potential of ultramafic rocks", 23rd Annual Technical Conference on Coal Utilization and Fuel Systems, Clearwater, Florida.

Goldstein, L., Newbury, D.E., Echlin, P. & Lyman, C.E. (2003), "Scanning electron microscopy and X-ray microanalysis", Kluwer Academic/ Plenum Publishers, New York.

Goodarzi, F. (2006), "Morphology and chemistry of fine particles emitted from a Canadian coal-fired power plant", *Fuel,* vol. 85, no. 3, pp. 273-280.

Grigorios, S.I., Socrates, I. & Nikolaos, K. (2009), "The effect of the particle size differentiation of lignite fly ash on cement industry applications", World of Coal Ash (WOCA), Lexington, Kentucky, USA.

Grossman, S.L. & Nathan, Y. (1988), "The mineralogy and chemistry of coal ash generated by the Hadera M.D power station", *Journal of Coal Quality,* vol. 7, no. 1, pp. 22-26.

Gunter, W.D., Perkins, E.H. & Hutcheon, I. (2000), "Aquifer disposal of acid gases: modeling of water-rock reactions for trapping of acid wastes", *Applied Geochemistry,* vol. 15, pp. 1085-1095.

Gurdeep, S. & Bradley, C.P. (2001), "Assessment of groundwater quality due to use of coal combustion by-products to control subsidence from underground mines", *Environmental International,* vol. 26, pp. 561-571.

Halstead, W.J. (1986), "Use of fly ash in concrete; Synthesis of highway practice" vol. 127, Transportation Research Board, National Research Council, Washington DC.

Hansen, Y., Notten, P.J. & Petrie, J.G. (2002), "The environmental impact of ash management in coal-based power generation", *Applied Geochemistry,* vol. 17, no. 8, pp. 1131-1141.

He, F. & Qin, D. (2006), "China's energy strategy in the twenty-first century", *China and World Economy,* vol. 14, no. 2, pp. 93-104.

Hinton, R.P. (1995), "Statistics Explained". Routeledge, London.

Hoehn, R.C. & Sizemore, D.R. (1995), "Acid mine drainage and its impact on a small Virginia stream." *Water Resources Bulletin,* vol. 13, pp. 153-160.

Huijgen, W.J.J. & Coman, R.N.J. (2003), "Carbon dioxide sequestration by mineral carbonation", Literature review, Energy Research Centre of the Netherlands, Petten, The Netherlands.

Huntzinger, D.N., Gierke, J.S., Sutter, L.L., Kawatra, K.S. & Eisele, T.C. (2009), "Mineral carbonation for carbon sequestration in cement kiln dust from waste piles", *Journal of Hazardous Materials,* .

Hwa, J.J. & Jeyaseelan, S. (1997), "Conditioning of oily sludges with MSWI ash", *Water Science and Technology,* vol. 35, no. 8, pp. 231-238.

Ilic, M., Cheeseman, C., Sollars, C. & Knight, J. (2003), "Mineralogy and microstructure of sintered lignite coal fly ash", *Fuel,* vol. 82, no. 3, pp. 331-336.

Intergovernmental Panel on Climate Change (2007), Climate Change Synthesis Report, IPCC Plenary XXVII, Valencia, Spain.

Intergovernmental Panel on Climate Change report (2005), "Mineral carbonation and industrial uses of carbon dioxide"

International Center for Diffraction Data, Powder diffraction file, "PDF" database, (1998), Newton Square, Pennslyvania, USA.

Iyer, R. (2002), "The surface chemistry of leaching coal fly ash", *Journal of Hazardous Materials,* vol. 93, no. 3, pp. 321-329.

Jankowski, J., Ward, R.C., French, D. & Grores, S. (2006), "Mobility of trace elements from selected Australian fly ash and its potential on aquatic ecosystems.", *Fuel,* vol. 85, pp. 234-256.

Jarvis, K.E., Gray, A.L. & Houk, R.S. (1992), "Handbook of Inductively coupled plasma mass spectrometer", *Chromatographia,* vol. 34, no. 9-10, pp. 546-551.

Jones, D.R. (1995), "The leaching of major and trace elements from coal ash" in "Environmental aspects of trace elements in coal", Kluwer Academic Publishers, Netherlands, pp. 221-262.

Kaakinen, J.W., Jordan, R.M., Lawasani, M.H. & West, R.E. (1975), "Trace element behaviour in coal fired power plants", *Environmental Science and Technology,* vol. 9, pp. 862-869.

Kaibouchi, S. & Germain, P. (2003), "Comparative study of physicochemical and environmental characteristics of (MSWI) bottom ash resulting from classical and selective collection for a valorization in road construction" in "Progress on the road to sustainability", Fifth International Conference on the Environmental and

technical implications of construction with alternative materials," San Sebastian, Spain, pp. 645-653.

Kakizawa, M., Yamasaki, A. & Yanagisawa, Y. (2001), "A new CO_2 disposal process via artificial weathering of calcium silicate accelerated by acetic acid", *Energy,* vol. 26, no. 4, pp. 341-354.

Kalnicky, D.J. & Singhvi, R. (2001), "Field portable XRF analysis of environmental samples", *Journal of Hazardous Materials,* vol. 83, no. 1-2, pp. 93-122.

Kalogirou, S.A. (2005), "Seawater desalination using renewable energy sources", *Progress in Energy and Combustion Science,* vol. 31, no. 3, pp. 242-281.

Kharaka, Y.K., Thordsen, J.J., Hovorka, S.D., Seay Nance, H., Cole, D.R., Phelps, T.J. & Knauss, K.G. (2009), "Potential environmental issues of CO_2 storage in deep saline aquifers: Geochemical results from the Frio-I Brine Pilot test, Texas, USA", *Applied Geochemistry,* doi:10.1016,j.apgeochem.2009.02.010, ISBN, 0883-2927.

Kim G.A, Kazonich .G & Dahlberg .M, (2003), "Relative solubility of cations in Class F fly ash", *Environmental Science and Technology,* vol. 37, pp. 4507-4511.

Kim, A.G. & Hesbach, P. (2009), "Comparison of fly ash leaching methods.", *Fuel,* vol. 88, pp. 926-937.

Kimmel, W.G. (1993), "The impact of acid mine drainage on the stream ecosystem" in "The Pennsylvania Coal: resources, technology and utilization", The Pennsylvania Academy of Sciences Publishing, Pennsylvania, USA, pp. 424-437.

Klass, L.D. (2003), "A critical assessment of renewable energy usage in the USA", *Energy Policy,* vol. 31, no. 4, pp. 353-367.

Klein, D.H., Andren, A.W., Carter, J.A., Emery, J.F., Feldman, C., Fulkerson, W., Lyon, W.S., Ogle, J.C., Talmi, Y., Van Hook, R.I. & Bolt, N. (1995), "Pathways of thirty seven trace elements through coal fired power plants", *Environmental Science and Technology,* vol. 9, pp. 973-979.

Kruger, R.A. & Krueger, J.E. (2005), "Historical development of coal ash utilization in South Africa", CSIR, Pretoria, South Africa.

Kruger, R.A. (2003), "Fly ash beneficiation in South Africa: creating new opportunities in the market-place", *Fuel,* vol. 76, no. 8, pp. 777-779.

Kutchko, B.G. & Kim, A.G. (2006), "Fly ash characterization by SEM–EDS", *Fuel,* vol. 85, no. 17-18, pp. 2537-2544.

Lackner, K.S., Wendt, C.H., Butt, D.P., Joyce, E.L. & Sharp, D.H. (1995), "Carbon dioxide disposal in carbonate minerals", *Energy,* vol. 20, no. 11, pp. 1153-1170.

Le Dirach, J., Nisan, S. & Poletiko, C. (2005), "Extraction of strategic materials from the concentrated brine rejected by integrated nuclear desalination systems", *Desalination,* vol. 182, no. 1-3, pp. 449-460.

Lederman, E., Cohen, H., Polat, M. & Pelly, I. (2003), "Chemical scrubbing of acidic/organic effluents using coal fly ash", *Journal of Ore-dressing,* vol. 6, pp. 18-35.

Lee, R.E.J., Crist, H.L., Riley, A.E. & Macleod, K.E. (1975), "Concentration and size of trace metal emissions from a power plant, a steel plant and a cotton gin", *Environmental Science and Technology,* vol. 9, pp. 643-647.

Lemos de Sousa, M.J. & Rodriguez, C. (2008), "CO_2 geological storage in North Atlantic and Gondwana Coal-types: Comparative research using laboratory modelling vs pilot test", International Advancements in Engineering, Science and CO_2 Technologies (CCS) with specific emphasis on storage, monitoring, validation and legislation, Johannesburg, South Africa.

Lemos de Sousa, M.J., Rodriguez, C., Oliveira, G.m. & Dinis, M.A. (2008) "The European Union 2020 targets in terms of energy and environment: How the CO_2 geological storage can contribute?", International Advancement in Engineering, Science and CO_2 Technologies (CCS) with specific emphasis on storage, monitoring, validation and legislation, Johannesburg, South Africa.

Lenzen, M., Dey, C. & Hamilton, C. (2003), "Climate change" in Handbook of transport and the environment, 4th edition, Elsevier, Netherlands, pp. 37-60.

Lewis, A.E., Mokone, T.P. & van Hille, R.P., (2009), "Mechanisms responsible for particle formation during metal sulphide precipitation processes" International Mine Water Conference, CSIR, Pretoria.

Li, M., Hu, S., Xiang, J., Sun, L.S., Li, P.S., Su, S. & Sun, X. (2003), "Characterization of fly ashes from two Chinese municipal solid waste incinerators", *Energy and Fuels,* vol. 17, no. 6, pp. 1487-1491.

Li, X., Bertos, F.M., Hills, D.C., Carey, J.P. & Simon, S. (2007), "Accelerated carbonation of municipal solid waste incineration fly ashes", *Waste Management,* vol. 27, pp. 1200-1206.

Lin, L.K. (1989), "A concordance Correlation Coefficient to Evaluate Reproducibility", *Biometrics,* vol. 45, pp. 255-268.

Mangialardi, T., Paolini, A.E. & Sirini, P. (1999), "Optimization of the solidification/stabilization process of MSW fly ash in cementitious matrices", *Journal of Hazardous Materials,* vol. 70, no. 1-2, pp. 53-70.

Matsunaga, T., Kim, J.K., Hardcastle, S. & Rohatgi, P.K. (2002), "Crystallinity and selected properties of fly ash particles", *Materials Science and Engineering A,* vol. 325, no. 1-2, pp. 333-343.

McCarthy, M.J. & Dhir, R.K. (1999), "Towards maximizing the use of fly ash as a binder", *Fuel,* vol. 78, no. 2, pp. 121-132.

Mead, R. (1991), "The design of experiments - statistical principles for practical application", Cambridge University Press, New York.

Medina, M.G., Bond, G.M. & Rogelj, S. (2000), "Comparison of carbonic anhydrase isozymes for use as a catalyst in carbon dioxide sequestration process", 93rd Annual conference and exhibition of the air and waste management association, pp. 5996-6013, Pittsburg, Pennsylvania.

Meima, J.A., van der Weijden, R.D., Eighmy, T.T. & Comans, R.N.J. (2002), "Carbonation processes in municipal solid waste incinerator bottom ash and their effect on the leaching of copper and molybdenum", *Applied Geochemistry,* vol. 17, no. 12, pp. 1503-1513.

Mickley, M., Hamilton, R., Gallegos, L. & Truesdall, J. (1993), "Membrane concentrate disposal", American Water Works Association Research Foundation, Denver, Colorado.

Mimura, H., Yokota, K., Akiba, K. & Onodera, Y. (2001), "Alkali hydrothermal synthesis of zeolites from coal fly ash and their uptake properties of cesium ion", *Journal of Nuclear Science and Technology,* vol. 38, no. 9, pp. 766-772.

Montes-Hernandez, G., Pérez-López, R., Renard, F., Nieto, J.M. & Charlet, L. (2009), "Mineral sequestration of CO_2 by aqueous carbonation of coal combustion fly-ash", *Journal of hazardous materials,* vol. 161, no. 2-3, pp. 1347-1354.

Montgomery, D.C. (2009), "Design and Analysis of Experiments", 7th edition, John Wiley and Sons Inc., New Jersey.

Mooketsi, I.O., Ginster, M., Matjie, H.R. & Riedel, J.K. (2007), "Leachate characteristics of ash residues from a laboratory scale brine encapsulation simulation process", World of Coal Ash (WOCA), Kentucky, USA.

Morse, J.W. & Bender, M.L. (1990), "Partition coefficients in calcite: Examination of factors influencing the validity of experimental results and their application to natural systems", *Chemical Geology,* vol. 82, pp. 265-277.

Mulder, E. (1996), "Pre-treatment of MSWI fly ash for useful application", *Journal of Waste Management,* vol. 16, no. 1-3, pp. 181-184.

Murad, E.U.S., Jerry, M.B. & Carlson, C.L. (1994), "Mineralogical characteristics of poorly crystallized precipitates formed by oxidation of Fe^{2+} in acid sulfate waters.", *American Chemical Society,* vol. 13, pp. 191-200.

Nakicenovic, N. & Swart, R. (2000), IPCC Special Report: Emissions Scenarios, Cambridge University Press.

Nathan, Y., Dvorachek, M., Pelly, I. & Mimran, U. (1999), "Characterization of fly ash from Israel.", *Fuel,* vol. 78, pp. 205-213.

Nikolaos, K., Vasilatos, C., Itskos, G., Mitsis, I. & Moutsatsou, A. (2009), "Removal of heavy metals from wastewater using CFB-coal fly ash zeolitic materials", *Journal of hazardous materials,* doi:10.1016/j.hazmat.2009.08.126 .

Nishikawa, T., Suzuki, K., Ito, S., Sato, K. & Tabeke, T. (1992), "Decomposition of synthesized ettringite by carbonation", *Cement and Concrete Research*, vol.22, no. 1, pp. 6-14.

Notten, P.J. (2001), "LCA of large scale resource based process industries; A focus on coal based power generation", Published PhD thesis, Department of chemical engineering, University of Cape Town.

O'connor, W.K., Dahlin, D.C., Nilsen, D.N., Gedermann, S.J., Rush, G.E., Walters, R.P. & and Turner, P.C. (2001), "Research status on the sequestration of carbon dioxide by direct aqueous mineral carbonation", 18th Annual Pittsburgh Coal Conference, Newcastle, Australia.

Parekh, S., Farid, M.M., Selman, J.R. & Al-hallaj, S. (2003), "Solar desalination with a humidification-dehumidification technique - a comprehensive technical review", *Desalination,* vol. 160, no. 2, pp. 167-186.

Penner, J.E., Lister, D.H., Griggs, D.J., Dokken, D.J. & McFarland, M. (1999), IPCC Special Report: Aviation and the global atmosphere, Cambridge University Press, London.

Perez-Lopez, R., Montes-Hernandez, G., Nieto, J.M., Renard, F. & Charlet, L. (2008), "Carbonation of alkaline paper mill waste to reduce CO_2 greenhouse gas emissions into the atmosphere.", *Applied Geochemistry,* vol. 23, pp. 2292-2300.

Persechino, M.J. & von Gottenberg, J.M.A. (2001), "Integrated membrane systems for water reuse", Membrane technology for waste water reclamation and reuse, Tel-Aviv, Israel.

Peters, T. & Pintó, D. (2008), "Seawater intake and pre-treatment/brine discharge environmental issues", *Desalination,* vol. 221, no. 1-3, pp. 576-584.

Petrik, F.L., White, A.R., Klink, J.M., Somerset, S.V., Burgers, L.C. & Fey, V.M. (2003), "Utilization of South African fly ash to treat acid coal mine drainage and high quality zeolite synthesis from the solids produced", International ash utilization symposium, Lexington, Kentucky, USA.

Petrik, L., Lewis, A.E. & Hendry, B.A. (2007), "Brine treatment and disposal", Coaltech Report, South Africa.

Petrik, L.F., Gitari, W.M., Etchebers, O., Nel, J., Kumar, V.R.V., Fatoba, O.O., Nyamhingura, A., Akinyemi, S.A. & Antonie, M.J. (2008), "Towards the development of sustainable salt sinks: Fundamental studies on the co-disposal of brines within inland ash dams", Eskom/ Sasol Report, University of the Western Cape.

Pieterson, H.S. (1993), "Reactivity of fly ash and slag in cement", Published Msc thesis, Delft University of Technology, The Netherlands.

Piper, A.M. (1944), "A geographic procedure in the geochemical interpretation of water analyses", *American Geophysical Union Transactions,* vol. 25, pp. 914-923.

Potts, P.J. (1992), "A handbook of silicate rock analysis", Blackie and Sons Ltd, London.

Queralt, I., Querol, X., López-Soler, A. & Plana, F. (1997), "Use of coal fly ash for ceramics: a case study for a large Spanish power station", *Fuel,* vol. 76, no. 8, pp. 787-791.

Querol, X. & Pires, M. (2004), "Characterization of Candiota (South Brazil) coal and combustion by-products.", *International Journal of Coal Geology,* vol. 60, pp. 57-72.

Querol, X., Moreno, N., Umaña, J.C., Alastuey, A., Hernández, E., López-Soler, A. & Plana, F. (2002), "Synthesis of zeolites from coal fly ash: an overview", *International Journal of Coal Geology,* vol. 50, no. 1-4, pp. 413-423.

Querol, X., Plana, F., Alastuey, A. & López-Soler, A. (1997), "Synthesis of Na-zeolites from fly ash", *Fuel,* vol. 76, no. 8, pp. 793-799.

Ramesh, A. & Kozinski, J.A. (2001), "Investigations of ash topography/morphology and their relationship with heavy metals leachability", *Environmental Pollution,* vol. 111, no. 2, pp. 255-262.

Randall, S. (2002), "Energy and sustainable development in South Africa", Sustainable Energy Watch Report, Helio International, South Africa.

Reardon, E.J., Czank, C.A., Warren, C.J., Dayal, R. & Johnston, H.M. (1995), "Determining controls on element concentrations in fly ash leachate", *Waste Management & Research,* vol. 13, no. 5, pp. 435-450.

Reddy, K.J., Gloss, S.P. & Wang, L. (1994), "Reaction of CO_2 with alkaline solid wastes to reduce contaminant mobility", *Water Resources,* vol. 28, no. 6, pp. 1377-1382.

Rendek, E., Ducom, G. & Germain, P. (2006), "Influence of organic matter on municipal solid waste incineration bottom ash carbonation", *Chemosphere,* vol. 64, pp. 1212-1218.

Reynolds, K., Kruger, R. & Rethman, N. (1999), "The manufacture and evaluation of an artificial soil (slash) prepared from fly ash and sewage sludge", International ash utilization symposium, Centre for Applied Energy Research, University of Kentucky, USA, pp. 378-385.

Rhee, S., Reible, D.D. & Constant, W.D. (1993), "Stochastic modeling of flow and transport in deep-well injection disposal systems", *Journal of Hazardous Materials,* vol. 34, no. 3, pp. 313-333.

Robb, G.A. & Robinson, J.D.F. (1995), "Acid drainage from mines", *The Geographical Journal,* vol. 161, pp. 47-54.

Rosen, C.J. & Bierman, P. M, Olson, D. (1994), "Swiss chard and Alfalfa responses to soils amended with MSWI ash; Growth and elemental composition", *Journal of Agriculture and Food Chemistry,* vol. 42, pp. 1361-1368.

Sabbas, T., Polettini, A., Pomi, R., Astrup, T., Hjelmar, O., Mostbauer, P., Cappai, G., Magel, G., Salhofer, S., Speiser, C., Heuss-Assbichler, S., Klein, R. & Lechner, P. (2003), "Management of municipal solid waste incineration residues", *Waste Management,* vol. 23, no. 1, pp. 61-88.

Safi, M.J. & Korchani, A. (1999), "Cogeneration applied to water desalination: Simulation of different technologies", *Desalination,* vol. 125, no. 1-3, pp. 223-229.

Saikia, N., Kato, S. & Kojima, T. (2006), "Compositions and leaching behaviours of combustion residues", *Fuel,* vol. 85, no. 2, pp. 264-271.

Saripalli, K.P., Sharma, M.M. & Bryant, S.L. (2000), "Modeling injection well performance during deep-well injection of liquid wastes", *Journal of Hydrology,* vol. 227, no. 1-4, pp. 41-55.

Sarkar, A., Rano, R., Udaybhanu, G. & Basu, A.K. (2006), "A comprehensive characterisation of fly ash from a thermal power plant in Eastern India", *Fuel Processing Technology,* vol. 87, pp. 259-277.

Scholes, R.J. & Van der Merwe, M.R. (1998), "South Africa greenhouse gas emissions inventory for the year 1990 - Phase 1", Council for Scientific and Industrial Research (CSIR), Pretoria, South Africa.

Schwartz, M.O. & Ploethner, D. (2000), "Removal of heavy metals from mine water by carbonate precipitation in Grootfontein- Omatako canal, Namibia", *Environmental Geology,* vol. 39, no. 10, pp. 1117-1126.

Seifritz, W. (1990), "CO_2 disposal by means of silicates", *Nature,* vol. 245, pp. 486-492.

Shaffer, L.H. & Mintz, M.S. (1980), "Electrodialysis" in "Principles of desalination, Part A", 2nd edition., Academic Press, New York, pp. 257-357.

Shi, Y.L., Jun-Qing, Q., Zhang-Gui, W., Wei-Dong, Y., Guo-Feng, W., Yi-Bin, P. & Kai, Y.Z. (2009), "Application of statistical method to evaluate immobilization variables of trypsin entrapped with sol-gel method.", *Journal of Biochemical Technology,* vol. 1, no. 3, pp. 79-84.

Show, K.Y., Tay, J.H. & Goh, A.T.C. (2003), "Reuse of incinerator fly ash in soft soil stabilization", *Journal of Materials in Civil Engineering,* vol. 15, no. 4, pp. 335-343.

Simsek-Ege, F.A., Bond, G.M. & Stringer, J. (2002), "Polyelectrolyte cages for a novel biomimetic CO_2 sequestration system" in "Environmental challenges and Green house gas control for fossil fuel utilization in the 21st century", Kluwer Academic/Plenum Publishers, New York, pp. 133-146.

Simsek-Ege, F.A., Bond, G.M. & Stringer, J. (2001), "A biomimetic route to environmentally friendly CO_2 catalyst immobilization", *Electrochemical Society Proceedings,* vol. 2000, no. 20, pp. 162-170.

Somerset, V., Petrik, L. & Iwuoha, E. (2008), "Alkaline hydrothermal conversion of fly ash precipitates into zeolites 3: The removal of mercury and lead ions from wastewater", *Journal of Environmental Management,* vol. 87, pp. 125-131.

Somerset, V.S., Petrik, L.F., White, R.A., Klink, M.J., Key, D. & Iwuoha, E. (2004), "The use of X-ray fluorescence (XRF) analysis in predicting the alkaline hydrothermal conversion of fly ash precipitates into zeolites", *Talanta,* vol. 64, no. 1, pp. 109-114.

Soong, Y., Fauth, D.L., Howard, B.H., Jones, J.R., Harrison, D.K., Goodman, A.L. & Frommell, E.A. (2006), "CO_2 sequestration with brine solutions and fly ashes", *Energy Conversion and Management,* vol. 47, pp. 1676-1685.

Soong, Y., Goodman, A.L., McCarthy-Jones, J.R. & Baltrus, J.P. (2004), "Experimental and simulation studies on mineral trapping of CO_2 with brine", *Energy Conservation & Management,* vol. 45, pp. 1845-1859.

Speiser, C., Baumann, T. & Niessner, R. (2000), "Morphological and chemical characterization of calcium-hydrate phases formed in alteration processes of deposited municipal solid waste incineration waste bottom", *Environmental Science and Technology,* vol. 34, pp. 5030-5037.

Stolaroff, J.K., Lowry, G.V. & Keith, D.W. (2005), "Using CaO and MgO rich industrial waste streams for carbon sequestration", *Energy Conversion and Management,* vol. 46, pp. 687-699.

Sukrut, S.T., Mirko, S. & Edward, L.D. (2002), "Morphology and composition of the fly ash particles produced in incineration of municipal solid wastes", *Fuel Processing Technology,* vol. 75, no. 173, pp. 184.

Sushil, S. & Batra, S.V. (2006), "Analysis of fly ash heavy metal content and disposal in three thermal power plants in India", *Fuel,* vol. 85, pp. 2676-2679.

Szostak, R. (1989), "Molecular sieves, principles of synthesis and identification", Van Nostrand Reinhold, New York.

Takahashi, T., Takeuchi, T. & Sassa, K. (2006), "ISRM Suggested Methods for borehole geophysics in rock engineering", *International Journal of Rock Mechanics and Mining Sciences,* vol. 43, no. 3, pp. 337-368.

Tarazona, M., Rosa, M. & Spears, D.A. (1996), "The fate of trace elements and bulk minerals in pulverized coal combustion in a power station", *Fuel Processing Technology,* vol. 47, pp. 79-92.

Tay, J.H. & Goh, A.T.C. (1991), "Engineering properties of incinerator residue", *Journal of Environmental Engineering,* vol. 117, no. 2, pp. 224-235.

Taylor, H.F.W. (1998), "Cement chemistry", 2nd edition, Thomas Telford, London.

Tiwari, G.N., Singh, H.N. & Tripathi, R. (2003), "Present status of solar distillation", *Solar Energy,* vol. 75, no. 5, pp. 367-373.

Tunc, G.I., Turut-Asik, S. & Akbostanci, E. (2007), "CO_2 emissions vs CO_2 responsibility; An input-output approach for Turkey", *Energy Policy,* vol. 35, no. 2, pp. 855-868.

Turek, M. & Bandura, B. (2007), "Renewable energy by reverse electrodialysis", *Desalination,* vol. 205, no. 1-3, pp. 67-74.

United States, Department of Energy (1999), "Fossil energy, carbon dioxide sequestration research and development", USA.

Van Gerven, T., Van Keer, E., Arickx, S., Jaspers, M., Wauters, G. & Vandecasteele, C. (2005), "Carbonation of MSWI-bottom ash to decrease heavy metal leaching, in view of recycling", *Waste Management,* vol. 25, no. 3, pp. 291-300.

Virgil, L.A. & McLean, A.R. (1974), "Design of Experiments, A realistic approach", Marcel Drekker Inc., New York.

Ward, R.C. & French, D. (2006), "Relation between coal and fly ash mineralogy based on quantitative XRD methods", *Fuel,* vol. 85, pp. 2268-2277.

Waterson, B.J., Rajbhandari, B. & Hounsell, N.B. (2003), "Simulating the impacts of strong bus priority measures", *Journal of Transportation Engineering,* vol. 129, no. 6, pp. 642-647.

Watson, R.T. (2001), "Land use, land-use change and forestry", Cambridge University Press, London, ISBN 13-9780521800839

Wendt, C.H., Butt, D.P., Lackner, K.S. & Ziock, H.J. (1998), "Thermodynamic calculations for acid decomposition of serpentine and olivine in $MgCl_2$ melts I", Los Alamos National Laboratory, New Mexico, USA.

Willemse, N. (2009), "Future fuel? Marine algae pilot project launched in the Eastern Cape", Engineering News, South Africa.

Wolf, H.G., Chizmeshya, A.V.G., Diefenbacher, J. & Mc Kelvy, J.M. (2004), "In Situ observation of CO_2 sequestration reaction using a novel micro reaction system", *Environmental Science and Technology,* vol. 38, no. 3, pp. 932-936.

Wuebbles, D.J. & Jain, A.K. (2001), "Concerns about climate change and the role of fossil fuel use", *Fuel Processing Technology,* vol. 71, no. 1-3, pp. 99-119.

Wu-Jang, H., Min-Hsiu, S. & Feng-Hung, T. (2007), "Stabilization of lead in MSWI baghouse ashes by steam enhanced carbonation reaction", *Journal of Materials in Civil Engineering Management,* vol. 17, no. 2, pp. 123-128.

www.dme.gov.za/energy/coal.stm (accessed on 17th April 2009)

www.eskom.co.za (accessed on 20th May 2008)

www.southafrica.info/doing_business/economy/infrastructure/energy.htm (accessed 15th June 2008)

Xiaoxun, M., Kaneko, T., Tashimo, T., Yoshida, T. & Kato, K. (2000), "Use of limestone for SO_2 removal from flue gas in the semidry FGD process with a powder-particle spouted bed", *Chemical Engineering Science,* vol. 55, no. 20, pp. 4643-4652.

Xuedu, L., Jiahua, P. & Ying, C. (2006), "Sustaining economic growth in China under energy and climate security constraints", *China and World Economy,* vol. 14, pp. 85-97.

Zevenhoven, Ron., Teir, Sebastian & Eloneva, Sanni. (2008), "Heat optimization of a staged gas-solid mineral carbonation process for long-term CO_2 storage", Energy, vol.33, pp. 362-370.

APPENDICES

Appendix 1: Elemental concentration of the carbonation leachates for Runs 1 to 14 (Values in ppm; nd means not detected).

Element	Run 1	Run 2	Run 3	Run 4	Run 5	Run 6	Run 7	Run 8	Run 9	Run 10	Run 11	Run 12	Run 13	Run 14
B	198.8	44.2	17.27	116.3	58.26	174	8.119	12.55	17.97	77.38	19.28	14.04	47.02	544.7
Mg	1192	35.87	333.9	1338	72.31	828.3	288.7	185.6	406.3	1396	375.8		11.45	614.9
Al	0.6982	0.2598	0.2127	0.3869	2.541	0.5864	0.2578	0.2381	0.4027	1.116	0.3064	0.1064	7.059	13.59
K	114.4	105.1	106.8	106	142.3	114.9	117.3	118.2	110.4	105.2	114.4	111.5	121.8	110.2
Ti	0.0227	0.01253	0.00606	0.02101	1.187	0.04877	0.01218	0.02996	0.00786	0.0328	0.01142	0.0114	0.01365	0.9905
V	9.275	0.3618	1.851	13.16	1.81	5.606	0.6617	1.345	2.064	8.82	2.131	1.669	1.482	7.192
Cr	12.84	0.2341	0.143	7.357	0.06991	8.725	0.01995	1.336	0.6185	0.9318	0.3578	1.229	3.961	14.76
Mn	0.1236	0.00756	0.02852	0.1268	0.2626	0.04137	0.08893	0.3915	0.05761	0.1324	0.02322	0.7098	0.00438	0.1373
Fe	0.8021	0.12	0.0686	0.09978	10.5	0.1145	0.0669	0.1111	0.05072	0.06814	0.07279	0.0122	0.1059	1.442
Co	0.0019	6.6E-05	0.00064	0.00624	0.00812	0.00195	0.00065	0.00708	0.00111	0.00381	0.00113	0.0069	0.00052	0.00284
Ni	0.2589	0.09348	0.1382	0.3412	0.105	0.1135	0.1599	0.1609	0.1573	0.2375	0.1525	0.2021	0.1048	0.1566
Cu	0.0590	0.0060	0.00053	0.01326	0.07288	0.01055	nd	0.02238	0.0058	0.01194	0.00418	0.0045	0.00616	0.0443
Zn	0.0254	0.06287	0.01037	0.00972	0.158	0.2422	0.0664	0.01857	0.01615	0.04026	0.03472	0.0252	0.02857	0.06684
As	0.4542	0.03539	0.07002	0.7181	0.04551	0.1434	0.02954	0.1831	0.0783	0.5019	0.07154	0.2607	0.02523	0.07961
Se	0.1433	0.03774	0.05227	0.15	0.2676	0.08313	0.1018	0.05776	0.02931	0.146	0.04494	0.0934	0.09836	0.08931
Mo	2.089	1.137	0.3159	1.539	0.6141	2.218	0.2142	0.2267	0.2689	0.9624	0.3042	0.2585	1.301	2.896
Cd	nd	nd	nd	0.00013	0.00014	0.00034	nd	nd	nd	nd	nd	nd	nd	0.00052
Ba	0.21	0.07713	0.111	0.2471	0.1808	0.265	0.1036	0.2407	0.09344	0.1688	0.06046	0.2263	0.129	0.6218
Pb	0.0689	0.00955	0.00404	0.00504	0.01027	0.00714	0.00749	0.00220	0.00263	0.00207	0.00499		0.00120	0.01029
Ca	422.3	55.6	60.9	83.4	65.5	28.4	49.2	58.2	78.9	67.4	75.3	92.4	64.3	33.8
Na	3408	3560.8	3601.4	3337.8	3562.3	3405.5	3672.4	3642.5	3820.7	3424.8	3724.6	3716.1	3460.0	3399.1
Si	26.4	4.0	27.3	91.4	22.8	26.6	36.3	50.6	40.7	95.1	33.2	61.8	13.1	23.1
Sr	12.6	9.6	4.1	21.6	5.1	5.7	8.8	15.4	5.3	20.3	4.0	19.4	8.0	9.1
Cl	2589	2296	2372	2141	2461	2322	2275	2345	2365	2277	2402	2343	2267	2405.0
NO$_3$	nd	nd	nd	nd	nd	nd	nd	nd	nd	nd	nd	nd	nd	nd
SO$_4$	9390	7342	8045	6116	7628	7581	7781	8306	8127	7945	8125	8151	7226	8970.0

173

Appendix 2: Elemental concentration of the carbonation leachates for Runs 16 to 31 (Values in ppm; nd means not detected).

Element	Run 16	Run 17	Run 18	Run 19	Run 20	Run 21	Run 22	Run 23	Run 24	Run 25	Run 26	Run 27	Run 28	Run 29	Run 31
B	9.026	72.91	25.62	15.95	14.39	127.6	328.7	7.947	75.41	27.72	6.519	13.9	44.39	7.96	2.72
Mg	1.166	713.1	370	326.1	0.3739	494.7	2220	1.009	1292	401.7	297.7	224.8	76.22	316.4	1.522
Al	0.1459	0.08326	0.1534	0.4468	0.0347	0.8086	0.1971	6.509	0.2768	0.1432	0.1445	0.2754	0.9151	0.0993	nd
K	125.3	118.8	118.1	113.7	135	93.28	110.9	128.5	101.1	122	110	117.7	119	119.2	9.75
Ti	0.0151	0.03047	0.0092	0.0523	0.0037	0.0408	0.0517	0.0034	0.1238	0.0077	0.0164	0.0027	0.0314	0.0103	nd
V	0.0515	6.132	3.446	1.271	0.0532	1.74	22.44	0.2234	5.52	2.668	1.14	0.3004	0.39	1.244	0.15
Cr	1.073	6.752	2.754	0.0999	1.143	5.506	20.33	1.067	6.082	1.774	nd	0.0030	0.0533	0.0396	0.001
Mn	nd	1.228	1.192	0.4372	nd	0.0356	0.1268	nd	0.1998	0.0700	1.625	0.0542	0.0123	1.506	nd
Fe	0.1459	0.08672	0.0642	0.0713	0.1091	0.1692	0.1252	0.0614	0.0617	0.0569	0.0499	0.0679	0.101	0.0453	nd
Co	nd	0.01348	0.0167	0.0033	nd	0.0022	0.0064	nd	0.0045	0.0013	0.0153	0.0002	0.0013	0.0111	0.002
Ni	0.0718	0.3207	0.2994	0.0775	0.0585	0.1235	0.3243	0.0975	0.2104	0.1827	0.3048	0.2096	0.1078	0.249	nd
Cu	0.0049	0.06808	0.0603	0.0068	nd	0.0251	0.0245	nd	0.0139	0.0087	0.0098	nd	nd	0.0102	nd
Zn	0.0160	0.13	0.0282	0.2594	0.0077	0.1	0.0879	0.0249	0.0208	0.0229	0.0438	0.0094	0.0319	0.0707	nd
As	0.0014	0.6223	0.4836	0.1122	0.0019	0.0965	1.267	0.0067	0.3391	0.1011	0.1191	0.0267	0.0173	0.1276	nd
Se	0.0662	0.1343	0.0688	0.3681	0.0896	0.0750	0.2322	0.0448	0.1307	0.0381	0.1733	0.0204	0.0409	0.2237	nd
Mo	0.7041	1.114	0.4175	0.3693	0.8893	1.677	2.643	0.5876	1.175	0.4265	0.162	0.3817	1.042	0.1708	0.069
Cd	nd	nd	nd	nd	nd	nd	0.0004	nd	nd	nd	nd	nd	nd	nd	nd
Ba	0.2556	0.4659	0.4465	0.2466	0.1393	0.0845	0.4798	0.2739	0.4223	0.1011	0.2156	0.0502	0.0611	0.2558	0.008
Pb	0.0029	0.0013	0.0007	0.0015	0.0008	0.0013	0.0019	0.0012	0.0003	nd	0.0002	nd	0.0006	0.0011	nd
Ca	51.6	56.3	44.1	65.3	75	46.7	34.4	94.3	69.8	42.1	85.1	84.9	62.1	47.8	25.5
Na	3798.6	3524.9	3581.5	3595.8	3471.4	3240.7	3355.3	3429.9	3380.4	3517.3	3457.8	3534.8	3555.6	3504	3201
Si	1.6	58	76.9	39.2	0.4	8.8	59.1	12.6	34.6	27	58.9	16.7	11.9	60.2	nd
Sr	16.8	22.6	16.9	12.6	12.3	5.1	20.5	14.4	19.7	6.8	23.7	4.6	5.5	17.9	nd
Cl	265.0	2295	2261	2220	2246	2298	2322	2256	2331	2233	2342	2400	2341	2300	2193
NO$_3$	nd	15	nd	nd	nd	nd	nd	nd	nd	nd	nd	nd	nd	nd	nd
SO$_4$	1069.0	6497	8101	7943	7502	6282	8224	6791	8239	7397	8029	7684	7219	8197	7511

174

Appendix 3: Phase quantification of the carbonation residues (Values in wt %; nd means not detected)

	Amorphous	Calcite	Magnetite	Mullite	Plagioclase	Quartz	Bassanite	Anhydrite	Aragonite
Run 1	64.8	4.03	0.82	18.94	2.04	9.38	1.58	0.29	0.22
Run 2	57.7	7.92	1.11	19.26	1.9	12.11	0.53	0.29	0.22
Run 3	58.04	5.28	0.98	19.22	2.35	12.08	2.06	0.07	nd
Run 4	63.91	3.99	0.79	19.47	2.06	9.78	1.3	0.47	nd
Run 5	59.11	3.89	1.12	17.15	4.37	14.33	0.66	0.82	0.49
Run 6	58.92	6	1.06	19.38	3.36	11.27	1.2	0.54	nd
Run 7	58.75	3.8	1.39	16.57	4.41	14.97	0.37	0.88	nd
Run 8	60.18	5.22	1.07	19.24	2.37	11.76	0.16	0.53	nd
Run 9	58.27	5.22	1.1	19.15	2.34	12.06	1.85	0.27	0.1
Run 10	61.43	4.79	0.94	19.22	2.06	11.51	0.97	0.26	0.07
Run 11	59.53	5.15	0.92	19.16	2.11	11.51	1.63	0.33	0.17
Run 12	59.55	4.96	0.9	20.07	2.55	11.94	0.83	0.35	nd
Run 13	60.84	5.1	1.07	19.02	2.63	11.2	1.26	0.39	nd
Run 14	63.54	3.38	0.87	19.91	2.85	9.46	1.92	0.56	nd
Run 16	62.01	3.48	1.15	19.16	2.16	11.68	1.42	0.28	0.1
Run 17	64.48	2.99	0.84	19.88	2.29	9.53	1.54	0.37	0.17
Run 18	63.05	3.42	0.78	20.47	2.08	10.02	0.82	0.51	0.16
Run 19	59.84	2.63	1.23	16.39	4.48	14.86	0.67	0.88	nd
Run 20	62.78	3.81	1.04	19.02	1.8	11.26	1.12	0.31	0.27
Run 21	62.35	3.85	0.83	19.77	3.05	10.16	1.38	0.39	0.33
Run 22	63.6	3.3	0.87	20.32	2.32	9.59	1.86	0.39	nd
Run 23	60.21	4.49	1.01	19.73	2.63	11.85	1.28	0.3	0.15
Run 24	63.66	3.18	0.82	20.14	2.08	10.12	1.77	0.21	0.08
Run 25	58.66	0.77	1.51	16.98	4.72	16.32	0.38	0.79	nd
Run 26	60.19	6.11	0.88	19.33	2.06	11.42	1	0.27	0.29
Run 27	59.3	6.96	0.97	18.26	2.67	11.84	0.27	0.48	nd
Run 28	59.9	6.07	1.14	19.12	2.24	11.54	1.45	0.11	nd
Run 29	60.86	1.21	1.1	17.45	4.36	14.43	0.2	0.93	nd
Run 31	59.46	4.99	1.22	19.31	3.28	11.74	1.94	0.32	nd

Appendix 4: Trace element partition within the various particle size ranges for Tutuka fresh ash (Values in ppm)

Traces (ppm)	bulk	>150 μm	150μm-106μm	106μm-90μm	90μm-75μm	75μm-63μm	63μm-53μm	53μm-45μm	45μm-32μm	32μm-25μm	25μm-20μm	<20μm
Nb	33.5	30.6	28.3	26.6	33.1	33	34.5	34.2	34.5	33.5	37.1	41
Zr	503.3	390	373	379.1	516.9	509.2	539.1	525.9	554.2	521.3	582	634.8
Y	76.7	58.9	55.1	56	79.2	85	89.1	87.9	92	85.8	93.2	102.2
Sr	1903.9	1398.9	1406.1	1465.3	1903	1965.8	2054.9	2025.3	2129	2000.8	2209.5	2489
U	6.1	0.6	4.8	4.7	8.6	9.1	6.2	7	6.9	5.8	10.3	11.1
Th	42.1	27.6	28.9	28.4	41.6	46.6	45.6	47.4	47.7	43.6	48.4	55.1
Rb	41.2	58.2	50.4	42.6	43.9	40.8	40.9	38.4	40.3	38	40.3	40.4
Pb	45.5	21.1	21.7	23.6	40	49.4	50.4	52.9	58.1	52.4	63.7	71.4
Mo	4.2	2.8	1.9	1.5	<1.1	3.9	4.9	4.4	4.4	4.8	5.5	6
Zn	50.2	45.9	30	29.4	42.7	55.1	60.7	59.9	63.5	61.1	68.6	87
Cu	43.3	38.1	32.7	32.7	39.8	48.5	47.3	49.8	51.8	84.7	74.1	108.8
Ni	59.1	45.8	45.8	46.9	52.8	58.8	61.5	63.9	68.2	62.6	74.7	90.1
Co	23.9	18.6	17.1	17.9	21.9	24.3	24.6	26.9	30.4	27	29.4	38.6
Mn	464.4	464.2	464.3	464.4	464.4	464.4	464.5	464.4	464.5	464.4	464.5	464.7
Cr	226.1	178.6	166.9	171.6	204.7	228.2	232	240.5	245.6	237.3	257.3	272.4
V	130.4	120.6	115.6	109.7	130.4	139.6	139.7	143.9	145.4	140.8	142.6	158.3
Ba	1306.6	1077.1	1038.3	1025.8	1170.9	1311.6	1317.9	1354.8	1420	1346.8	1452.3	1651
Sc	33.7	26.2	24.1	24.9	30.2	34.6	34.5	34.8	36.5	35	36.5	42.4
S	2764	1390.7	1113	1282	2268	3032.1	2960.1	3060.1	2973	2988.1	3065	3305

Appendix 5: Trace element partition within the various particle size ranges for Secunda fresh ash (Values in ppm)

Traces (ppm)	bulk	>150 μm	150μm-106μm	106μm-90μm	90μm-75μm	75μm-63μm	63μm-53μm	53μm-45μm	45μm-32μm	32μm-25μm	25μm-20μm	<20μm
Nb	35.3	27.1	25.5	31	28.1	36.1	36.1	38.1	37.7	38.3	39.2	37.2
Zr	638.8	381.3	475.3	574.3	627.1	652.3	663.8	703.6	682.7	734.3	696.4	655
Y	81.1	49.2	60	72	82.5	85.6	86.4	88.4	87.6	94.6	91.6	89.5
Sr	4059.3	2416.4	3325	3880.5	4194	4243.5	4216.1	4365.2	4213.9	4502.5	4296.5	4263.7
U	7.4	3.9	5.3	5.7	9.1	8.8	10.3	9.1	9.7	8.2	10	12.1
Th	52.8	31.3	38.1	45.4	52.4	59.2	58.4	62.1	58.4	65.5	63.5	62.6
Rb	33.1	26.9	32	32	32.2	34.4	35.2	35.6	35.2	38.3	38.2	35.8
Pb	30	13.1	15.3	21	28.8	38.4	35.4	42.3	39	47.9	48.5	46.4
Mo	3	<1.1	<1.1	1.6	<1.1	15.5	2.6	2.5	2.9	3.1	3.9	2.6
Zn	33.8	15.6	18	22.5	27.5	33.4	33.4	34.7	36.6	39.4	41.1	46.4
Cu	48.2	31	35.1	37.6	43.9	50.9	50.1	53.7	56.5	58.3	64.1	74.6
Ni	43.3	35.9	38	39.9	41.9	45.8	45.1	45.3	47.4	46.9	49	55.8
Co	11.2	8.1	7.9	7.6	11	10	10	11.1	12.8	11.4	12.2	13.3
Mn	464.3	464.2	464.2	464.3	464.4	464.4	464.4	464.4	464.4	464.4	464.4	464.4
Cr	203.6	173.5	163.3	181.8	209.4	209.6	216.1	219.4	216.5	217.4	223.2	224
V	138.2	114.9	117.1	122.7	133.4	138.5	135.1	135.3	136	140.6	137.9	147.4
Ba	2290.7	1429.5	1760.5	1859.5	2026.9	2180.2	2165.1	2217.7	2263.2	2306.9	2323.8	2647.3
Sc	32.1	21.2	26.3	25.4	30.1	32.3	31.1	33.4	32.7	34.3	34.4	37.6
S	1932.9	2600.5	1919.4	1649.5	1797.8	1841	1821.9	1892.5	1879.9	1903.4	1889.3	1772.6